# COMPUTATIONAL PREDICTION AND EXPERIMENTAL VERIFICATION OF GENE

# REGULATORY ELEMENTS IN NEURONAL DEVELOPMENT

**by**

**SUNG TAE DOH**

A Dissertation submitted to the

Graduate School-New Brunswick

Rutgers, The State University of New Jersey

and

The Graduate School of Biomedical Sciences

University of Medicine and Dentistry of New Jersey

In partial fulfillment of the requirements

For the degree of

Doctor of Philosophy

Graduate Program in Biomedical Engineering

Written under the direction of

Dr. Li Cai

And approved by

_____

_____

_____

_____

_____

New Brunswick, New Jersey

October, 2010

# ABSTRACT OF THE DISSERTATION

**Computational Prediction And Experimental Verification Of Gene Regulatory Elements**

**In Neuronal Development**

**By Sung Tae Doh**

**Dissertation Director:**

**Li Cai**

Completion of the human genome sequence along with other species allows for greater understanding of the biochemical mechanisms and processes that govern healthy as well as diseased states. Non-coding regions have been shown to play a critical role as gene regulatory elements. Enhancers that regulate transcription processes have been found in intergenic regions. Many regulatory elements found in non-coding regions are highly conserved across different species. While current sequence based computational methods are continuously improving in accuracy and scope, determining the time and tissue specific function of gene regulatory elements remain largely elusive.

The goal of this dissertation is to identify novel gene regulatory elements involved in neuronal development using a combined approach which utilizes both computational prediction and experimental verification. We describe a method for utilizing genomes, annotations, computational tools, expression data, and molecular genetics methods to predict gene regulatory elements and confirm the function of these elements. In particular, the non-coding regions of homologous and functionally related genes are analyzed to identify highly conserved regions

predicted to have gene regulatory function.  To facilitate in the acquisition of desired sequences,

a web tool was created to retrieve non-coding sequences based on annotations.  Using multiple

pair-wise alignments of non-coding sequence, over 502 conserved regions have been identified,

at least 3 of which are well characterized, known enhancer elements.  Previous studies utilized

transgenic animals to experimental confirm the function of conserved regions.  These animals are

time consuming and expensive to generate.  In contrast this study uses *in ovo* and *in vivo*

electroporation of a plasmid DNA reporter construct for the confirmation of function. By

transfecting the plasmid DNA reporter constructs into an animal model, enhancer function can be

confirmed by the expression pattern of the reporter gene.  Ten novel enhancers have been

experimentally verified of which 2 have been characterized for the purpose of this study.

Identification of novel gene regulatory elements allows for a better understanding of the

mechanisms of gene regulation which may lead to the eventual control of gene expression.  This

has important implications and applications ranging from directing stem cell differentiation to

designing new sequence based therapeutics.

**ACKNOWLEDGEMENT**

To my family, friends and wife thank you for all your love and support.

Thank you to all my professors and advisors who have helped to shape the work that

came to be this dissertation.

**TABLE OF CONTENTS**

**LIST OF TABLES**

## LIST OF ILLUSTRATIONS

**CHAPTER 1    INTRODUCTION**

**1.1     Background**

Completion of the human genome sequence along with other species allows for greater understanding of the biochemical mechanisms and processes that govern healthy as well as diseased states. The large size of the genome sequences has made them difficult to study using traditional methods. There are many studies focusing on the protein coding sequences, however, not much is known about the function of non-coding regions of the genome. It has been demonstrated that parts of the non-coding region play a critical role as gene regulatory elements. Enhancers that regulate transcription processes have been found in intergenic regions. Furthermore, it is observed that many regulatory elements found in non-coding regions are highly conserved across different species. However, computational predictions of regulatory elements are not as straightforward as it may first seem.  Gene regulatory elements are often spatially and temporally restricted in their function.  While current sequence based computational methods are continuously improving in accuracy and scope, determining the time and tissue specific function of gene regulatory elements remain largely elusive.

The goal of this dissertation is to identify novel gene regulatory elements involved in neuronal development using a combined approach which utilizes both computational prediction and experimental verification. We describe a method for utilizing genomes, annotations, computational tools, expression data, and molecular genetics methods to predict gene regulatory elements and confirm the function of these elements.  In particular, the non-coding regions of homologous and functionally related genes are analyzed to identify highly conserved regions (CR) predicted to have gene regulatory function.  To facilitate in the acquisition of desired sequences, a web tool was created to retrieve non-coding sequences based on annotations.  Using multiple pair-wise alignments of non-coding sequence, 1053 CRs have been identified, at least 3 of which are well characterized, known enhancer elements.  These predicted enhancers are then

experimentally tested for enhancer activity. Previous studies utilized transgenic animals to experimental confirm the function of CRs. These animals are time consuming and expensive to generate. In contrast this study uses *in ovo* and *in vivo* electroporation of a plasmid DNA reporter construct for the confirmation of CR function. This construct contains the CR sequence, a basal promoter and a reporter gene that expresses fluorescent protein. By transfecting the plasmid DNA reporter constructs into an animal model by *in ovo* or *in vivo* electroporation, enhancer function can be confirmed by the expression pattern of the reporter gene. Ten novel enhancers have been experimentally verified of which 2 have been characterized for the purpose of this study. Identification of novel gene regulatory elements allows for a better understanding of the mechanisms of gene regulation which may lead to the eventual control of gene expression. This has important implications and applications ranging from directing stem cell differentiation to designing new sequence based therapeutics.

### 1.1.1  Motivation

The broad long-term objective of this research is to identify gene regulatory elements of genes involved in neural development. While the body has the capability to heal and regenerate the majority of the body's tissue types, once damaged, neurons do not regenerate. Many of those conditions involving neuronal damage or degeneration therefore do not currently have effective treatments. Spinal cord injury, macular degeneration and Parkinson's disease are but a few of the devastating conditions that may benefit from treatments that offer neuronal regeneration or replacement therapies. While stem cell research is a very promising field, the events that drive differentiation and how environmental cues determine cell fate are only now beginning to be investigated. In order to understand how neurons differentiate and develop from their progenitor cells the genes involved in orchestrating and controlling development must be identified. Furthermore we need to understand how these key genes are regulated. While many of the genes involved in development have already been identified we are only beginning to understand how they are regulated and how this in turn affects the control of overall

development. Identification of gene regulatory elements such as enhancers is a key step in beginning to unraveling the complex mechanisms and regulatory networks involved.

### 1.1.2    Functional Roles of Non-Coding Sequences

Annotation efforts and gene prediction methods have begun the process of identifying protein-coding genes, however robust high-throughput methods for detecting functional non-protein-coding elements remains elusive [1].  Only about 2 percent of the human or mouse genomes consist of DNA sequences that are protein-coding regions [2].  The remaining vast majority of the genome consists of non-coding sequences [3-5].  It has been shown that gene regulatory elements (GREs) reside in the non-coding sequences.  GREs have been broadly placed into two major functional groups: promoters and enhancers.  Promoters are sequences that direct the precise locations of transcription start sites.  Promoters are therefore usually located close to the 5′ start of the gene.  Enhancers are sequences that bind gene regulatory proteins and influence the transcription activity of a gene.  Enhancers can be located upstream, downstream, or even internal to the target gene.  Enhancers, therefore, act as switches to turn gene expression on or off and as modulators to increase or decrease expression.  Traditionally, non-coding sequences have not received as much attention from investigators as protein coding sequences and GREs are generally poorly defined, mostly as only sequence motifs.  Research is now increasingly focusing on non-coding sequences and specifically the search for non-coding sequences with regulatory function.  Identifying functional non-coding sequences and understanding their mechanism of operation will shed new insights into the understanding of the regulatory functions of transcription, DNA replication, chromosome pairing, and chromosome condensation [2, 6].  In order for the full understanding and eventual control of biological function, not only must the genes involved be identified but the means through which regulatory elements trigger and control biochemical pathways that determine expression be well understood.  However, searching for functional GREs within the non-coding sequences that comprise roughly 98% of the genome is not a simple task. The size and scope of this search brings with it many intellectual and

experimental challenges that span computational biology and comparative functional genomics [7].

## 1.2 Computational Prediction of Gene Regulatory Elements

There are two commonly used methods for identification of functional GREs. The first uses gene expression analysis and the second uses comparative genomics. DNA microarray gene expression profiling is capable of evaluating thousands of genes across various experimental conditions. Bioinformatics approaches are used to cluster subsets of genes that show similar patterns of expression. Once genes with similar patterns of expression are identified, they are searched within their upstream non-coding sequences to identify over-represented or conserved sequence motifs [8-11]. The second method utilizes sequence alignment algorithms to identify conserved sequences from diverse species in non-coding regions located within and around genes with the same function, known as homologous genes. Genes from different species with the same function should also share some of the same regulatory mechanisms and elements. Therefore, non-coding regions that are highly conserved amongst distantly related species should have regulatory function that can be identified using alignment analysis. Functional regions (which consist of protein coding regions along with regulatory regions) should experience selective pressure against change and therefore have a higher level of sequence conservation across a wide range of species than non-functional regions. Ideally, selective pressures allow for non-functional sequences to diverge due to evolutionary drift while leaving functional regions with high similarity [1, 12-19]. DNA sequence comparison of the human and mouse orthologous genes have indicated that conserved non-coding sequences are enriched significantly in regulatory sequence regions [5, 20, 21]. Transcriptional regulatory regions in genes from humans, mouse, Fugu fish, *Caenorhabditis elegans*, *Drosophila*, and yeast have been identified through identifying conserved non-coding sequences [3, 6, 22-26]. The power of comparative genomics analysis is enhanced significantly when genomic sequences are available from a number of related species that have diverged sufficiently. This reduces the chances of

conservation among non-functional elements. By comparing multiple genomes, it can help to determine which conserved elements are more likely to be functional [3, 25, 27, 28]. Therefore multiple pair-wise alignments are performed to allow for identification of non-coding CRs that are shared among a set of distantly related species.

Co-regulated or co-expressed genes can also be analyzed through multiple pair-wise alignments. Microarray and SAGE analysis measure mRNA levels under specific conditions to identify sets of genes that show similar patterns of expression [29]. If genes are in fact co-regulated or co-expressed then they should share *cis*-regulatory elements. *Cis*-regulatory elements are sequence specific regions that interact with regulatory proteins or other *cis*-regulatory elements to regulate gene expression [30]. Since these *cis*-regulatory elements are conserved they can be identified in their non-coding sequences through sequence alignment analysis. Targeting computational study on those regions most likely to contain *cis*-regulatory elements may increase the accuracy with which transcription factor binding sites are identified using rVista [31]. Transcription factor binding sites interact with transcription factor proteins to regulate gene expression. Identifying the transcription factor binding sites present can narrow the field of potential transcription factors and may help to identify a specific subset of transcription factors or a pattern of transcription factors from which once can elucidate the biological function of the CR.

Ultimately, the computational prediction of potential enhancers allows for the selection of only those CR that have the greatest likelihood for regulatory function for further experimental study will increase the efficiency and throughput of the enhancer element identification process. Once CRs have been identified, scoring the CRs allows for a ranking system which can help to prioritize those CRs which are most likely to possess biological function and therefore increase overall efficiency.

**1.3      Confirmation of Biological Function**

Gain-of-function assays using transgenic mice is a well established method for studying development [32]. However, the use of transgenic mice is very time-consuming. Electroporation can be used with mice, rats, or chicks and multiple plasmids can be electroporated at once. Thus, *in vivo/ovo* electroporation offers a rapid alternative to the use of transgenic mice for gain-of-function assays. While the expression of transfected genes is not permanent it is long enough to study the development of the animal model [33, 34]. This method has been used to study the function of various genes [34], the cell specificity of particular promoters [33], and the study of enhancers [35]. *In vivo/ovo* electroporation will be used in this as a key method for studying normal development and for the experimental verification of CRs for enhancer function.

# CHAPTER 2    DEVELOPMENT OF A NON-CODING SEQUENCE RETRIEVAL SYSTEM AND IMPLEMENTATION IN BUILDING AN ENHANCER CANDIDATE DATABASE

## 2.1    Prologue

Enhancers are non-coding sequences that regulate gene expression in a spatio-temporal specific manner.  Enhancers may provide critical insight into gene regulation and reverse engineering the mechanisms through with they function may provide biomedical engineers the tools necessary for advances towards clinical therapies. These sequences have been found upstream, downstream, and within the intronic region of the gene they regulate.  They can be located as close as a few kb away from the transcription start site or as far as hundreds of kb away.  Furthermore non-coding sequences account for approximately 98% of the entire genome.  Therefore to randomly search for these sequences would be extremely difficult, time consuming and wasteful of both time and lab resources.  Computational sequence analysis has provided some critical tools necessary for guiding the search for enhancers and narrowed the overwhelming scope of this search to a much more manageable task.  We describe here an approach for predicting enhancers and a pair of web based tools that were created.  The first was designed to aid in the collection and distribution of sequences and the second to store and conveniently present our computational results.

## 2.2    Abstract

Completion of the human genome sequence along with other species allows for greater understanding of the biochemical mechanisms and processes that govern healthy as well as diseased states. The large size of the genome sequences has made them difficult to study using traditional methods. There are many studies focusing on the protein coding sequences, however, not much is known about the function of non-coding regions of the genome. It has been

demonstrated that parts of the non-coding region play a critical role as gene regulatory elements. Enhancers that regulate transcription processes have been found in intergenic regions. Furthermore, it is observed that regulatory elements found in non-coding regions are highly conserved across different species. However, the analysis of these regulatory elements is not as straightforward as it may first seem. The development of a centralized resource that allows for the quick and easy retrieval of non-coding sequences from multiple species and is capable of handing multi-gene queries is critical for the analysis of non-coding sequences. Here we describe the development of a web-based non-coding sequence retrieval system and its implementation to generate multiple genome alignment based predictions of enhancers.

The Non-Coding Sequences Retrieval System (NCSRS) is a web-based bioinformatics tool that performs fast and convenient retrieval of non-coding and coding sequences from multiple species related to a specific gene or set of genes. This tool has compiled resources from multiple sources into one easy to use and convenient web based interface. With no software installation necessary, the user needs only internet access to use this tool.  NCSRS was used along with LAGAN to identify 1053 conserved regions (CR) surrounding 89 genes, 53 of which are involved in neuronal development.  These CR were then scored and ranked to estimate the likelihood of containing gene regulatory elements that exist in non-coding regions.  These results were then compiled into a searchable and web browser friendly database that includes 502 high scoring CR (score > 75). The web based application can be accessed on the internet at: http://cell.rutgers.edu/ncsrs/.

## 2.3    Introduction

While annotation efforts and gene prediction methods have begun the process of identifying protein-coding genes, robust high-throughput methods for detecting functional non-protein coding elements remain elusive [1].  Only about 2 percent of the human or mouse genomes consist of DNA sequences that are protein-coding regions [2].  The remaining vast majority of the genome consists of non-coding sequences (NCS).  It has been shown that gene regulatory

elements (GREs) reside in the NCS [3, 5, 36, 37]. GREs have been broadly placed into two major functional groups: promoters and enhancers. Promoters are sequences that direct the precise locations of transcription start sites. Enhancers, repressor, and silencers, etc. are sequences that bind gene regulatory proteins and influence the transcription activity of a gene. GREs can be located upstream, downstream, or even internal to the target gene. GREs, therefore, act as switches to turn gene expression on or off and as modulators to increase or decrease expression. Traditionally, NCS have not received as much attention from investigators as protein coding sequences and GREs are generally poorly defined, mostly as only sequence motifs. Research is now focusing increasingly on non-coding sequences and specifically the search for NCS with regulatory functions. Identifying functional NCS and understanding their mechanism of operation will shed new insights into the understanding of the regulatory functions of transcription, DNA replication, chromosome pairing, and chromosome condensation [2, 6]. In order for the full understanding and eventual control of biological function, not only must the genes involved in a particular function be identified but the regulatory elements that trigger and control the biochemical pathways that determine each gene's expression must also be well understood. However, searching for functional GREs within the NCS that comprise roughly 98% of the genome is not a simple task. The size and scope of this search brings with it many intellectual and experimental challenges that span computational biology and comparative functional genomics [7].

There are two commonly used methods for identification of functional GREs. The first uses gene expression analysis and the second uses comparative genomics. DNA microarray gene expression profiling is capable of evaluating thousands of genes across various experimental conditions. Bioinformatics approaches are used to cluster genes that show similar patterns of expression. Once genes with similar patterns of expression are identified, they are searched within their upstream sequences to identify over-represented or conserved sequence motifs [10, 11]. Sequence alignment algorithms employed by the comparative genomic methods are powerful in

identifying conserved sequences in non-coding regions located in and around genes with the same function, known as homologous genes, from diverse species.  Homologous genes usually have the same function and may also have similar regulatory elements that control this function. Functional regions (which consist of protein coding regions along with regulatory regions) experience selective pressure against change and therefore have a higher level of sequence conservation across a wide range of species than non-functional regions.  Ideally, selective pressures would allow for non-functional sequences to diverge due to evolutionary drift while leaving functional regions with high similarity [1, 13-15, 17-19, 38, 39].  DNA sequence comparison of the human and mouse orthologous genes have indicated that conserved NCS are enriched significantly in regulatory sequence regions [5, 20, 21]. Subsequent to the identification of putative regulatory elements by sequence comparison, the confirmation of biological function will depend upon experimental assays. Transcriptional regulatory regions in genes from humans, mouse, Fugu fish, *Caenorhabditis elegans*, *Drosophila*, and yeast [3, 6, 22-26] have been identified. The power of comparative genomics analysis is enhanced significantly when genomic sequences are available from a number of related species that have diverged sufficiently.  This reduces the chances of conservation among non-functional elements. By comparing multiple genomes, it can help to determine which conserved elements are more likely to be functional [3, 25, 27, 28].

Whether the focus is on genes with similar expression patterns or those expected to have the same function, both analysis methods require the retrieval of NCS for the identification of functional sequence elements.  Currently, the process of retrieving these sequences is performed manually from a wide range of sources. No efficient method is available for retrieving NCS quickly and systematically at a single source. To facilitate the analysis of NCS for functional regulatory elements, we present here a web-based Non-Coding Sequences Retrieval System (NCSRS) that performs the automated retrieval of non-coding sequences among genomes of different species. A previously developed application for retrieving NCS, called Retrieval of Regulative Regions

(RRE) [40] parses annotation and homology data from NCBI to identify NCS.  This parser

**Table 1 - Statistics of gene annotation for ENSEMBL and NCBI**

**ENSEMBL - as of 12/06/06**

| *Organism* | *Assembly* | *Genebuild Date* | *Version* | *Known* | *Novel* | *Total Predictions* |
|---|---|---|---|---|---|---|
| *Human* | NCBI 36 | Aug 2006 | 41.36c | 22205 | 1019 | 69185 |
| *Mouse* | NCBI m36 | Apr 2006 | 41.36b | 21839 | 2599 | 71259 |
| *Chicken* | WASHUC 1 | Dec 2005 | 41.1p | 5123 | 5417 | 76146 |

**NCBI - taxonomy browser and Unigene as of 12/06/06**

| *Organism* | *Assembly* | *GenBank Date* | *UniGene Build* | *Entrez Genes* | *Total Unigene Clusters* |
|---|---|---|---|---|---|
| *human* | NCBI 36 | Oct 2006 | 197 | 38597 | 85590 |
| *mouse* | NCBI m36 | Oct 2006 | 159 | 60745 | 64618 |
| *chicken* | WASHUC 1 | Aug 2006 | 31 | 24313 | 30837 |

Known - genes that have species-specific protein sequences already available in the public sequence databases. Novel – genes that could not be mapped with confidence to existing entries. Total Predictions – the number of 'known', 'novel' and 'pseudogenes' predicted by the Ensembl analysis and annotation pipeline.

Entrez Genes – number of genes defined by sequence and/or located in the NCBI Map Viewer. Total Unigene Clusters – the number of non-redundant sets of gene-oriented clusters automatically partitioned by UniGene.

requires local installation but also requires a local copy of desired genomes and annotation files. A web based application is also available but only a few genomes are currently available and RRE utilizes annotation data from only NCBI.  The NCSRS requires no installation or local management of genome sequence databases and utilizes annotation information from both NCBI and Ensembl. Currently, NCSRS has 15 genomes (containing over 85 Gigabyte of DNA sequence data) with sufficient annotations available for NCS retrieval.

**2.4     Implementation**

*2.4.1    Annotation and Sequence Information*

**Table 2 - Statistics of homology prediction for human, mouse, and chicken**

| *Ensembl (mart 41)* | | *Baseline Species for Homology Search* | | |
|---|---|---|---|---|
| | | *Human* | *Mouse* | *Chicken* |
| *Species of Homologous Genes* | *Human* | - | 13049/ 46.7% | 9839/ 50.7% |
| | *Mouse* | 12036 / 38.6% | - | 11698/ 60.3% |
| | *Chicken* | 11773 / 37.7% | 12187/ 43.6% | - |
| *Total number of genes* | | 31206 | 27964 | 19399 |

| *Homologene (release 53)* | | *Baseline Species for Homology Search* | | |
|---|---|---|---|---|
| | | *Human* | *Mouse* | *Chicken* |
| *Species of Homologous Genes* | *Human* | - | 16325 / 73.0% | 10498 / 84.0% |
| | *Mouse* | 16325 / 41.2% | - | 10299 / 83.3% |
| | *Chicken* | 10498 / 26.5% | 10299 / 46.6% | - |
| *Total number of genes* | | 39605 | 22364 | 12500 |

The homolog data table files for each of the baseline species (available for download at ftp://ftp.ensembl.org/pub/current_mart/data/mysql/ensembl_mart_41/) were queried to find the total number of genes along with the number of homologous genes that are present in another given species' genome.  Similarly the homologene.data file (ftp://ftp.ncbi.nih.gov/pub/HomoloGene/current/homologene.data) was used to generate the homologene statistics.  Shown are the number of homologs and the percentage of coverage (the number of genes that have homologs in a particular species' genome divided by the total number of genes for the baseline species.)

There are two major groups currently working on genome annotation.  Data from these two sources serve as the source of the annotation information that comprises the core for this tool.  These include NCBI RefSeq [41] and Ensembl [42].  RefSeq is a partially manually curated annotation database which includes information based on predicted mRNAs and proteins.  The genes with manually curated mRNA information are labelled with the "NM" prefix while the genes based on predicted mRNA information are labelled with an "XM" prefix.  Ensembl's gene predictions are automated but all predictions are based on experimental mRNA evidence.  The

Ensembl annotation system marks predicted genes as either known or novel based on the level of experimental support and information from other annotation sources. The number of genes annotated by Ensembl and Refseq are listed in Table 1 and 2. Table 3 shows the number of genes annotated in Refseq are also included in the Ensembl system along with the percentage of overlap between the two with respect to the total number of annotated genes in the Ensembl system. The pros and cons of each will not be discussed here but rather it is emphasized that this tool offers users the freedom to choose.

**Table 3 - Analysis of known and predicted genes for chicken, rat, mouse, and human from Ensembl Mart v.41**

| Species | NM (known) | | | XM (predicted) | | |
|---|---|---|---|---|---|---|
| | Refseq known to Ensembl | Ensembl | Percentage | Refseq known to Ensembl | Ensembl | Percentage |
| Chicken | 2726 | 24939 | 10.93% | 1 | 24910 | 0.00% |
| Rat | 9119 | 37825 | 24.11% | 9731 | 38778 | 25.09% |
| Mouse | 21336 | 36898 | 57.82% | 16931 | 46566 | 36.36% |
| Human | 29836 | 62076 | 48.06% | 9849 | 63575 | 15.49% |

| TOTAL | | | |
|---|---|---|---|
| Species | Refseq known to Ensembl | Ensembl | Percentage |
| Chicken | 2727 | 49849 | 5.47% |
| Rat | 18850 | 76603 | 24.61% |
| Mouse | 38267 | 83464 | 45.85% |
| Human | 39685 | 125651 | 31.58% |

The RefSeq annotation data (RefGene.txt, RefLink.txt) is obtained for each genome from the Human Genome Browser at UCSC [43] ftp site (ftp://hgdownload.cse.ucsc.edu/goldenPath/) as are some of the genome sequences. The remaining genome sequences along with the Ensembl data (gene, transcript, and structure files for each genome) are obtained from Ensembl's ftp site (ftp://ftp.ensembl.org/pub/current_mart/). Both sets of gene annotations are downloaded and then processed to serve as the basis for building a genome map that contains the location of each gene and all its exons. In those cases where multiple transcripts are available, the

transcript with the greatest number of exons is used. Because not all the transcript information is used to define sequences in the intron region there is the potential that an exon from an unused transcript variant may not be shared with the utilized transcript.  In this case, the unshared exon would be "hidden" from the annotation and returned as part of the non-coding sequence. However this is not relevant in the majority of cases as "hidden" exons are not the norm. Furthermore, this is limited to only the intragenic region and would not affect the up and down stream sequences.

### 2.4.2   Homology Prediction

The RefSeq annotation information is the basis for the homologous gene prediction system. It is called Homologene (http://www.ncbi.nlm.nih.gov/entrez/query.fcgi?db=homologene).  This system is implemented in the NCSRS by using the single "homologene.data" file for gene annotation information from RefSeq.  This file is a list of the sets of homologous genes for all genes annotated by RefSeq.  Ensembl has its own homology prediction method and its output is organized in a set of multiple files.  The Ensembl annotation information is the basis for its homologous gene prediction and therefore when using Ensembl's annotation information Ensembl's homology prediction results are used.  Simple analysis of the data generated by the two homology prediction methods shows that both systems have good coverage for those genomes most commonly used for research (see Table 2).  As the annotations improve, the results of the predictions will also improve in accuracy and percent coverage.

**Figure 1 - Snapshot of the web based user interface for the NCSRS**

# Non-Coding Sequence Retrieving

- Non-Coding sequences
- Ortholog will retrive other species

| Sequence information |
|---|
| Input Type: ○ Gene ID (LocusLink ID) ⦿ Gene Symbol |
| Species: [Human ▾] |
| Pull all otholog sequences: [Yes ▾] |
| Extend the sequence to next adjacent gene? ⦿ Yes ○ No, extend [          ] bp. |
| Exon Masking: [No ▾] |
| Load from file? ⦿ No, input below: |
| pde6g<br>gas7<br>crx<br>rdh5<br>rom1 |
| ○ Yes, [                    ] Browse... |
| Output Compression: ⦿ zip ○ tar ○ gzip |
| Submit     Reset |

## Links

UCSC genome
NCBI map view

The user interface allows the user to input the HUGO (Human Genome Organization) ID, i.e., Entrez gene ID (LocusLink ID), Gene Symbol, and Ensembl ID numbers and set the other search options.

*2.4.3 Input*

The user's input of the desired search options on the user interface (Fig. 1) determines the work-flow path (Fig. 2). The search options include the input type, genome or genomes from which sequences will be extracted, range of sequence extension, exon masking, and output format. The user inputs the individual gene or set of genes of interest. The input can be either the Entrez gene id or HUGO gene symbol (default) but must be the same for all the genes of a given search. The non-coding sequences from a specific species can be returned by selecting the desired species from a pull down menu or from all species with a known orthologous gene, by activating the "pull all ortholog sequences" option according to the homologene database (ftp://ftp.ncbi.nih.gov/pub/HomoloGene/current).

*2.4.4 Mapping*

Using the annotation information all annotated genes are sorted based on chromosomal position. Then the start and stop locations for all coding regions are identified. By identifying the coding regions we can also determine the locations of the non-coding regions using genomic position information, or mapping, of a specified gene and its flanking genes. The non-coding sequences are identified simply as those located between the adjacent identified exons. The information for each gene's non-coding region is then written to a new set of files that are used by the NCSRS. This non-coding region annotation serves as the basis for the locations of the end points for each intergenic and intragenic region.

*2.4.5 Retrieval of Non-coding Sequences*

Using the locations of non-coding regions the appropriate genomic sequence is identified. The genome sequence file is read and the specified sequences are extracted and copied to a new file according to the appropriate position information. The NCSRS by default outputs the non-coding sequence of the specified gene starting from the end of its adjacent gene and ending with the start of the other adjacent gene (as marked with 2 "X"s in Fig. 1). Unless specified otherwise the

**Figure 2 -** **Work flow diagram of the NCSRS**
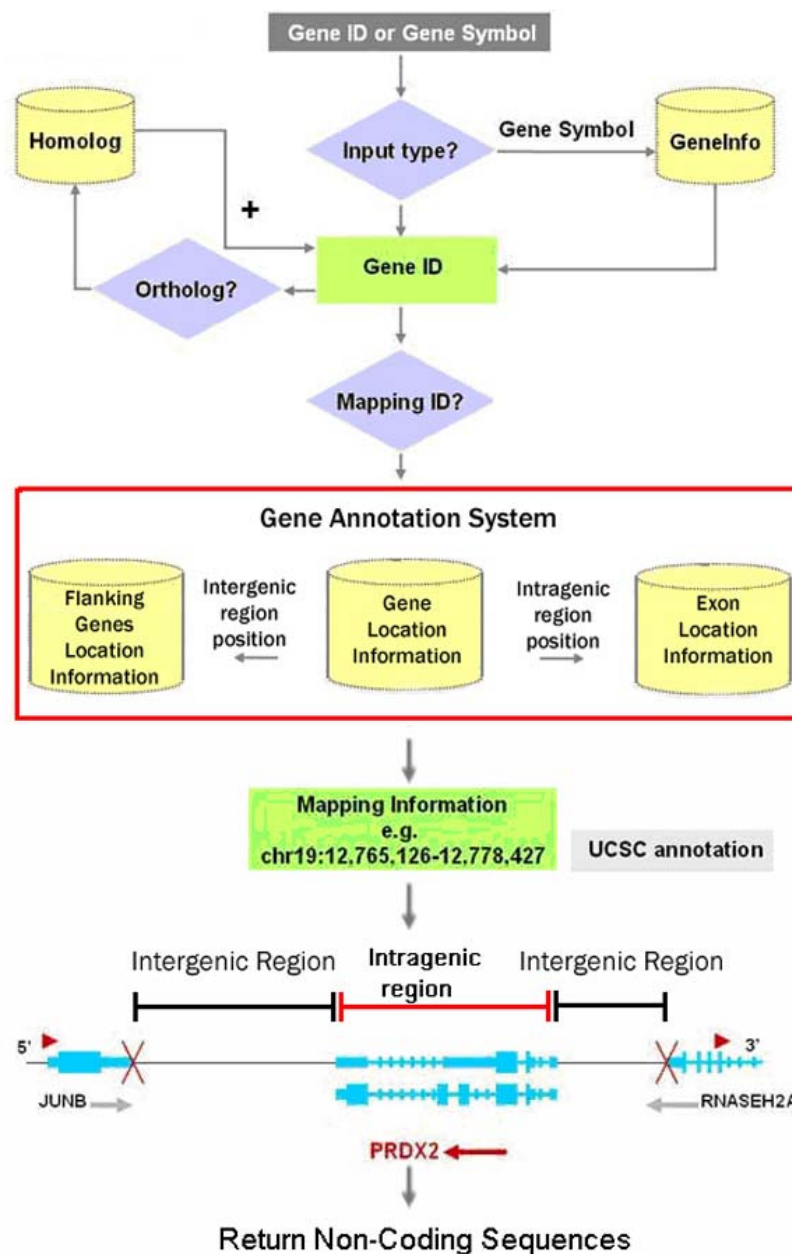
The Refseq annotation uses Entrez gene IDs as the database key while Ensembl uses gene stable IDs. The input ID is converted into the appropriate database key if necessary. Entrez gene IDs are used directly for the Refseq annotation but are converted to gene stable IDs for the Ensembl annotation. Gene symbols are translated into Entrez gene IDs and gene stable IDs. Once the database keys are acquired, the homologous genes can be identified using the available homology databases if the "pull ortholog" option is activated. The database key is then used to access the mapping information that has been compiled from the annotation data. The mapping information is then used to locate the relevant sequences. These sequences are extracted then copied to a new ".fa" file with FASTA sequence format; and the annotation information about the exons is written to the ".exon" file. Thus, for each requested gene, there are one pair of files for each genome.

NCSRS also outputs the intergenic sequences, exons and introns. The boundaries for the flanking regions can be arbitrarily set by specifying the extension length in the options, e.g., with a specified extension length of 5000bp. Then, 5000bp up- and down-stream of the queried gene will be included in the extraction irrespective of the location of neighboring genes.  Each sequence has a pair of associated files: FASTA format sequence file with file extension ".fa" and EXON definition file with file extension ".exon", both with file names generated using the UCSC annotation format.  The ".fa" file contains the sequence in FASTA format.  The first line of the ".exon" file defines the span of the coding region.  The first line also contains other information such as the name of the gene the chromosome the gene is located and the chromosomal position of the extracted NCS.  The following lines list pairs of locations which represent the start and end of all the exons.  These locations are relative to the start of the sequence in the ".fa" file. The set of sequences and exon annotation files are packaged as a compressed file that is available for download through a link on the results webpage (Fig. 3).  The result webpage also has a table of the gene or genes returned, for each genome that is currently available, along with a link to the results for each genes query of NCBI's entrez gene site (http://www.ncbi.nlm.nih.gov/entrez/query.fcgi?db=gene), a gene map view from UCSC's genome bioinformatics website (http://genome.ucsc.edu/), and further gene information at Ensembl's website (http://www.ensembl.org).

## 2.4.6   Updating

Both annotation systems, Refseq and Ensembl, are works in progress and with each releases, the annotations are improving in scope and accuracy.  New genome assemblies will also continue to be released for new and existing genomes.  As the sequence and annotation information which serve as the basis for this system are refined, the sequences generated by this system will improve.  Therefore, it is critical that the genomes and annotation information are kept up to date.  The NCSRS will be updated automatically on a weekly basis to ensure that the most recent information is always available.

**Figure 3** – An example webpage that display the results for the NCSRS

The sequences and annotation information written to the FA and EXON files respectively are bundled and zipped into a single file that can be accessed by the "Download Results!" link. A table with links to NCBI, UCSC genome browser and Ensembl for the gene and specific species is also provided.
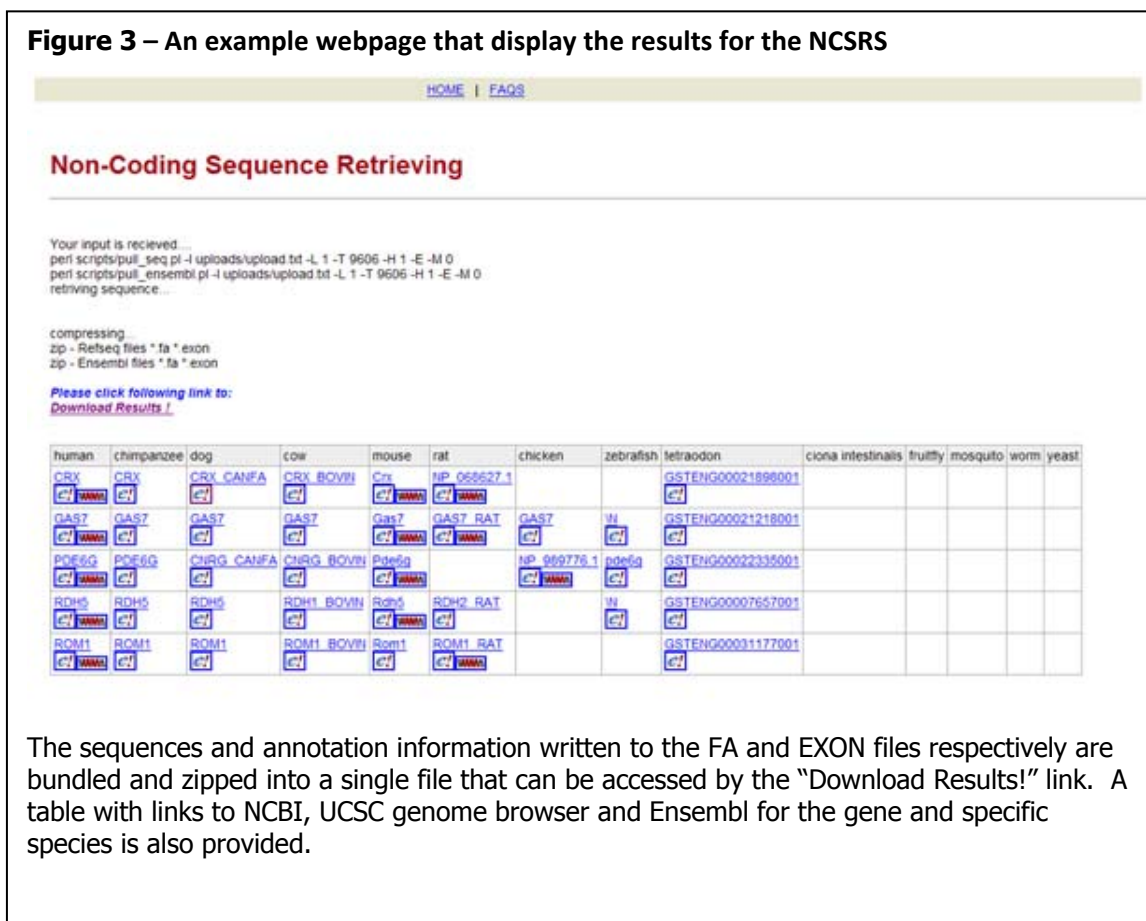
### 2.4.7 Hardware and Software

The NCSRS uses a single computer that acts as both the server and database. There is also a developmental computer which is used for updating, designing new applications, and troubleshooting. The main server ("cell.rutgers.edu") uses Dual Intel® Xeon® Processors at 3.0GHz, with 4 Gb RAM and 500 GB Hard Disk space and runs apache 2.2 as its web server. The scripts and programs used by NCSRS for building and accessing the databases are written predominantly in PHP and Perl.

### 2.4.8 Sequence Alignments and Scoring

Non-coding regions do not code for proteins and should not be under selective pressure to be conserved across evolutionary distant species unless they have some other important sequence

specific function. If for example, a non-coding region were to have an important functional role such as gene regulation it would be under selective pressure to be conserved. Therefore multiple genome alignments that identify highly conserved non-coding sequences should predict evolutionarily conserved gene regulatory elements (GRE) [3, 23, 44, 45]. The sequences and annotations of analyzed genes along with their homologs from the various other genomes depending on availability (possible genomes include: human, cow, dog, rat, opossum, chick, zebrafish, and tetradon) were retrieved using NCSRS [46]. These sequences consist of the upstream intergenic non-coding region, the coding region, intronic sequences and the downstream intergenic non-coding region. These sequences were then aligned using multi-LAGAN [18] to identify sequences of at least 75% identity over a 100 bp span. Annotations were submitted to multi-LAGAN along with their respective sequences to ensure that highly CRs of interest were non-coding regions. The percent identity and the length of the conserved sequence was used to calculate a score for each CR (score = percent identity + (length/60)). While the length of the CR may indicate that the high level of conservation may be more statistically significant the minimum required length of 100 bp was sufficient to ensure significance. A limit of 2 kB was implemented because wanted to isolate individual enhancers for study. Based on this scoring system the percent identity was more heavily weighted to ensure that shorter (i.e., 200 bp) very highly conserved sequences are not ranked below longer (i.e., 1000 bp) sequences with lower levels of conservation.

## 2.5    Results

### 2.5.1    NCSRS

We have developed a web-based sequence retrieval system that quickly and easily extracts non-coding sequences associated with a specific user defined gene set from a single and/or multiple genomes. The NCSRS efficiently delivers non-coding sequences for specified genes or gene sets using a user-friendly interface from a single site. This system eliminates the need to manually sift though genome sequences and look for annotation information from multiple sources. This

will help eliminate human errors as well as increase throughput for those investigating gene regulatory elements.  The system also allows the user to specify the gene or set of genes for retrieval while maintaining a simple user interface, enabling the user to apply their expert knowledge without having to spend a lot of time learning how to use the system.  Another option that is important for those seeking to elucidate functional NCS is masking.  Repetitive sequence elements found in the genome can cause sequence alignment algorithms to predict conserved elements that do not have gene regulatory function.  For this reason, there is an available option to mask sequences as repeated sequences to allow for alignment algorithms to ignore repeated sequences [1].

This system has great flexibility in its potential applications.  An important and unique feature is that if the user intends to apply this tool to a comparative genomics approach, the user can obtain the sequences for multiple species by simply selecting the "pull all orthologs" option.  Once the sequences are returned, a multiple sequence analysis can be performed for each set of homologous gene sequences.  The system's ability to return sequences from multiple genomes in one run greatly increases the efficiency and speed of the system.  Furthermore, it has been shown that increasing the number of genomes used in alignment analysis increases the signal-to-noise ratio and if specific genomes are selected carefully increase the likelihood of correctly predicting functionality [1].  If microarray data is the basis for analysis, the system's ability to handle multiple genes in a single query allows for the user to input multiple genes with similar expression patterns at one time to return the desired sequences.  It is even possible to combine the two approaches and obtain sequences for all homologous genes of a set of genes with similar expression profiles.  This allows for the system to be utilized by those who seek to learn more about genome-wide networks through their analysis [29].

**Table 4 - Predicted enhancers involved in motor neuron development and their scores listed by location relative to their respective gene.**

| DOWN STREAM | | | INTERNAL | | | UP STREAM | | |
|---|---|---|---|---|---|---|---|---|
| Gene name | Region | Score | Gene name | Region | Score | Gene name | Region | Score |
| Nkx2-2 | CR3 | 93.6 | Hoxc5 | CR4 | 103.7 | Nkx6-2 | CR2 | 90.8 |
| Hoxc6 | CR9 | 92.8 | Dbx2 | CR1 | 99.2 | Nkx6-2 | CR3 | 89.0 |
| Nkx2-2 | CR2 | 91.5 | Bcl11b | CR11 | 96.0 | Hoxc6 | CR8 | 88.8 |
| Hoxc8 | CR8 | 87.1 | Bcl11b | CR18 | 84.5 | Hoxc6 | CR2 | 88.6 |
| Nkx2-2 | CR1 | 84.6 | Bcl11b | CR13 | 83.5 | Hoxc6 | CR3 | 88.1 |
| Bcl11b | CR5 | 84.0 | Bcl11b | CR23 | 82.8 | Hoxc6 | CR5 | 87.4 |
| Hoxc8 | CR5 | 83.7 | Notch2 | CR11 | 78.7 | Hoxc6 | CR6 | 87.0 |
| Bcl11b | CR9 | 83.0 | Notch2 | CR4 | 75.0 | Hoxc6 | CR7 | 87.0 |
| Bcl11b | CR10 | 80.1 | | | | Dbx1 | CR9 | 85.6 |
| | | | | | | Nkx6-2 | CR1 | 85.5 |
| | | | | | | Hoxc6 | CR1 | 85.2 |
| | | | | | | Hoxc5 | CR2 | 84.3 |
| | | | | | | Dbx2 | CR4 | 82.5 |
| | | | | | | Hoxc6 | CR4 | 82.4 |
| | | | | | | Hoxc5 | CR1 | 81.8 |
| | | | | | | Runx3 | CR5 | 81.6 |
| | | | | | | Notch2 | CR1 | 80.4 |
| | | | | | | Hoxc8 | CR1 | 79.8 |
| | | | | | | Dbx2 | CR3 | 77.5 |

*2.5.2   Enhancer Candidate Database*

A literature search was performed in the selection of 89 developmental genes of which 53 are related to retinal and/or motor neuron cell development, for analysis.  The homologous non-coding sequences of inter/intragenic regions flanking these genes were retrieved using NCSRS. These sequences were aligned using the multiple pairwise sequence alignments tool LAGAN to identify CR.  The resulting 1053 CRs from these alignments was then annotated and ranked using a simple scoring method that compared the level of sequence identity and the length of the CR to help determine which regions were the most likely to contain functional gene regulatory elements.  A database of these results was compiled and formatted to be accessed locally using a standard web browser.  Through this analysis 502 CRs, with a score of at least 75, have been

**Table 5 - Predicted enhancers involved in retinal development and their scores listed by location relative to their respective gene**

| down stream | | | internal | | | up stream | | |
|---|---|---|---|---|---|---|---|---|
| *Gene name* | *ID* | *Score* | *Gene name* | *Region* | *Score* | *Gene name* | *Region* | *Score* |
| Irx3 | CR7 | 85.1 | Pax6 | CR8 | 93.7 | Olig2 | CR7 | 100.1 |
| Irx3 | CR6 | 80.5 | Pax6 | CR6 | 91.0 | Olig2 | CR10 | 92.4 |
| Otx2 | CR3-5 | 76.1 | Pax6 | CR11 | 90.2 | Olig2 | CR6 | 87.9 |
| | | | Notch1 | CR4 | 88.4 | Rpgrip1 | CR1 | 85.2 |
| | | | Kiaa1411 | CR1 | 88.4 | Notch1 | CR1 | 81.1 |
| | | | Notch1 | CR2 | 86.9 | Neurod1 | CR2 | 80.7 |
| | | | Nrl | CR3 | 85.7 | Rho | CR2 | 75.7 |
| | | | Otx2 | CR19 | 80.9 | Otx2 | CR13 | 75.4 |
| | | | Notch1 | CR3 | 74.4 | Rho | CR1 | 75.1 |
| | | | | | | Otx2 | CR14 | 75.0 |
| | | | | | | Rho | CR3 | 42.9 |



**Figure 4 – A well characterized known downstream enhancer element successfully predicted for the Otx2 gene**
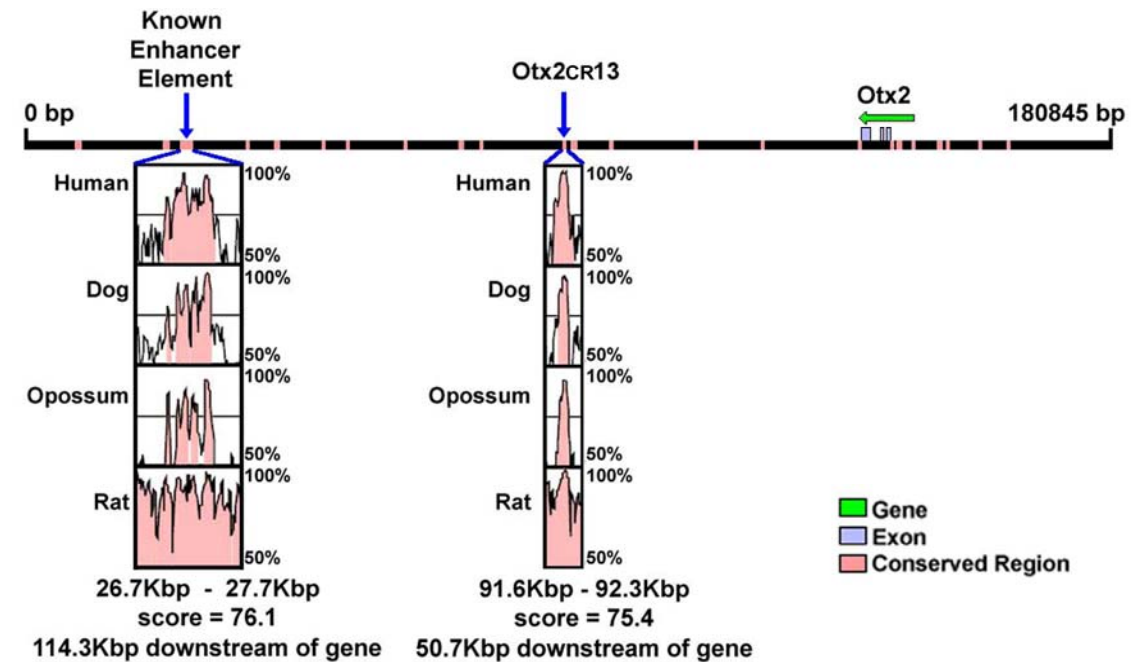
Each alignment corresponds to the same region of the mouse genome. The percent identity of the alignment is between 50% and 100%. Any conserved regions with at least 75% identity are shaded in pink.

**Figure 5 - An example from the enhancer candidate database showing the alignment and data from the first 10 kbp of the Hoxc8 entry**
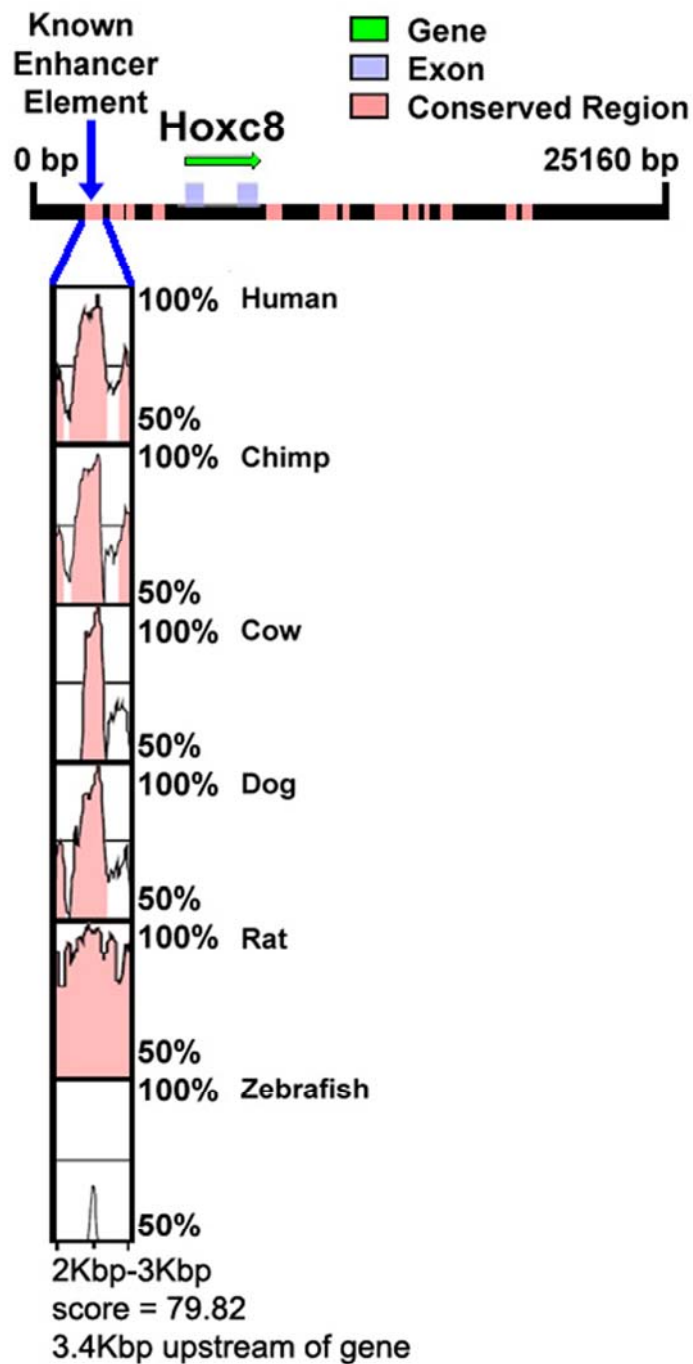
Each entry includes a graph of the alignments and the data from the alignments including the chromosomal positions and level of conservation. The mouse genome is used as the baseline genome for each pair-wise alignment. The x-axis represents the location with respect to the start of the mouse sequence. The y-axis ranges from 50% to 100% identity for each alignment. The blue regions are exons and pink regions have at least 75% identity between the mouse baseline sequence and the comparison sequence.

identified from 89 different genes as enhancer candidates (Table 4. and Table 5). Of the 58

enhancer candidates identified using this computational method; three have been previously

identified as enhancer elements [45-49]. The successful prediction of RhoCR3, Otx2CR3-5 [46,

47] (Fig. 4), and Hoxc8CR1 [50] (Fig. 5) as enhancers shows that the use of multiple pair-wise

alignments of distantly related homologs was successful at identifying sequences containing

enhancer elements. The known enhancers for Rho, Otx2, and Hoxc8 score 42.9, 76.1 and 79.8

respectively with this system. Given that there are over 500 predicted enhancer candidates with

higher scores, there is significant potential for the discovery of novel enhancers using this

method. The database allows for the user to easily navigate or search for alignment results of a

gene of interest based on gene name, ensemble id, or gene ontology. The sequence of every

CR, the graph of each alignment, and the statistics of the alignments (strand orientation,

chromosomal position, level of conservation, genomes used) are all available on this database.

For example the link for Hoxc8 returns the results shown in Figure 6.



**Figure 6 – A well characterized known early enhancer for the Hoxc8 gene**

Alignments were able to successfully predict as CR1, a well known enhancer (Wang, et al. 2004) of the Hoxc8 gene as shown in Figure 3. Each alignment corresponds to the same region of the mouse genome. The percent identity of the alignment is between 50% and 100%. Any conserved regions with at least 75% identity are shaded in pink.
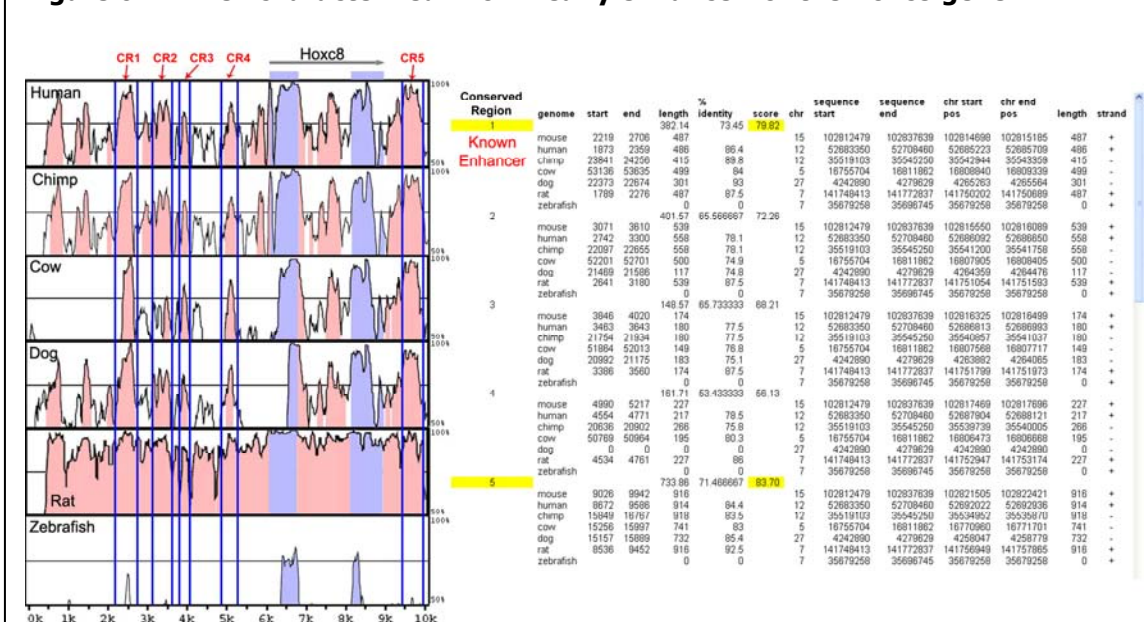
## 2.6    Discussion

NCSRS combines a number of available genomic resources (a total of over 70 Gb sequences) and applies them to the specific task of identifying and retrieving non-coding sequences in an up to date web based application that is easy to use and requires no maintenance by the user.  The unique features of this tool will be very helpful for those studying gene regulatory elements that exist in non-coding regions.  We have incorporated NCSRS into the workflow of analyzing non-coding sequences using a multi-sequence alignment algorithm and identified highly conserved regions [14, 17-19, 38, 39] to increase the speed and accuracy of this analysis by automating the workload involved in searching and retrieving sequences and eliminated the human error that commonly occurs during such tedious repetitive tasks.  A scoring system was implemented to rank each CR according to the likelihood of functionality using statistics associated with sequence identity and length of CRs.  Using this scoring system a database was created that combined all the alignments results obtained, the sequences of CRs, gene ontology of the associated gene.  This database was then formatted into a user friendly interface.  This database will serve as the basis for directing experimental work that will seek to verify the enhancer function of conserved elements and provide a theoretically basis for regulatory function and therefore increase overall efficiency.

**CHAPTER 3    ANALYSIS OF RETINAL CELL DEVELOPMENT IN CHICK EMBRYO BY**

**IMMUNOHISTOCHEMISTRY AND *IN OVO* ELECTROPORATION**

**TECHNIQUES**

## 3.1    Prologue

The embryonic chick model has been established as an important tool in the study of development.  Among its benefits are its relative ease and lower cost of use.  By combining alternative transcript plasmids with *in ovo* electroporation methods this system has become a powerful tool capable of overexpression, knockdown, and reporter gene experiments.  Reporter gene experiments in particular can resolve the spatio-temporal regulation of gene expression of enhancers.  However, conventional *in ovo* electroporation methods lack some critical capabilities when it comes to the study of enhancers.  For example, while earlier time points of development are easier to study in the chick, transient transfections of the retina resulting from electroporation at these early stages only lasts a few days and is not able to label all the major retinal cell types.  In order to analyze spatio-temporal regulation the ability to examine all the major cell types throughout extended periods of development would necessary.  *In vivo* electroporation of postnatal day 0 mice has its own weaknesses as it is able to study only late born cells.  Therefore we have modified the electroporation method in the chick to target the retina at embryonic day 3-4 (E3-4) in an attempt to extend the duration of transfection.  We were able to successfully obtain prolonged transfection of the retina (beyond E18) and able to label all the retinal cell types.  These new method further increases the value of the chick model and establishes it as a powerful complement to *in vivo* methods for studying retinal development and enhancer function.

## 3.2    Abstract

Retinal cell development has been extensively investigated; however, the current knowledge of dynamic morphological and molecular changes is not yet complete.

This study was aimed at revealing the dynamic morphological and molecular changes in retinal cell development during the embryonic stages using a new method of targeted retinal injection, *in ovo* electroporation, and immunohistochemistry techniques. A plasmid DNA that expresses the green fluorescent protein (GFP) as a marker was delivered into the sub-retinal space to transfect the chick retinal stem/progenitor cells at embryonic day 3 (E3) or E4 with the aid of pulses of electric current. The transfected retinal tissues were analyzed at various stages during chick development from near the start of neurogenesis at E4 to near the end of neurogenesis at E18. The expression of GFP allowed for clear visualization of cell morphologies and retinal laminar locations for the indication of retinal cell identity. Immunohistochemistry using cell type-specific markers (e.g., Visinin, Xap-1, Lim1+2, Pkc$\alpha$, NeuN, Pax6, Brn3a, Vimentin, etc.) allowed further confirmation of retinal cell types. The composition of retinal cell types was then determined over time by counting the number of GFP-expressing cells observed with morphological characteristics specific to the various retinal cell types.

Conventional methods using injection and electroporation at E1.5 have had difficulty maintaining transfection for extended periods and labeling late born neurons. This new method of retinal injection and electroporation at E3 – E4 allows the visualization of all retinal cell types, including the late-born neurons, e.g., bipolar cells at a level of single cells. Based on data collected from analyses of cell morphology, laminar locations in the retina, immunohistochemistry, and cell counts of GFP-expressing cells, the time-line and dynamic morphological and molecular changes of retinal cell development were determined. These data provides a more complete account of retinal cell development and serves as a reference for future investigations in retinal development and diseases.

## 3.3    Introduction

*3.3.1    Retina Development*

The vertebrate retina contains seven major cell types, six neuronal and one glial. These cells are derived from multipotent retinal stem/progenitor cells. Previous studies have revealed that the development of the vertebrate retina is a conserved process of cell genesis with the following order of cell birth: ganglion cells, horizontal cells, cone photoreceptors, amacrine cells, bipolar cells, rod photoreceptors, and Müller glia. Similar to other parts of the central nervous system, the retina contains a layered structure with photoreceptors (rods and cones) located in the outer nuclear layer (ONL), short projection neurons (bipolar cells) and local circuit neurons (horizontal and amacrine cells) in the inner nuclear layer (INL), and long projection neuron (ganglion cells) in the ganglion cell layer (GCL) [47]. During early stages of retinal development, the outer neuroblastic layer (ONBL) consists almost entirely of mitotic progenitor cells, while newborn neurons (mostly consisting of amacrine and ganglion cells) reside in the inner neuroblastic layer (INBL). The position of mitotic progenitors within the ONBL varies depending upon their progress through the cell cycle, with S phase cells found on the vitreal side of the ONBL near the border with the INBL and M-phase cells found on the scleral side of the ONBL abutting the retinal pigment epithelium [48, 49].

An important aspect in understanding retinal anatomy and function is to trace the development of various cell types during embryonic stages. Although significant progress has been made, a complete developmental process underlying retinal cell differentiation during embryonic development is still lacking. Previous studies have provided information of retinal development on the rate of progression through the cell cycle [50-53], the mode of cell divisions, e.g., symmetrical versus asymmetrical [54-61], cell migration [62], and the order of cell birth [48, 49, 63-66]. A cell is born when it withdraws from the cell cycle and undergoes differentiation. These studies are mainly based on DNA synthesis analysis using tritiated-thymidine ($^3$H-TdR) or 5'-bromon-2'deoxy-uridine (BrdU) labeling methods. $^3$H-TdR or BrdU is incorporated into the genomic DNA of stem/progenitor cells during the S-phase of cell cycle before they withdraw from the cell cycle and undergo differentiation. These methods are particularly useful in determining

the start and end of cell genesis. In addition, using cell type-specific markers, the onset of differentiation can be determined by identifying the earliest time points for which immunolabeling is observed [67, 68]. However, a major drawback to these methods is that DNA replication occurs in the nuclei thus only the nuclei of the labeled cells are observed. In addition, many cell type-specific markers also label only the nuclei of cells. Cell type-specific markers may be able to distinguish between cellular subtypes but fail to reveal the subtle morphological differences that determine key functional differences. Furthermore, morphological changes were observed in previous studies of retinal degenerative diseases caused by mutation or loss of gene function [69, 70]. Thus, important morphological information of the whole cell that accompanies molecular changes is critical to understanding normal development and disease states.

Here, we report studies aimed at revealing dynamic morphological and molecular changes in retinal cell development of the chick embryo. A plasmid DNA that expresses green fluorescent protein (GFP) as a marker was directly delivered into the embryonic chick subretinal space and electric pulses were applied to facilitate DNA uptake by retinal stem/progenitor cells using a rapid and convenient *in ovo* electroporation technique. With this technique, GFP-expressing plasmids were efficiently transfected into retinal stem/progenitor cells with little damage to the chick embryos. GFP expression has been found in all cell types of the developing chick retina and allowed for clear visualization of cell morphologies. Immunohistochemistry was performed to further confirm retinal cell types with specific molecular markers. By tracking the cell counts of various cell types based on cellular morphology, laminar location, and molecular markers, the composition of various cell types of the developing retina at different stages has been determined. Thus, this study provides more complete insight into both the morphological and molecular changes during chick embryonic retinal development.

## 3.4    Materials and Methods

### 3.4.1    Chicken Embryos

**Figure 7 – In ovo electroporation method targeting E3-E4 chicken retina**
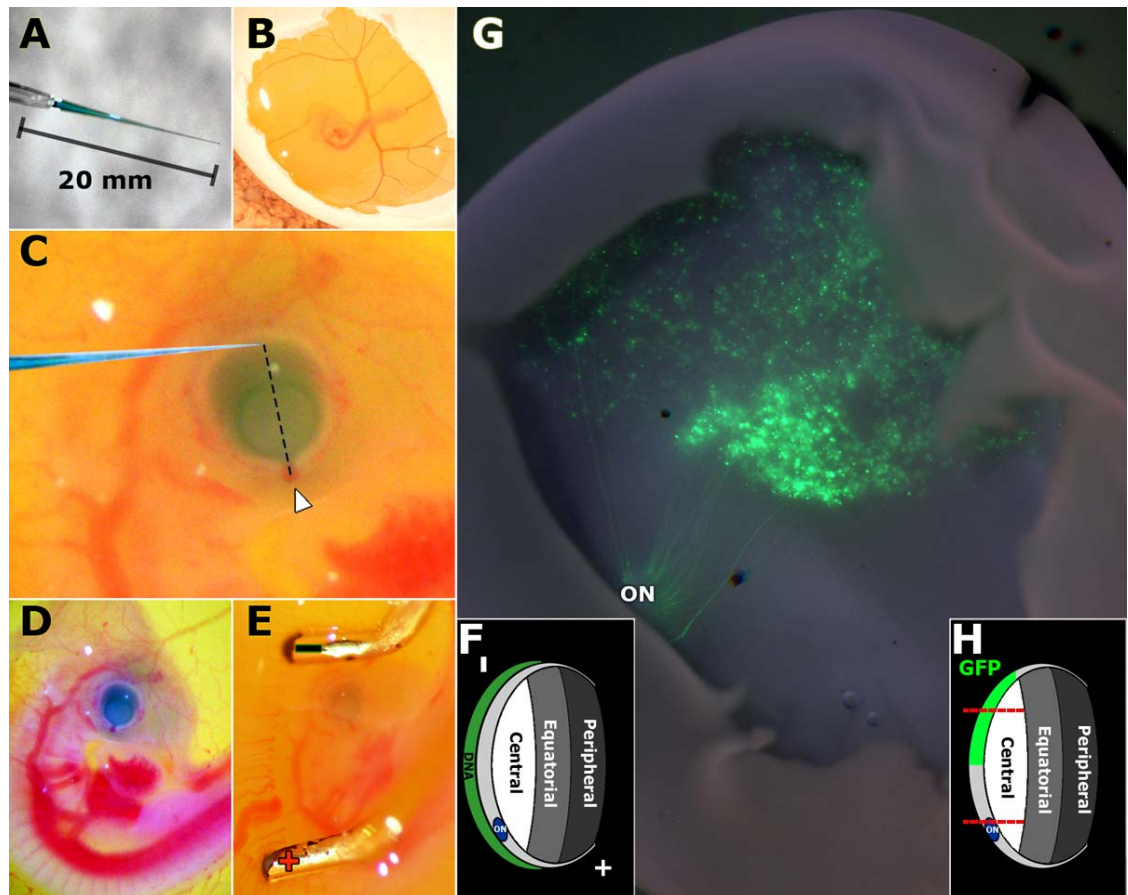
Glass capillary tubes were pulled to fabricate needles with a tip opening at 0.1 µm in diameter and a 20 mm taper (A). The needle is loaded with DNA/0.025% fast green solution. Eggs were rotated to release the embryo and the shells were sterilized by wiping with 70% ethanol then windowed using forceps (B). The trajectory of the needle approached the eye from behind the head, toward the beak, and tangent to the retina surface (C). The outermost region of the retina opposite of the main bundle of blood vessels entering the eye (arrowhead, C) was targeted for injection. Successful injection was verified by observing that the subretinal space of the eye was filled with DNA/fast green solution (D). Electroporation was performed with the negative electrode placed above the head of the embryo and deeper in the albumin than the eye. The positive electrode was placed below the spine and on the surface of the albumin (E). Electroporation using this orientation drives the DNA in the subretinal space toward the positive electrode and into the retinal progenitor cells (F). The egg was sealed and incubated until tissue harvest at desired time points. Electroporated retinal tissues were then checked for GFP expression. A wholemount image of a retina with GFP expression at E14 (G) shows axons of ganglion neurons originating in the central retina and extending to the optic nerve (ON). Approximately 1/3 of the central retina was transfected with decreasing levels of GFP expression in more peripheral regions (G, H). Using this method of electroporation at E3-4, the central region of the developing chick retina (area between the two red dotted lines in H) was consistently and stably transfected with CAG-GFP throughout *in ovo* developmental stages.

Fertilized pathogen-free (SPF) white leghorn chicken (*Gallus domesticus*) eggs were obtained from Sunrise Farms (Catskill, NY). These eggs were incubated at 37.5°C and 60% humidity (GQF manufacturing, Savannah, GA) for 88-92 hours (~3 - 4 days) to obtain embryos that are at the developmental stage HH21. Stages of the chick embryo were determined according to Hamburger and Hamilton [71]. All of the animal experiments were approved by the Institutional Animal Care and Facilities Committee at Rutgers University.

### 3.4.2   In Ovo *Electroporation*

Microinjections were performed using a micropipette needle made from pulled glass capillary tubes with a tip opening at about 0.1 μm in diameter and a 20 mm taper (Fig. 7A).  Needles with larger tips have difficulty piercing the vitelline membrane while smaller tips have difficulty loading and delivering the DNA solution. The taper minimizes damage to the embryo while maintaining enough structural integrity in the needle for handling microinjections. The needles were attached to a 0.1 ml Hamilton Gastight 1710 syringe (Reno, NV) mounted on a WPI M3301-M3 micromanipulator (Sarasota, FL). The needle was loaded with a mixture of DNA (CAG-GFP; 1.5 μl with concentration ranging 3.0-6.0 μg/μl) and 0.025% fast green dye (0.2 μl) to allow visualization of the injection (Fig. 7A). This amount of DNA loaded per needle is enough for about a dozen egg injections. The condition and location of the embryo can be seen by candling the egg.  The vitelline membrane of the egg was freed from the inner membrane with gentle rotation. The egg was placed with the larger end up and windowed (Fig. 7B) as previously described [72] with minor changes being that the windowing was placed immediately above the air cell and albumen was not removed. The vitelline membrane was not removed as the needle was sharp enough to easily pierce through this membrane. Injection into the vitreous humor allows DNA to diffuse away from the retina and therefore requires more DNA to be injected or results in poor transfection. To maximize the travel of the needle point in the subretinal space, the needle should approach the eye such that it is almost at a tangent to the section of the retina targeted for transfection (Fig. 7). To prevent critical damage to the brain or heart the needle was

inserted by approaching from caudal to rostral direction towards the beak. The targeted injection site was along the dorsal region of the eye contralateral to the main bundle of blood vessels entering the eye (Arrowhead in Fig. 7C). When injecting at this angle, continually injecting the DNA while slowly retracting the needle allows visualization of the DNA/fast green solution either filling the subretinal space or the vitreous humor. Injection of the subretinal space can be verified by the filling of DNA/fast green solution following the outline of the eye (Fig. 7D) rather than diffusing away or filling into the middle of the eye. Every attempt was made to consistently target the same injection site for each embryo to minimize variation from retina to retina. The injection site was electroporated using a BTX ECM 830 electroporation system (Harvard Apparatus, MA). The BTX Genetrodes (model 514) were spaced 3-5 mm apart. The electrodes were placed in parallel so that the developing eye was situated between the electrodes (Fig. 7E). Electroporation with the electrodes placed in this manner transported DNA located in the subretinal space towards the positive electrode and into the retina (Fig. 7F) resulting in approximately half of the central retina being transfected (Fig. 7G-H). The electroporation settings were 5 pulses of 15 mV for 50 ms with 950 ms pauses between each pulse. After electroporation, the window on the operated eggs was sealed with clear scotch tape, and the egg was returned to the incubator.

### 3.4.3   Tissue Processing and Sectioning

Chick embryos were harvested at various times after injection, electroporation, and placed in cold 1x PBS (Phosphate buffered saline, Fischer Scientific). Retinas were dissected at embryonic day 8 (E8) or older stages, while retinas younger than E8 were left intact in the embryo to minimize damage. Tissues were fixed by immersion in 4% paraformaldahyde (in 1x PBS) for 90 minutes at 4°C and then infiltrated overnight in 30% sucrose (in 1x PBS).

For retinas at E8 and older, the peripheral regions of the cryoprotected retinas were removed to ensure only the central region of the retina was included for analysis. The face of a clock will be used to describe the regions of the whole retina. The retina was oriented such that from an

**Figure 8 – Diagram depicting the central region of the retina included for analysis**
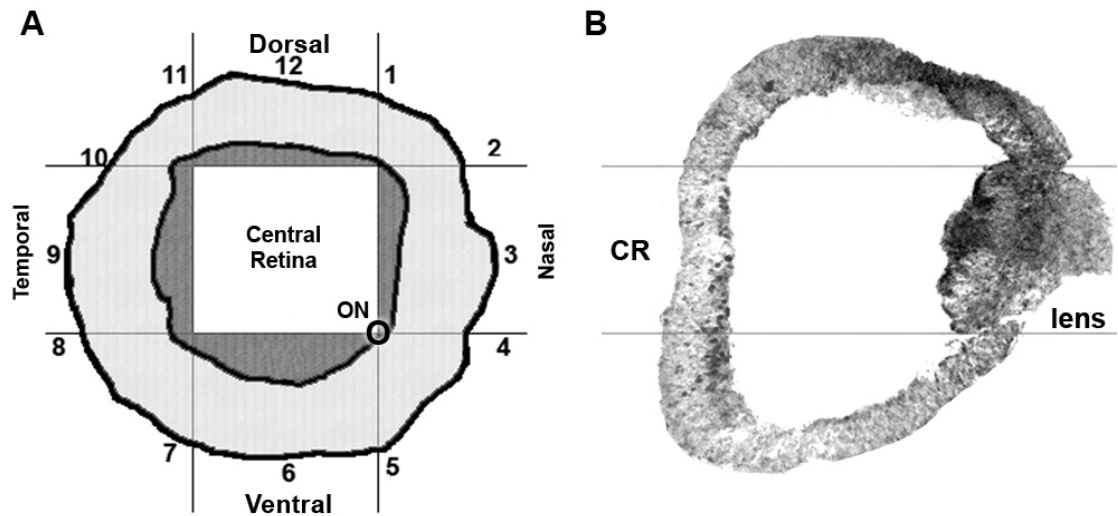


A. For retinas at E8 and older, the peripheral regions of the cryoprotected retinas were removed to ensure only the central region of the retina was included for analysis.  The face of a clock will be used to describe the regions of the whole retina.  The retina was oriented such that from an overhead view the dorsal region was oriented at 12 o'clock and the ventral region to the 6 o'clock position.  Once situated in this orientation, a first cut is made from the 2 o'clock to the 10 o'clock positions.  A second cut is made from the 4 o'clock to the 8 o'clock positions (red dotted lines in Fig. 3H).  A third cut from the 1 o'clock to the 5 o'clock positions; and a final cut from the 7 o'clock to the 11 o'clock positions. The resulting square piece in the center is designated as central retina region.
B. For retinas younger than E8, the whole eye was sectioned along with the head at the horizontal plane. The central region (CR) of the retina was defined as the area that opposite to the lens.

overhead view the dorsal region was oriented at 12 o'clock and the ventral region to the 6 o'clock position.  Once situated in this orientation, a first cut is made from the 2 o'clock to the 10 o'clock positions.  A second cut is made from the 4 o'clock to the 8 o'clock positions (red dotted lines in Fig. 7H).  A third cut from the 1 o'clock to the 5 o'clock positions; and a final cut from the 7 o'clock to the 11 o'clock positions. The resulting square piece in the center is designated as central retina region (Fig. 8A).  In most of the cases, this central square region contained the vast majority of GFP expressing cells.

For retinas younger than E8, the whole eye was sectioned along with the head at the horizontal plane (Fig. 8B).  Only sections of the retina that contain the lens were used to ensure that the

central region (CR) of the retina is analyzed. The central region of the retina was defined as the area that opposite to the lens as shown in the figure 8B.

For embryos injected with CAG-GFP, successful transfection (Fig. 7G) was verified by examining the retinas under a fluorescent dissection microscope, Leica MZ16FA (Leica Microsystems, Germany) before embedding and sectioning. Tissues were embedded in OCT (Electron Microscopy Sciences, Hatfield, PA) and stored at -80°C until ready for sectioning. Retina tissues sections at 10-15 µm were cut using a cryostat (Thermo 0620E), mounted on Superfrost slides (Fisher Scientific) and air-dried. Immunohistochemistry was performed immediately afterwards.



**Figure 9 – Negative control for antibody staining**
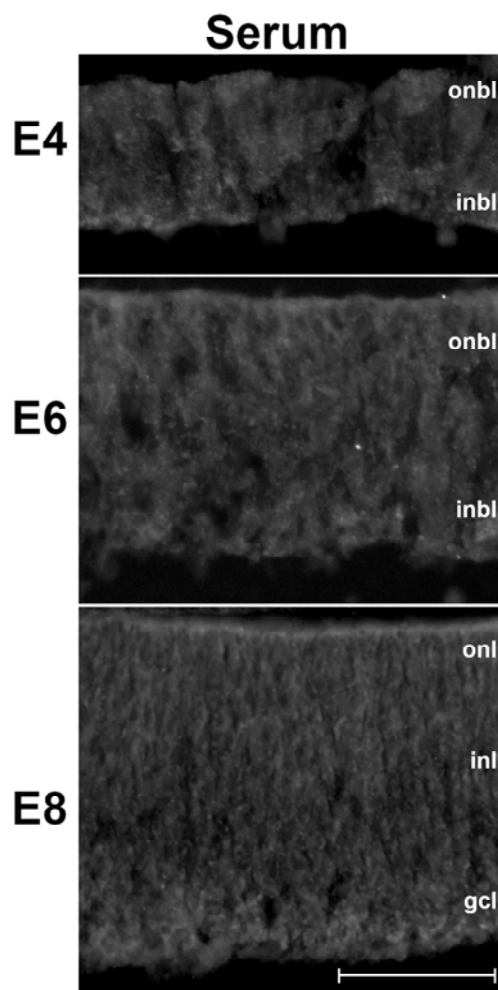
Retina tissue from chicken embryos were harvested at E4, E6, and E8, sectioned, and treated with serum and secondary antibody.

ONBL  - outer neuroblastic layer
INBL   - inner neuroblastic layer
ONL    - outer nuclear layer
INL     - inner nuclear layer
GCL    - ganglion cell layer

Scale bar = 40 µm.

### 3.4.4   Immunohistochemistry

For immunofluorescence staining, tissue sections were fixed in 4% paraformaldahyde for 5 minutes and washed in PBS. Blocking solution (175 µl; 0.05% Triton X-100, 10% goat serum, 3% BSA in PBS) was applied on the slide and incubated for 30 minutes at room temperature followed by washing in PBS. Primary antibodies XAP-1 [73] (100 µl of 1:10 dilution; DSHB, IA), Xap-2 [73] (100 µl of 1:100 dilution; DSHB, IA), Visinin [74] (100 µl of 1:10 dilution; DSHB, IA), rho-4D2 [75] (100 µl of 1:100 dilution; R.S. Molday, University of British Columbia), Lim1/2 (4F2) [76-78] (100 µl of 1:10 dilution; DSHB, IA), Vimentin (H5) [79] (100 µl of 1:10 dilution; DSHB, IA), Pax6 [80] (100 µl of 1:100 dilution; DSHB, IA), Pkc$\alpha$ (100 µl of 1:400 dilution; Santa Cruz Biotechnology Inc, CA), Recoverin [81] (100 µl of 1:100 dilution; Millipore, MA),  Brn3a [67] (100 µl of 1:100 dilution; Millipore, MA), or NeuN [82] (100 µl of 1:1000 dilution; Millipore, MA) were applied to the wet slides. Incubation was carried out in a humidified box on a slow rocker at 4°C overnight. As a negative control, serum and secondary antibodies were applied but no primary antibody was added to the staining solution (Fig. 9). Slides were then washed with PBST (0.1% Tween-20 in 1x PBS) and Cy3-conjugated secondary antibodies (150 µl of 1:300 dilution; Jackson ImmunoResearch, West Grove, PA) was applied. After 30 min incubation at room temperature with gentle rocking, the slides were washed with PBST then cover slipped.  All washes were 5 min and repeated 3 times unless specified otherwise.

### 3.4.5   Imaging

Microscopy and imaging analysis were performed using an upright fluorescence microscope (Zeiss Axio Imager A1) with a monochrome digital camera Axiocam MRM (Zeiss, Germany). Images of GFP-expressing cells and secondary antibody Cy3 labeled cells were taken separately using FITC and DsRed filters, respectively. Imaging of Vimentin-labeled retinas was performed using a confocal microscope (Nikon Eclipse 80i) with a monochrome digital camera Nikon D-Eclipse C1 (Nikon, Japan).  Images of GFP-expressing cells and secondary antibody Cy3 labeled cells were taken separately using 488nm and 543nm wavelengths, respectively.  Images of Cy3

and GFP channels were then overlaid using Adobe Photoshop CS to create pseudo-colored double-labeled images.

### 3.4.6    Cell Counts

Retinas electroporated with CAG-GFP were harvested as described above at each time point (E10, E12, E14, E16, and E18).  At least three retinas from each time point with confirmed GFP expression were then sectioned and imaged.  To avoid counting cells that span multiple sections more than once, only one image was counted from any given set of 5 serial sections.

### 3.4.7    Determining Cell Type for Cell Counts

In the majority of cases, the morphology and laminar location criteria are sufficient for the determination of a cell type. For photoreceptor cells, Visinin labeling starts in the ONBL as early as E4 and is restricted in the ONL from E8 and beyond.  Furthermore no other cell types other than Müller cells were observed through antibody staining to be in the ONL.  However, the cell body of Müller cells is generally not located in the ONL.  Therefore, all cells restricted to only the ONL were identified as photoreceptors.  Horizontal cells, in the time frame of E10-E18, were shown to be strictly restricted to the outermost region of the INL by Lim1/2 staining.  The morphologies as revealed by GFP show round cell bodies with the majority of processes extending toward the OPL.  Therefore cells with round cell bodies found in the outermost region of the INL that have processes generally restricted to the OPL were identified as horizontal cells. Ganglion cells were labeled with Brn3a and found only in the GCL between E10 and E18.  The cell bodies of ganglion cells are also known to be round and among the largest of all the cell types in the retina.  Therefore, cells located in the GCL with round cell bodies were identified as ganglion cells.  There may be a small number of displaced amacrine cells that were counted as ganglion cells; however, we believe that this should not significantly affect the accuracy of our cell counts. Bipolar cells were known to be restricted to the INL (which was confirmed by staining with Pkc$\alpha$) with round cell bodies and two distinct bi-directional processes.  The greatest difficulty in

identifying this cell type was in distinguishing bipolar cells from Müller cells and migratory cells as each of these cell types could have their cell bodies in the INL. We have found, however, that even in their progenitor state after E10 they do have subtle but distinct morphological characteristics that allow for them to be distinguished from each other. Müller glial cells have multiple branching processes extending from the cell body. Migratory cells have elongated cell bodies and are usually clustered with other migratory cells. Bipolar cells have rounder cell bodies and at most 2 processes which, if present, are transversely opposed from each other. Pax6 is known to label horizontal, amacrine, and ganglion cells. NeuN is known to label amacrine and ganglion cells. Comparing the staining patterns of these two markers between E10 and E18 shows that the inner half of the INL and the GCL are consistently labeled by both markers. Based on these staining patterns amacrine cells were determined to be restricted to the inner half of the INL between E10 and E18. Amacrine cells also have round cell bodies with processes that are directed toward the IPL. Therefore, all cells with round cell bodies, processes directed toward the IPL, and located in the inner half of the INL were counted as amacrine cells. In all cases characteristic laminar location of cell types narrows down the potential identity of the cell, while morphological characteristics which became increasingly distinguished over time increased the accuracy of cell type identification.

*3.4.8   Statistical Analysis*

For each cell type, its percentage of the total GFP-expressing cells was calculated each retina. The data was then plotted and the standard error of the mean (SEM) was calculated for each set of retinas of the same time point using Prism version 4.03 (GraphPad Software, Inc. La Jolla, CA).

**3.5    Results**

The chick embryo has been the most advanced model organism suitable for experimental embryology and for studying the development of higher vertebrates [83]. In this report, the chick

retina was used for the study of cellular morphological and molecular changes during embryonic development using *in ovo* electroporation and immunohistochemistry techniques. All results reported in this study were focused on the central portion of the developing chick retina.

*3.5.1    Onset and Expression Pattern of Retinal Cell Type-Specific Markers*

To determine the onset of the marker expression of various cell types in the embryonic chick retina, cell type-specific antibodies, e.g., Xap-1 [73] and Visinin [74] for photoreceptors; Lim1/2 for horizontal cells [84-88], and Brn3a for ganglion cells [67, 89-91] were used to stain retina sections harvested at various time points during retinal development from E4 to E18 (Fig. 10). The development of the many retinal cell types could be tracked independently by observing the onset and dynamic changes in expression patterns of these cell type-specific markers as detected by immunofluorescence labeling.

The expression of a photoreceptor marker Xap-1 [73, 92-94] was observed only in the outer segment of the outer nuclear layer (ONL), and its expression starts sometime between E8 and E10 (Fig. 10A-D). The intensity of Xap-1 labeling continued to increase through E18 (Fig. 10E-F). The expression of another photoreceptor marker Visinin, a retinal photoreceptor protein which is believed to be cone specific [68, 74, 95], starts around E4 (Fig. 10G) which is much earlier than Xap-1 expression. At E6, its expression had increased in intensity but individual cells were still distinguishable (Fig. 10H). Visinin labeling then increased in intensity and the labeled cells composed a significant portion of the ONL at E8 (Fig. 10I). The intensity of Visinin labeling continued to increase and peaked at about E10 (Fig. 10J) when it was expressed in the entire ONL. In later stages (Fig. 10K-L), Visinin labeling continued to remain strong in the outer segment but diminished in the inner segment of the ONL. The differences in expression may suggest that Xap-1 and Visinin coincide with different stages of photoreceptor development.

**Figure 10 – The expression of chick retinal cell-type specific marker determined by immunohistochemistry method**
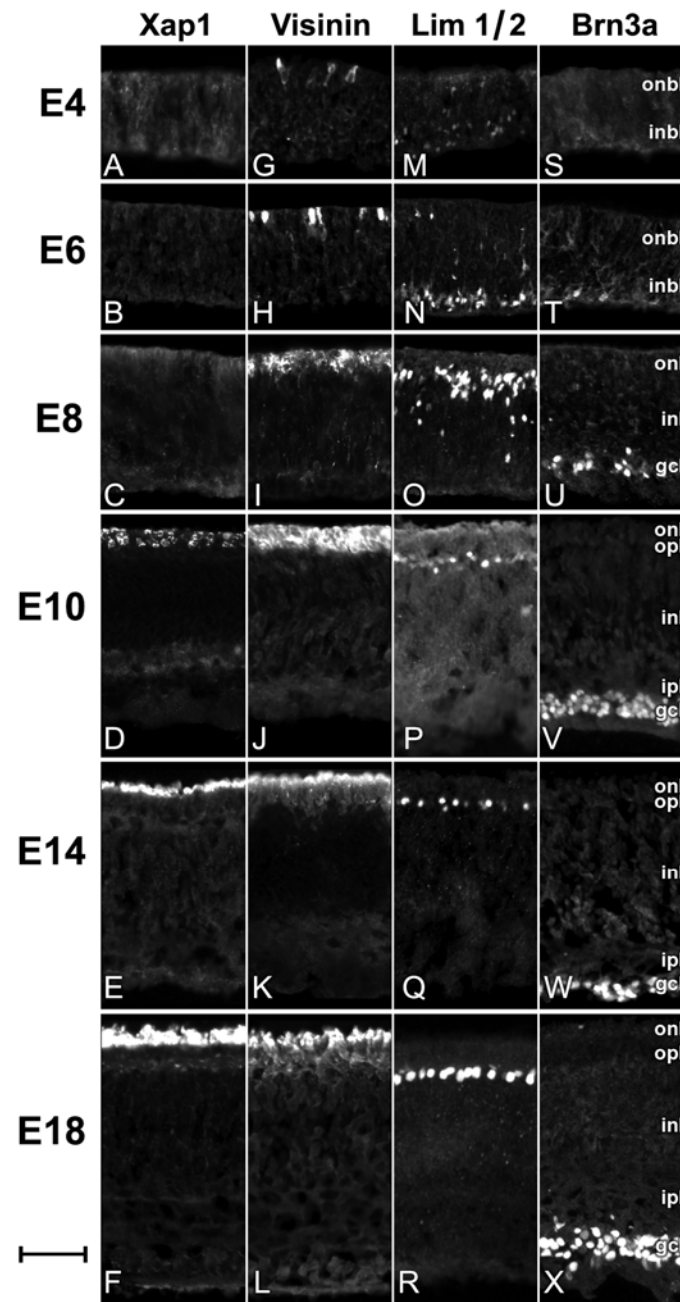
Retina tissue from chicken embryos were harvested at various time points during development, sectioned, and stained with retinal cell type specific antibodies Xap-1 (A-F), Visinin (G-L), Lim1+2 (M-R), and Brn3a (S-X). Xap-1 is known to selectively stain only the outer segments of photoreceptor cells, while Visinin is known to selectively stain the entire photoreceptor cells. Lim1+2 labels horizontal cells exclusively. Brn3a selectively labels as subset of ganglion cells. By staining retinas at various times during development, the onset of each cell type specific marker and their changes through out development were observed. ONBL, outer neuroblastic layer; INBL, inner neuroblastic layer; ONL, outer nuclear layer; INL, inner nuclear layer; GCL, ganglion cell layer. Scale bar = 40 μm.

Other photoreceptor specific antibodies against Recoverin and Xap-2 did not show

immunoreactivity in any of the stages (E4-E18) of chicken retina tested (results not shown).

The expression of a horizontal cell marker Lim1/2 [84-87] started in the retinal neural epithelium

around E4 (Fig. 10M). A few Lim1/2 positive cells were observed in the inner neuroblastic layer

(INBL) where newborn neurons appear. At E6, (Fig. 10N) the majority of Lim1/2 positive cells

are near the edge of INBL, while some are migrating through the inner nuclear layer (INL)

towards the outer portion of the INL where mature horizontal cells reside. Migration of Lim1/2

positive cells continues through E8 (Fig. 10O) and nears completion by E10 (Fig. 10P) when cells

begin to align as a single layer adjacent to the ONL where synaptic endings of the photoreceptor

cells located. By E14 (Fig. 10Q), the majority of Lim1/2 positive cells align on the outer portion

of the INL. The space between the Lim1/2 positive horizontal cells were almost evenly spaced.

This pattern was observed in all the later stages during chick retinal development. The horizontal

cells at E18 (Fig. 10R) appear to be more mature than previous stages with larger and more oval

cell bodies and are better aligned to the outer most region of the INL.

The expression of a retinal ganglion cell marker Brn3a [67, 90, 91] was observed to start in the

GCL around E6 (Fig. 10T). Brn3a positive cells were organized into 3-4 cell layers in thickness by

E8. Brn3a expression increased significantly in both intensity and in number of cells that

expressed Brn3a at E8 (Fig. 10U), and its expression was restricted to the GCL. This increasing

trend of staining continued at E10 (Fig. 10V) when the majority of cells in the GCL were Brn3a-

positive. The borders of the INL, GCL, and the optic nerve fiber layer were clearly defined by

Brn3a expression. From E10 (Fig. 10V) to E18 (Fig. 10X), Brn3a expression remained constant.

The expression pattern of Brn3a at E21 (data not shown) was similar to that observed from E10

to E18.

In addition, the expression pattern of neuronal specific markers, e.g., Pax6 and NeuN, and a

radial glial cell/progenitor cell marker, Vimentin, were also examined (Fig. 11). Vimentin is an

intermediate filament protein that is responsible for maintaining cell integrity [96] and is used to

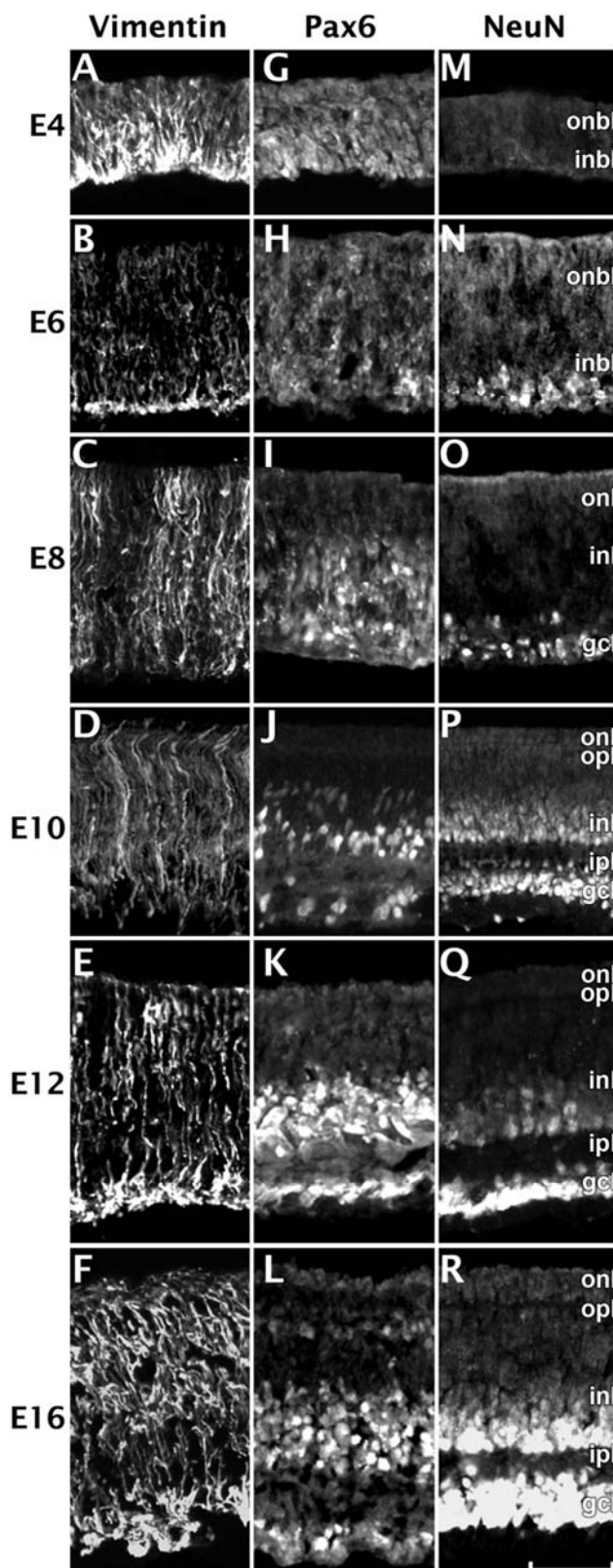**Figure 11 – Expression of glial and neuronal markers in the developing retina.**

Retina tissue from chicken embryos were harvested at various time points during development, sectioned, and stained with antibodies Vimentin (A-F), Pax6 (G-L), and NeuN (M-R). While these markers are not cell-type specific, they label proteins that are involved in retina development. Vimentin labels radial glia in retina at early embryonic stages and Müller glia cells in retina at late embryonic stages. The Vimentin labeling resulted in the characteristic striated banding that stretched across the layers of the retina. Pax6 labels horizontal, amacrine, and ganglion cells. NeuN is a marker of early neurons and in the retina labels amacrine and ganglion cells.

ONBL - outer neuroblastic layer
INBL - inner neuroblastic layer
ONL - outer nuclear layer
INL - inner nuclear layer
GCL - ganglion cell layer

Scale bar = 40 μm.

label radial glial cell/progenitor cell and Müller glia cells in the chicken retina [41, 42]. Müller glia cells span all the retinal layers, possess radially polarized processes, and have arborizations called "end-feet" toward the GCL [97]. Vimentin positive cells were found in all stages tested (Fig. 11A-F) and were not seen to be specific to any cell layer. The Vimentin positive cells showed distinct striated banding throughout all layers. Immunoreactivity was usually most intense in the GCL, which is likely caused by the high concentration of processes in the end-feet of radial/Müller glial cells. Pax6 is a nuclear marker for ganglion, amacrine, and progenitor cells that is required for multipotency in retinal cells [98]. Pax6 was first detected at E4 in a small number of progenitor cells located in the INBL (Fig. 11G). Over the next few days, the overall number of cells detected increased and by E8 (Fig. 11I) included cells located in the INL. At E10 (Fig. 11J), ganglion cells, amacrine cells, and migrating cells are all clearly labeled by Pax6. By E16 (Fig. 11l), as found in previous reports, some horizontal cells are also labeled but labeling is weaker than that found in amacrine or ganglion cells [99]. NeuN is a neuron-specific nuclear protein marker [82]. The onset of immunoreactivity of this marker indicates terminal differentiation of the neuron. Previously, use of NeuN antibodies in the mouse retina showed immunoreactivity in the GCL and to a much lesser extent in the INL [82]. In the chicken retina, NeuN labeling is seen in the INBL beginning at E6 (Fig. 11N), and in the INL at E8 (Fig. 11O). By E10 (Fig. 11P), the INL and GCL can be very easily distinguished by the NeuN expression pattern. The intensity of NeuN expression was more intense and widespread in the GCL than the INL at E12 (Fig. 11Q). By E16 (Fig. 11R), the entire GCL and amacrine cell portion of the INL were labeled by NeuN.

### 3.5.2 *Morphological Analysis of Developing Chick Retina Using* In Ovo *Electroporation Technique*

To reveal the dynamic morphological changes during retinal cell development, the *in vivo* electroporation method was adapted and optimized for chick retinal study (*in ovo* electroporation) [72, 100]. Although *in ovo* electroporation is a widely used technique for the study of neural development, the technique has been mainly performed in neural tube injection

**Figure 12 – Tracking development and migration of chicken embryonic retina cells using GFP labeling by in ovo electroporation technique**
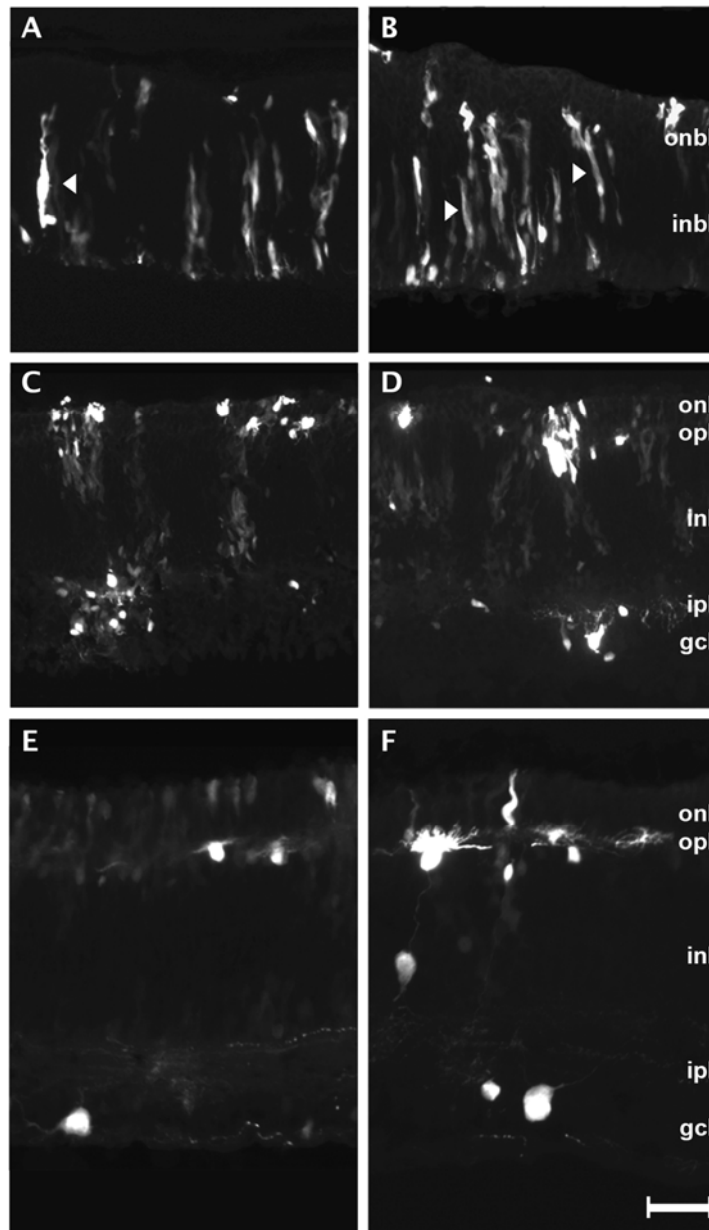


Chicken embryos are injected with CAG-GFP and electroporated at embryonic day 4 (E4). GFP expression is observed during early stages of development, E7-E8 (A-B). These cells are elongated which is characteristics of cell migration. The cells span the whole width of the neural epithelial layer. In subsequent stages E9-E10 (C-D), cell layers begin to show distinct boundaries and cells begin to settle into their final layers. Cells also take on a rounder morphology and begin to extend their processes. The appearance of well defined cell type specific morphologies begins around E12 (E). Processes are more clearly visible and help to form clearly visible boundaries between layers. The clearest and most distinct and definitive cell morphologies are observed in GFP–expressing cells at E18 (F) (see Figure 4). ONBL, outer neuroblastic layer; INBL, inner neuroblastic layer; ONL, outer nuclear layer; INL, inner nuclear layer; GCL, ganglion cell layer. Scale bar = 50 μm.

and electroporation. Targeted retinal injection and *in ovo* electroporation at E3-4 is considered a novel method for the study of chick retinal development (See Methods section for technical detail). The CAG-GFP DNA was injected into the sub-retinal space of E3-E4 chicken embryo (Fig. 7A-D) followed by electroporation (Fig. 7E-F). The plasmid DNA construct, CAG-GFP, was previously shown to produce ubiquitous GFP expression without altering normal development [100]. *In ovo* electroporation of CAG-GFP consistently resulted in the highest level of GFP expression in the central retina with decreasing GFP expression in more peripheral regions of the retina. Few if any cells in the peripheral retina were observed to express GFP (Fig. 7G-H). Immunohistochemistry revealed GFP expression in retinal stem/progenitor cells during early chick embryonic retinal development (Fig. 12A-B), and all six differentiated major cell types during late chick embryonic retinal development (Fig. 12C-F and Fig. 13). Visualization of cytoplasmic GFP expression revealed the cross section morphology of cell bodies and processes (axons and dendrites). The location of individual cells with respect to the retina layers was also clearly visible (Figs. 12-13). The determination of a specific retinal cell type was based on the cellular morphology, laminar location, and expression of molecular markers of the cell.

By observing development between E7 (Fig. 12A) and E18 (Fig. 12F), the changes in laminar location were determined. During early development, the vast majority of cells are still proliferating and some have started their migration process (Fig. 12A-B). Migratory cells have elongated cell bodies that can span both the ONBL and INBL (arrows in Fig. 12A-B). Once migratory cells reach their respective laminar locations (Fig. 12C-E), they terminally differentiate into specific mature cell types. Differentiated cells (Fig. 12F and Fig. 13) have cell type-specific morphologies and more defined axons and dendrites. At E18, the characteristic morphologies and locations of all six major cell types found in a more developed retina were clearly seen through GFP labeling (Fig. 13). Visualization of GFP allows for the cell bodies as well as the processes (axons and dendrites) to be observed in great detail. Photoreceptor cells (Fig. 13A) are localized exclusively in the ONL and have elongated cell bodies like rods and cones that span the ONL. Their synaptic bodies are found along the boundary of the ONL and the outer plexiform layer

**Figure 13 – Characteristic morphology of various cell types in chicken retina at E18 with GFP labeling by in ovo electroporation technique**
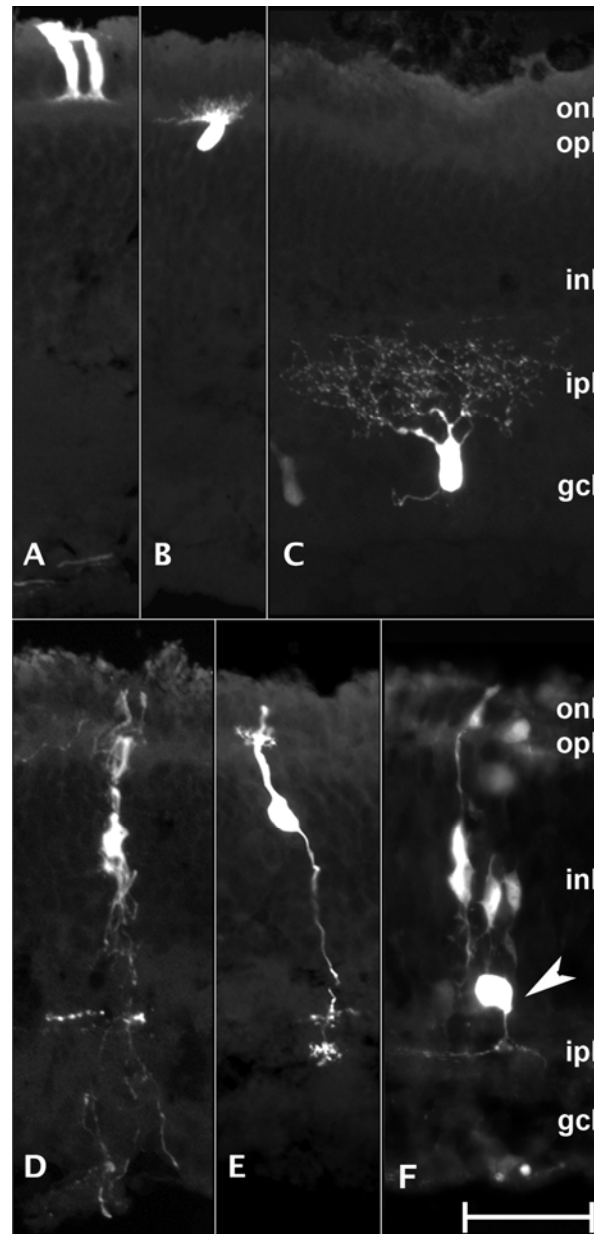


Expression of GFP is observed in all six cell types found in retina tissue through E18. Visualizing GFP expression at this stage shows cells localized in distinct layers and each of the cell type specific morphologies. Photoreceptors (A) have a cylindrical shape and are located in the outer nuclear layer (ONL). Horizontal cells (B) have processes located at the boundary of the inner nuclear layer (INL) and ONL with their cell bodies in the INL. Ganglion cells (C) are located in the GCL and have processes which mostly point toward the INL. Müller glial cells (D) span the entire retina with their cell bodies in the INL. Bipolar cells (E) have two distinct processes one that extends from the cell body in the INL to the ganglion cell layer (GCL) and the other to the ONL. Amacrine cells (F) have cell bodies in the INL and have processes that extent toward the GCL. OPL, outer plexiform layer; IPL, inner plexiform layer; Scale bar = 20 μm.

(OPL). Horizontal cells (Fig. 13B) have oval cell bodies found in the region of the INL closest to the OPL. Their cell bodies align in a single cell layer with dendrites in the OPL that reach towards the ONL. Ganglion cells (Fig. 13C) are located in the GCL, their cell bodies seem to be the largest in all cell types in the retina. Their dendrites reach towards the INL and the inner plexiform layer (IPL). The size of their cell bodies and the number of dendrites can greatly vary depending on their subtype. Morphologically distinct cells (cell body size, process number, and process direction) were observed in the GCL at E18 (Fig. 12F, Fig. 13C). Based on the laminar location of these observed cells and the known morphological diversity among ganglion cells, it is concluded that multiple subtypes of ganglion cells were able to be labeled by this technique. Müller glial cells (Fig. 13D) are the principal glial cells of the retina. They form architectural support structures stretching radially across the thickness of the retina and are the limits of the retina at the outer and inner limiting membrane, respectively. They are also the least frequently found cell type in the retina accounting only about 2.7% of the total cell population in the mature mouse retina [48, 49]. Their cell bodies sit in the INL and project thick and thin processes irregularly in either direction to the outer limiting membrane and the inner limiting membrane. Bipolar cells (Fig. 13E) have their cell bodies in the INL and reach from the ONL to the ganglion cell layer (GCL) but have only a single axon and dendrite in opposite directions. Amacrine cells (Fig. 13F) have round cell bodies found in the INL and have a single axon that extends to the inner plexiform layer (IPL) where it then branches out to contact the cells in GCL [101].

### 3.5.3   *Confirming Retinal Cell Type of GFP-Expressing Cells by Immunohistochemistry*

To confirm that cell types were correctly identified by cellular morphology and laminar location and to determine composition of cell types of GFP-expressing cells, immunohistochemistry was performed on E10, E14 and E18 retina sections with CAG-GFP transfection. The cell types were determined using the GFP images (green cells in Fig. 14,) and confirmed by overlaying the images with cell type specific antibody labeling (red cells in Fig. 14,). At E10, a large number of GFP-expressing cells have immature cell morphology (Fig. 14 A, D, G, J, M, P). However, each

cell type has a defined laminar location with cell migration close to completion. The laminar

location combined with the morphological characteristics (described above and shown in Fig. 13)

allowed for the cell types to be quite accurately determined. The identification of each retinal cell

type at E14 (Fig. 14 B, E, H, K, N, Q) became even easier as the vast majority of cells have

already completed migration, and their characteristic morphologies, such as axons and dendrites,

were more clearly defined. GFP-expressing cells were stained with a cell type specific antibody,

e.g., Xap-1 (Fig. 14A-C) or Visinin (Fig. 14D-F) for photoreceptors, Lim1/2 (Fig. 14G-I) for

horizontal cells, Pkc$\alpha$ (Fig. 14J-L) for bipolar cells, Brn3a (Fig. 14M-O) for ganglion cells, and

Vimentin (Fig. 14P-R) for Müller glial cells. For photoreceptor cells, immunolabeling showed that

Visinin and Xap-1 staining was only found in ONL where photoreceptor cells reside. The results

of antibody labeling with GFP-expressing cells showed that cells in ONL were positive with Visinin

and Xap-1 staining. Visinin and Xap-1 labeled all photoreceptors in the ONL beginning at E10.

Xap-1 did not label the whole photoreceptor cell but as previously reported only the outer

segment [73]. Xap-1 has been shown to be expressed by photoreceptors exclusively under

conditions in which the outer segment membranes are properly assembled [92]. The fact that

Xap-1 expression was observed in the outer most region of the outer nuclear layer (ONL)

beginning at E8 and E10 may indicate that this outer most region stained by Xap-1 is the

developing outer segment of the ONL. Our results further indicate that development of the outer

segment of the ONL may start as early as E8. Each of the cells labeled with photoreceptor

specific markers were correctly identified based on laminar location and cellular morphology (Fig.

14A-F). Lim1/2 staining was only found in the outer region of the INL. GFP-expressing cells in

the outer border of the INL, with round cell bodies, showed Lim1/2 staining at each of the

developmental stages. Pkc$\alpha$ has been shown to specifically label bipolar cells in the developing

retina [102-104]. Pkc$\alpha$ labeling showed no staining at E10 (Fig. 14J). Staining at E14 (Fig. 14K)

showed labeled cells intermittently in the INL. Staining became more frequent and more intense

at E18 (Fig. 14L) in the INL where bipolar cells reside. Double labeling was first observed at E14
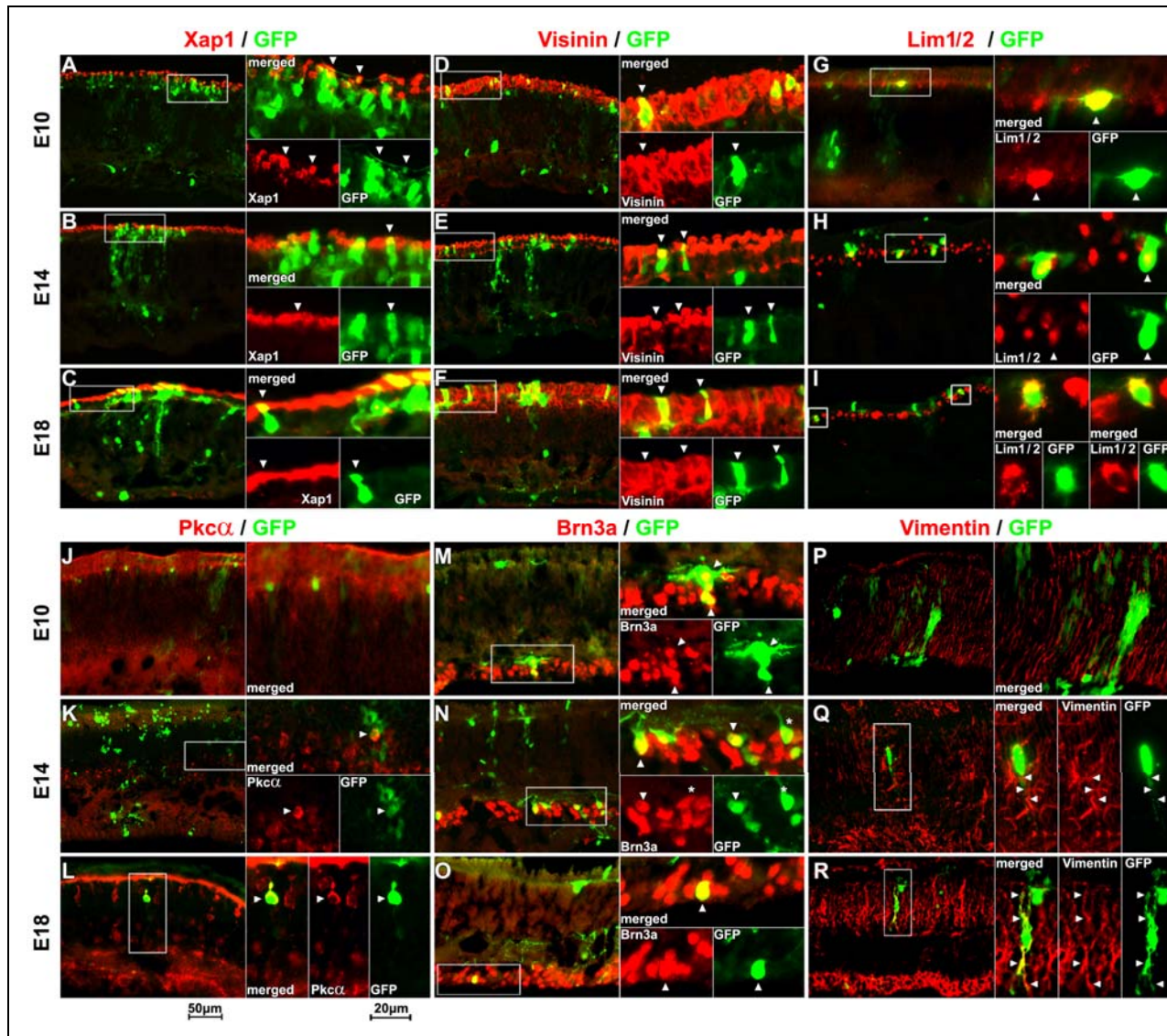
**Figure 14 – Determine retinal cell type of the GFP-expressing cells using immunohistochemistry method**

GFP-expressing retinal tissues at three developmental stages (E10, E14, and E18) were sectioned and stained with retinal cell type specific antibodies, e.g., Xap-1 (A-C) and Visinin (D-F) for photoreceptor cells, Lim1+2 for horizontal cells (G-I), Pkcα for bipolar cells (J-L), Brn3a for ganglion cells (M-O), and Vimentin for Müller glial cells (P-R). For each set of images (A-R) the entire retina cross section is shown to allow for the laminar location to be easily visualized. The image on the right shows a merged high magnification image and a pair of separate images showing the antibody staining and GFP fluorescence. The white-boxed region is shown in higher magnification on the right. Double labeled cells are indicated by arrowheads at higher power.

and became more frequent at E18.  Double labeled cells were only observed in the INL, showed round cell bodies, and characteristic processes were regularly observed at E18.  Brn3a staining was exclusively localized in GCL where ganglion cells reside.  A few GFP-expressing cells that showed ganglion cell-type specific characteristics were not labeled with Brn3a (Fig. 14N, marked with an asterisk). However, this finding does not exclude this cell from being a ganglion cell as Brn3a was shown to label the majority of but not all ganglion cells [101]. Labeling with Vimentin showed striated banding throughout all layers for all the various stages. Double labeling with GFP and Vimentin was not observed at E10 but migrating cells expressing GFP seemed to follow Vimentin labeled cells.  Double labeling was first seen at E14 (Fig. 14Q) and only in the processes of the cell (Fig. 14Q Q-R).  At all three stages, individual whole cell bodies were resolved by GFP labeling, as opposed to only the outer segment (Fig. 14A-C), entire layers (Fig. 14D-F), or only the nuclei (Fig. 13 and 14M-O) as resolved using antibody labeling.  The molecular identification of retinal cell types confirmed that the cell types of chick retina cells between E10 and E18 could be accurately determined based on cellular morphology and laminar location as revealed by GFP expression.

## 3.5.4    *Dynamic Changes in the Composition of GFP-Expressing Cell Types During Retinal Development*

To identify dynamic changes in the developing chicken retina, GFP-expressing cells were counted for each cell type from E10 to E18. At least three retinas with GFP expression were generated for each time point. The cell type of the GFP-expressing cells was determined, categorized, and counted. The percentage of each cell type among the entire population of GFP-expressing cells (composition of each retinal cell type) was calculated at each time point (Fig. 15). Cell types were determined based on their morphology, laminar location, and molecular marker. The cell counts showed a dramatic decrease in the number of migratory cells from E10 to E18 (Fig. 15). This finding indicates that the number of migrating cells decreased steadily as fewer migratory cells were being generated and more migratory cells differentiated during this time frame. By E18, the

**Figure 15 – Cellular composition at various stages during embryonic development of the chicken retina**
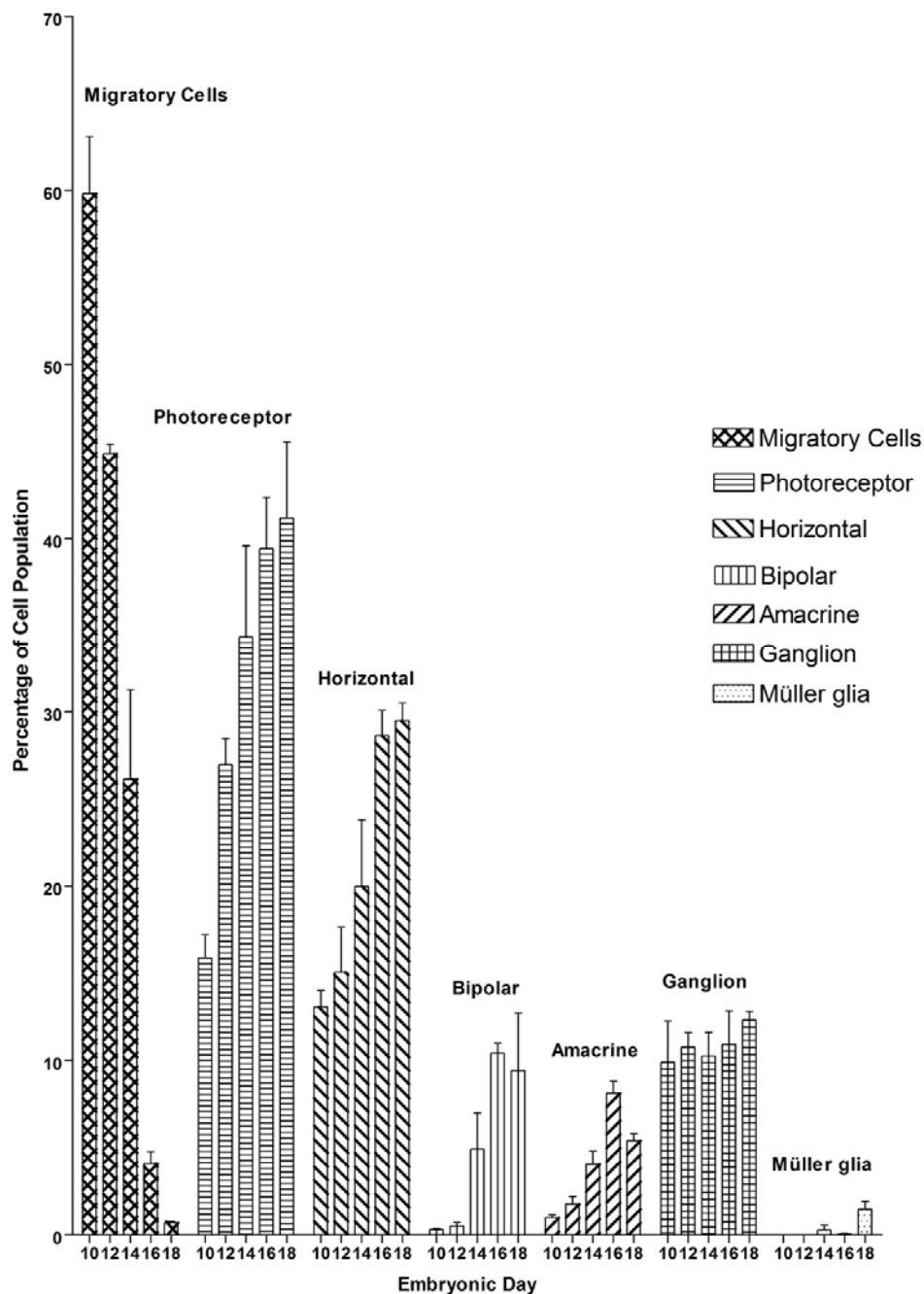


Three retina samples were collected every other day from E10 to E18. Retinal cells expressing GFP were categorized into one of seven cell types based on retinal laminar location, cellular morphology, and molecular marker. Cell counts of each cell type were used to determine the distribution of each cell type during development of the retina. The data shows that the number of ganglion cells remained fairly consistent throughout this time period. Photoreceptors and horizontal cells have a significant increase in population while the increase is less dramatic in bipolar and amacrine cells. As expected, with the increase in other cell types the number of migratory cells decreases.

percentage of migratory cells was less than 1%, suggesting that cell migration almost reached completion. The largest increases in differentiated cell types occurred at E12 for photoreceptors, E14 for horizontal cells, and E16 for bipolar cells and amacrine cells. Ganglion cells did not show significant changes during these time periods. Morphologically mature Müller glia cells were first seen around E14 but still remained in very small proportion at E18.

By E18, the composition of retinal cell types is approximately 41.2% photoreceptor, 29.5% horizontal, 9.4% bipolar, 5.4% amacrine, 12.3% ganglion, 1.5% Müller glia, and 0.7% migratory cells (Fig. 15).

## 3.6     Discussion

The timing of neurogenesis in the chicken retina was previously determined using [3H] tymidine autoradiographs by Prada et al. However, due to technical limitations, retinal cell development with dynamic morphological changes in relation to the changes in molecular markers was not fully determined.  To address these limitations, we have adopted existing *in ovo* electroporation capabilities to develop a new method of *in ovo* electroporation that can specifically target retinal progenitor cells (E3-E4) resulting in the ability to visualize all six major retina cell types at the single cell level.  Conventional methods (electroporation at E1.5) have difficulty labeling late-born neurons in the retina such as bipolar cells.  This new method adds important capacities to allow possible future studies where the precise cell morphology of retinal neurons is required.  It can also be applied to gain/loss of function studies where a gene of interest can be targeted to study normal development and/or disease of the retina.  In this study, we have tracked the morphological and molecular development of each of the cell types in the developing chick retina and determined the relative abundance of each cell type within the total population over a developmentally critical time frame, thereby providing new insights into retinal development.

*3.6.1    Photoreceptors*

Almost all vertebrate retinas have two morphological types of photoreceptors (rods and cones) that mediate dim-light, color vision and fine-detail detection [105]. Although autoradiographic studies fail to distinguish rods and cones in the chick retina [106, 107], ultrastructural studies using scanning electron microscopy confirmed that both rods and cones do exist [108]. However, photoreceptor percentages vary with species, cones being a majority in the chick retina, i.e., 86% cones versus 14% rods [109]. In this study, the earliest time we observed photoreceptor marker Visinin expression was at E4 (Fig. 10G-L), which is about two days earlier than it has previously been reported at E6 [68]. Since Visinin preferentially labels cone photoreceptors [74, 95], this suggests that cone photoreceptor development in chick begins early at about E4. For rods, antibodies against Rhodopsin and Recoverin were used to immunostain the developing chick retina from E6-E18. No labeling was detected with Rhodopsin and Recoverin antibodies (data not shown), suggesting that either the rod-specific antibodies were not specific to chick rods due to differences in species, or that chick rods differentiate after the examined time-frame (E6-E18).

### 3.6.2   Horizontal and Amacrine Cells

For the study of retinal horizontal cell and amacrine cell development, we used the antibody against Lim1/2 [78, 84-86], Pax6 [80, 99] and NeuN [110, 111]. Transcription factor Lim1/2 is essential for horizontal cell development and its laminar position in the retina [84, 86, 112-115]. Pax6 homeobox gene is among the earliest genes expressed in the eye primordia and plays crucial roles in retina development [88, 98, 112]. It is also known to be an amacrine cell marker in later stages (after E8) during embryonic retinal development [99]. By E10, the cells labeled with Pax6 show three distinct layers consisting of migratory cells, amacrine cells, and ganglion cells which can be distinguished using their laminar location. Staining with Lim1/2 antibody showed that horizontal cells began differentiation as early as E4. Lim1/2 staining showed that the vast majority of Lim1/2 expressing horizontal cells completed migration to the outer region of the INL by E10. The dynamic expression pattern of Lim1/2 during horizontal cell differentiation in

our study (Fig. 10M-R) is consistent with previously observations as the differentiating horizontal cells undergo bi-directional interkinetic nuclear migration [86, 113]. Pax6 also weakly labeled some horizontal cells after E14. The staining patterns of Lim1/2 and Pax6 indicate that amacrine and horizontal cells can be distinguished from each other using laminar location information beginning at E10. The DNA-binding, neuron-specific protein NeuN, is present in most neuronal cell types of vertebrates. NeuN stained ganglion cells but labeled very few cells in the INL in adult human retinas [111] and in E12.5 mice [82]. We found that NeuN was strongly expressed in the majority of cells in both the GCL and INL, which is quite different from the one reported in mouse and human. It has been reported that NeuN staining in the adult chick retina is weaker in the INL than in the GCL [116]. This observation suggests that in amacrine cells, NeuN may be most highly expressed shortly after or during differentiation.

### 3.6.3    Bipolar Cells

In cell counts of GFP-expressing cells, bipolar cells were not observed with significant frequency until E14. Immunolabeling with Pkc$\alpha$ antibody was also not observed until E14 supporting the cell count data. Birth-dating studies of bipolar cells in rodents showed bipolar cells are among the later born cell types being born postnatally along with Müller cells [48, 49]. Consistent with previous studies [107], the bipolar cells in chick retina have been shown to be the last cell type to become postmitotic.

### 3.6.4    Ganglion Cells

Previous studies show that ganglion cells are produced over the period from E2 to E9 [107], with all cells initially born in the ventricular zone, followed by immediate differentiation and migration into the future ganglion cell layer [117]. The development of ganglion cells begins at the central region of the developing retina, gradually spreading to the peripheral region as a wave-like front [118]. The composition of GFP-expressing ganglion cells in this report did not show significant changes from E10 to E18, indicating that they were generated before E10. Brn3a is a

transcription factor that regulates the development, morphology, and function of retinal ganglion cells [67, 90, 91]. It is expressed specifically in the nuclei of cells that have finished migration and begun differentiating into ganglion cells. Previous findings have shown that Brn3a is expressed as early at E4.5 in the chick retina [89]. Combining the early onset of Brn3a antibody labeling and the consistent percentage of ganglion cells from E10 to E18, it is believed that the vast majority of ganglion cells complete development before E10. This observation is consistent with previous finding that all ganglion cells are born before E9 [107]. Since multiple subtypes of ganglion cells express GFP after *in ovo* electroporation of CAG-GFP, the fact that most of the GFP-expressing ganglion cells were also Brn3a-positive (Figs. 4.1 & 14A-F) indicates that Brn3a labels the majority of ganglion cell subtypes but not all ganglion cells [101].

### 3.6.5   *Müller Glial Cells*

The birth dating of Müller glial cells has been controversial. Electron microscopic studies indicate they are born early [119, 120]. However, results from $^3$H-TdR or BrdU labeling indicate that Müller glia cells are labeled only after injections were preformed at late stages during retina development. The immunolabeling results (Fig. 11 A-F) show that there is constant expression of Vimentin throughout the embryonic period from E4 to E18.  Vimentin is known to label radial glial cells, a type of progenitor cell in the central nervous system [79, 121, 122]. Müller glial cells are the only glial cell type in the retina suggesting that Vimentin-positive cells are either mature Müller glial cells in mature retina or retinal stem/progenitor cells in early embryonic retinal development. Radial glial cells or progenitors exist throughout the embryonic stages of retinal development and serve as structurally stabilizing scaffolds [123] and as cell migration guides [124]. GFP-expressing Müller glial cells with mature morphology (Fig. 13D, Fig. 14P-R) could only be observed after E14.  The proportion of GFP-expressing Müller glial cells was small, e.g., under 0.3%, at E14 and gradually increased to only 1.5% at E18 (Fig. 14R and Fig. 15). The low number of morphologically mature Müller glia cells expressing GFP observed between E10 and E18 could be because 1) they are naturally scarce during this time frame or 2) the late birth of

Müller glial cells makes them less compatible for labeling using the *in ovo* electroporation method described.  First, the early onset and high frequency of immunoreactivity of Vimentin suggests that a significant number of radial glial/progenitor cells are born as early as E4 and maintain a significant population throughout the examined time frame. Second, if their late birth results in the lack of Müller glial cell labeling, bipolar cells should also be rarely seen, since bipolar cells are born around the same time as Müller glial cells.  Third, GFP labeling at E18 showed similar proportions of retina cell population for ganglion cells (which are born early) and bipolar cell (which are born late).  Therefore, we believe that the time of birth should not significantly affect the proportion of cell types observed at E18 unless those cells are not yet born.  For these reasons, we conclude that the lack of cells with mature Müller glia morphology is not due to their inherent rarity or incompatibility with *in ovo* electroporation but that the majority of Müller glial cells do not exhibit morphological maturity before E18.  A possible explanation for the lack of morphologically mature Müller glia are that they may maintain their progenitor cell (radial glia) state for a significant period of time (at least 14 days) after being born. If this is the case, then the cells that serve as scaffolds and migration guides for the migratory neurons in the retina are radial glia cells/progenitor cells in early embryonic development.  In the mouse retina, the majority of Müller glia cells reach morphological maturity late in development [48, 49].   It is known that many of Müller glial cells continue to differentiate postnatally in the chick retina [125]. Alternatively, the staining of Vimentin in microglia cells and proliferating precursor cells is another consideration [126]. Microglia cells are known to be present in small numbers during the development of retina and involved in clearing dying cells that are part of the normal developmental processes [127, 128]. However, labeling of Vimentin in microglia cells may only slightly contribute to the early onset and high frequency of Vimentin labeling.   Furthermore, neither microglia nor proliferating precursor cells can account for the radially polarized staining pattern.

## 3.7    Conclusion

In conclusion, this study reveals the dynamic morphological and molecular changes during a critical period of chick embryonic retinal development. We have demonstrated that *in ovo* electroporation with CAG-GFP combined with immunohistochemistry is a very efficient technique for tracing cell proliferation, migration and differentiation processes during retinal development. We were able to label and identify all the major cell types of the developing retina based on their morphology and laminar location of the GFP-expressing cells. The cellular identities of GFP-expressing cells were further confirmed by immunostaining using cell type-specific antibodies. Although, this method has been used in study of retinal development, sustained reporter gene expression in the developing chicken retina has not reported to last for more than a few days [129, 130]. *In ovo* electroporation at HH10 (~E2) targeting the optic vesicle is able to transfect cells that develop to form the eye.  However, these cells have a very high turnover at this time and this method is not specific for retina cells.  It may be that the high cell turnover rate prevents sustained stable expression.   By E3, the embryo is developed enough that the major structures of the eye are all formed but young enough that the majority of cells in the retina are still retinal stem cells. The vitelline membrane is thin enough to allow for microinjection and the blood vessels are spaced far enough from the eye to allow for electroporation of the embryo without damaging the vessels.  As demonstrated in this study, we were able to optimize the *in ovo* electroporation method to successfully transfect the retinal stem/progenitor cells at E3-E4 resulting in all 6 major retinal cell types to express GFP through E18. Furthermore, GFP expression clearly shows the cellular morphology that other techniques, e.g., $^3$H-TdR or BrdU labeling methods, failed to provide. In rodents, retinas injected and electroporated with CAG-GFP at postnatal day 0 (P0) did not show GFP expression in early born cells, e.g., horizontal or ganglion cells, which indicates that the generation of these two types are completed by P0 in rodents.  By visualizing the morphology of whole individual cells in the developing retina, characterization of each cell type can be performed dynamically during normal development, disease states, or specific over-expression of critical retinal genes. As shown in our results this method can be easily combined with well established immunohistochemistry methods which will

be helpful for the understanding of the molecular events that accompany morphological changes during normal development or disease of the retina. This method can be applied to study the development and growth of the axons and dendrites of particular cell types or applied to produce sustained over-expression/knockdown of developmental genes or detection of gene regulatory in the chick retina using alternative DNA constructs.

## CHAPTER 4     EXPERIMENTAL VERIFICATION OF NOTCH1 ENHANCERS

### 4.1     Prologue

The methods developed and results obtained in the previous chapters were combined to allow for the work presented in this chapter.  Sequence analysis was performed to identify the specific non-coding regions with the greatest likelihood of possessing enhancer function and novel methods were designed and implemented in an effort to experimentally verify computationally predicted results.  A novel reporter gene based enhancer function assay, described in this chapter, was developed for the experimental verification and spatio-temporal characterization of enhancer function.  The novel *in ovo* method developed in combination with existing *in vivo* methods allowed for a fast and effective method for screening for enhancer function.  Two novel enhancers were discovered and detailed analysis of their function was performed.  For one of the enhancers the enhancer function in the retina was found to be conserved between the mouse and chick. The experimental verification of these novel enhancers of Notch1 was a culmination of the union between computational analysis and wet lab experimentation.

### 4.2     Abstract

Blindness affects about 45 million people worldwide and 3.3 million Americans age over 40, and these figures are projected to reach 76 million and 5.5 million respectively by the year 2020 [131]. One approach that is attractive to treat blindness or low vision is the use of retinal stem/progenitor cell-based therapy to repopulate the photoreceptors and other cells that are lost. The retinal progenitor cells can divide and differentiate into various retinal cell types, including photoreceptors. Müller cells are glial cells found in the vertebrate retina, which normally serve the function of glial cells in other regions of the central nervous system (CNS). However, following retinopathy and injury to the retina, Müller glial cells undergo dedifferentiation into multipotent progenitor cells [132, 133].

Notch and its signaling pathway has been extensively studied and shown to play an important role in normal development, e.g., cell fate determination [134], proliferation [135], and differentiation [136]. In particular Notch1 expression has been shown to be involved in maintaining progenitor cell properties and the selection of the glial cell fate by retinal progenitor cells. However, the mechanisms by which Notch expression is regulated are not well understood. Two highly evolutionarily conserved non-coding regions proximal to the Notch1 gene were identified using multiple genome sequence alignment analysis and tested for function as gene regulatory elements (GRE) in the lens and retina of postnatal mouse and embryonic chick using molecular genetic methods. The retinal enhancer of Notch1 was found to be preferentially active in retinal progenitor cells and nestin positive Müller glial cells. The characterization of this enhancer provides greater understanding of the regulatory mechanisms that control Notch1 expression in retinal progenitor cells and Müller glial cells. The lens enhancer was restricted to the central core of the mouse lens where primary fibers reside. These GFP expressing cells presented elongated thin morphologies and were compact and polarized in their orientation. Notch1 was shown to be involved in the timing of differentiation of both primary and secondary lens fiber cells and the lack of Notch1 expression resulted in postnatal degeneration of the lens [135]. The lens specific Notch1 enhancer provides a mechanism of regulation that maintains Notch1 expression that may prevent cell degeneration in the lens. The applications for stem cell research and tissue engineering have great clinical potential toward a cure for blindness.

## 4.3     Introduction

The vertebrate retina is an excellent model system for studying the development, function and diseases of the eye. Advances in *in ovo/vivo* electroporation methods now allow for the study of key developmental genes and their regulatory elements using overexpression, knockdown, or promoter/enhancer specific reporter gene assays. Due to these advances and its convenient accessibility, the retina is emerging as a model system to study stem cell biology of the central

nervous system (CNS) and ultimately engineer replacement therapies to treat diseases that cause vision loss.

*4.3.1    Stem/Progenitor Cells, Cell Fate Determination, and the Vertebrate Retina*

The vertebrate retina originates from the walls of the optic cup with the outer pigmented layer forming the retinal pigment epithelium and the inner neural layer differentiating into the neural retina.  The mature vertebrate retina consists of three distinct cellular layers and two synaptic layers [137-139]. The well-characterized laminar structure contains neural cell populations within each of the layers, i.e., six major types of neurons, along with a single type of glial cell [140, 141].  These diverse retinal cell types are derived from multipotent stem/progenitor cells in the proliferating neural epithelium.

Retinal development is performed as a highly orchestrated combination of four major tasks: proliferation, migration, differentiation, and formation of synaptic connections.  Regulation of these four tasks depends on a combination of extrinsic and intrinsic factors that must work together in concert for development to successfully occur.  First, secreted signaling molecules and cell-cell interactions must accurately transmit a combination of spatial and temporal cues (extrinsic).  Second the developing cell must correctly interpret these cues and appropriately respond (intrinsic).  This results in the generation of each of the cells types of the retina in the proper temporal order, relative number, and laminar location within the retina.  Previous studies have revealed that the development of the vertebrate retina is a conserved process of cell genesis with the following order of cell birth: ganglion cells, horizontal cells, cone photoreceptors, amacrine cells, bipolar cells, rod photoreceptors, and Müller glia.  Birthdating studies have shown that retinal cell types are generated in two major waves of overlapping intervals, with ganglion cells, cone photoreceptors, amacrine cells, and horizontal cells generated prior to birth, and bipolar neurons and Müller glia generated after birth in mice.  Rod photoreceptor cells (rods), the most abundant cell type in the retina, are born both pre- and postnatally, with a peak of genesis coincident with the day of birth in the mouse [48, 49].

The photoreceptors (rods and cones) are located in the outer nuclear layer (ONL), short projection neurons (bipolar cells) and local circuit neurons (horizontal and amacrine cells) in the inner nuclear layer (INL), and long projection neuron (ganglion cells) in the ganglion cell layer (GCL) [47]. During early stages of retinal development, the outer neuroblastic layer (ONBL) consists almost entirely of mitotic progenitor cells, while newborn neurons (mostly consisting of amacrine and ganglion cells) reside in the inner neuroblastic layer (INBL). The position of mitotic progenitors within the ONBL varies depending upon their progress through the cell cycle, with S phase cells being found on the vitreal side of the ONBL near the border with the INBL and M-phase cells being found on the scleral side of the ONBL abutting the retinal pigment epithelium [48, 49].

### 4.3.2   Radial Glia Cells

Radial glial cells are an essential cell type in the developing CNS involved in key developmental processes, e.g., provide guidance for neuronal migration and serve as progenitors during neurogenesis [142-144]. Radial glia arise early in development from neuroepithelial cells. Radial phenotype is typically transient, but some cells, such as Bergmann glia in the cerebellum and Müller glia in the retina, retain radial glia-like morphology postnatally. During the late stages of CNS development, radial glial cells divide asymmetrically in the ventricular zone to generate radial glial cells and intermediate progenitor cells that divide symmetrically to produce multiple neurons [145-147], including photoreceptors and bipolar cells in the retina [148, 149]. Notch1 activation has been shown to induce the radial glia-specific gene expression, e.g., the glial fibrillary acidic protein (GFAP) and the brain lipid binding protein (FABP7) [150].  In the cerebral cortex, Notch1 activation induces radial glia differentiation embryonically [151], but astrocyte differentiation postnatally [152].

### 4.3.3   Müller Glial Cells

Müller glial cells (or Müller glia) are the principal radial glial cells of the vertebrate retina. These cells span the entire thickness of the retina, making contact virtually with all retinal neurons [153, 154]. They exist throughout the embryonic stages of retinal development and serve as structurally stabilizing scaffolds and as cell migration guides [123]. In the vertebrate retina, the majority of Müller glia reach morphological maturity late in development, mostly during final stage of the postnatal development of the retina [48, 49]. Many studies have shown that the extracellular and intracellular signaling pathways can regulate Müller glial cell genesis. Previous studies have demonstrated that Notch1, rax, and Hes1 are expressed in retinal progenitor cells that they promote the formation of Müller glia [118]. The epidermal growth factor receptor (EGFR) and the cyclin dependent kinase inhibitors (CKIs, e.g., $p27^{K}ip1$) have been implicated in regulating the Müller glial cell fate determination [155-158]. Emerging evidence demonstrates that activation of the Notch signaling pathway plays a pivotal role in regulating Müller glia development as well as gliogenesis in other parts of the CNS [118, 149, 159, 160]. In addition to numerous functions, Müller glia have been shown to dedifferentiate into multipotent retinal stem cells [132, 161-165] in response to retinopathy or injury.

### 4.3.4    Role of Notch1 in Retina Cell Fate Determination

Notch was first suspected of being involved in cell-cell contact mediated signaling when Notch mutants were observed to lack the inhibition of neural cell fates observed in normal development [166]. This established that Notch must play a role in communication between cells. The structure of the Notch transmenbrane protein helped to elucidate the mechanisms through which Notch facilitates cell-cell signaling [167, 168]. Notch1 is a 300 kDa type I single-pass transmembrane protein [169, 170] with its amino end in the lumen and the carboxyl end in the cytosol [171]. Upon ligand (delta, serrate) binding, a series of proteolytic cleavages release the intracellular domain of Notch1 from the plasma membrane, allowing subsequent translocation into nucleus [169, 170]. Notch1 (intracellular domain) then, in association with Mastermind (MAM) and Su(H) (DNA-binding effector suppressor of hairless), turns on target genes such as

BLBP (brain lipid-binding protein) and bHLH transcriptional repressors Hes1 and Hes5 [150, 172, 173] (Fig. 16). It has been shown that Notch1 signaling involved in the generation of all germ layers and the development of all tissues [170, 174, 175]. Notch1 expression is mainly restricted to the progenitor cells located in the proliferating ventricular zone of the vertebrate retina. Its expression is down-regulated during neural differentiation [159]. Knock-out mice of Notch1 die before birth making the study of its function solely through knock-out animals impossible [176]. Various experiments involving the missexpression of Notch1 have resulted in a fuller understanding of its functional role in development and disease [118, 177-179].  The role of Notch1 in retina development was also observed using antisense oligos specific to Notch. *In vivo* injections of the Notch antisense oligos reduced the amount of functional Notch and showed the number of ganglion cells to be inversely related to Notch activity [180].  This inhibition was not limited to ganglion cell differentiation but more broadly to all neural cell types [177, 181, 182]. Without this inhibition a disproportionately high number of progenitor cells chose early cell fates, depleted the progenitor cell pool, and resulted in a decreased number of late born cells.  These results showed that Notch was involved in maintaining a progenitor cell state throughout retina development from which progenitor cells could differentiate into the various cell fates. Interestingly this inhibition activity did not seem to apply to the differentiation of glial cells [118, 148, 183].  It is now evident that Notch1 plays important roles in neural stem cells maintenance, e.g., Notch1 maintains stem/progenitor cells in the developing retina [118, 182] and brain [151, 170, 175]. Neural stem/progenitor cells are capable of self-renewal and differentiation into glia and neurons. However, studies employing retrovirus to deliver constitutive active Notch1 into rat retinal progenitors show that Notch1 does not simply function to maintain the progenitor state since the number of other late-born neurons does not increase, but instead the number of Müller glial cell increase at the expense of rod photoreceptors and bipolar cells [118]. It is proposed that Notch1 governs the decision between neuronal and glial lineages, e.g., it affects the formation of V2 interneurons and motoneurons in the developing spinal cord [184] and facilitates the generation of glial cell types by suppressing the photoreceptor fate in the retina [182, 185].

**Figure 16** – **Notch1 signaling promotes Müller Glia differentiation**
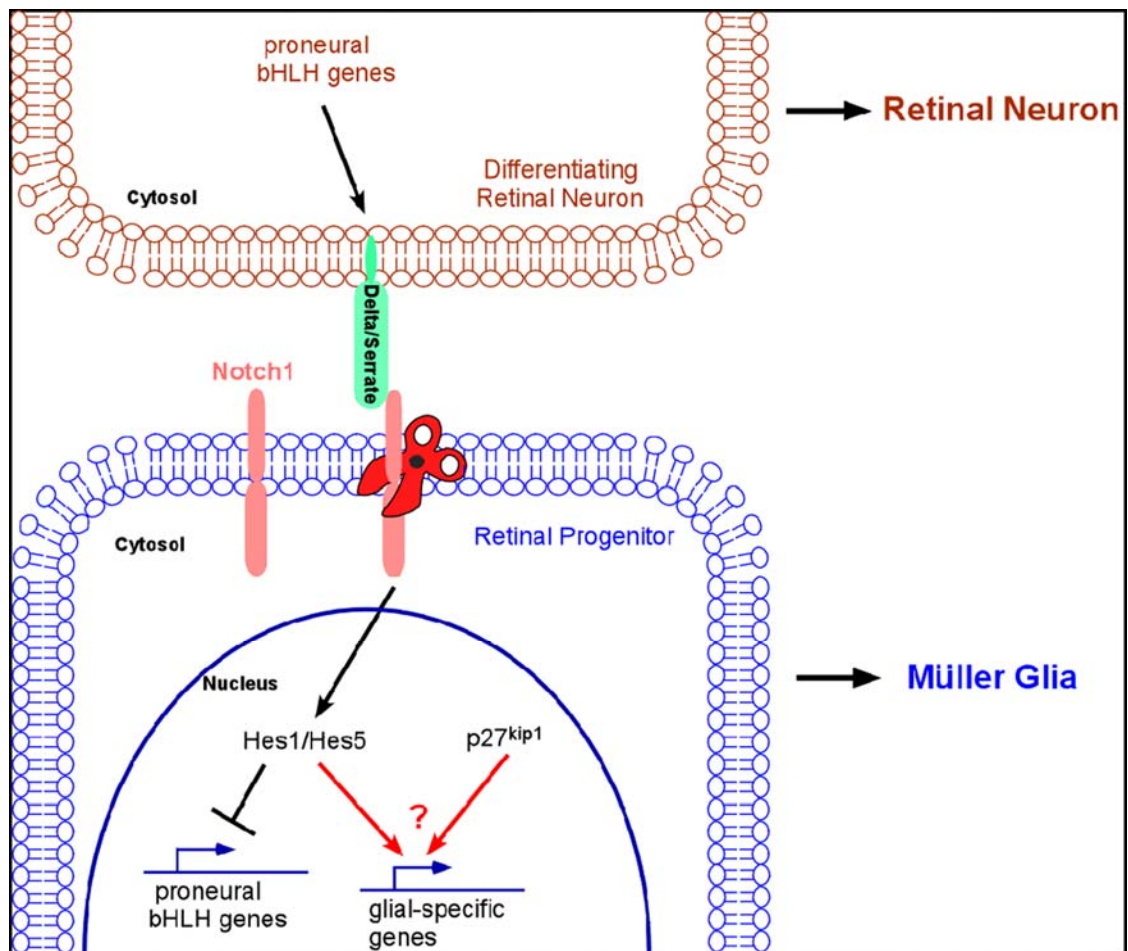


Differentiating retinal neurons express Delta that can bind to Notch1 receptors on neighboring retinal progenitors and activate proteolytic cleavage of Notch1 to release the cytosolic domain. Translocation of the Notch1 cytosolic domain into the nucleus activates the transcription of bHLH transcription repressors such as Hes1 and Hes5. Hes transcription repressors, by suppressing proneural bHLH genes, together with the action of p27Kip1 can promote differentiation of retinal progenitors into Müller Glial cells. This figure is adopted from Figure 1 in ref. [159].

Interestingly, only those progenitors from later stage of retinogenesis (e.g. late progenitor) seem to respond to constitutive active Notch1 to become Müller glia, whereas progenitors from early stage of retinogenesis (e.g. early progenitor) are refractory, in consistent with the model proposed by Cepko *et. al* that neural progenitors change over the course of neural development in their ability to respond to intrinsic and extrinsic cues [186]. The Notch1 expression profile in mouse is detectable from embryonic to postnatal stage. Notch1 is present in the developing brain, spinal cord (except the floor plate) and retina in both mouse and chicken [118, 148, 180]. Expression is detectable beginning at embryonic day 11 (E11) in mouse [187]. At E14.5, Notch1

co-localizes with Nestin, a neural progenitor cell marker and continues to be expressed in the neuroepithelium at lower levels until birth. Whether Notch signaling is instructive or simply permissive of the various cell fates possible during retinal development [137], the paramount importance of the Notch1 signaling pathway has been shown to shape the neurogenesis and gliogenesis process in the developing retina. However the transcription regulation of the key regulator of this pathway, Notch1, as by what mechanism governs the tissue-specific expression of Notch1 in retinal progenitors and Müller glial cells, remains to be determined [159].

## 4.3.5   Control of Tissue-Specific Gene Expression

Gene expression is largely controlled at the level of transcription which is influenced by both cis-acting elements (e.g. DNA sequences that defines promoters and enhancers), complexes of trans-acting elements (e.g. trans-acting factors such as transcription factors) that bind to cis-acting elements as well as the chromatin structure [188, 189]. The complex machinery required to regulate this control is still emerging from functional and evolutionary analysis of the genome architecture. Unlike promoters, which determine the transcription start sites, other cis-elements are required for the spatial/temporal control of gene expression. One important class of such cis-elements is the enhancer. Enhancer elements may reside in introns, upstream or downstream regions of a gene. They can regulate gene expression irrespective of their orientation. It is clear later on that the chromatin structure which defines the epigenetic control of transcription is an extension of genetic elements that control gene expression. Enhancers contain DNase I hypersensitive sites (DHS) where sequence-specific transcription factors can interact and recruit chromatin remodeling complexes [190, 191]. Analysis of the developmentally regulated globin gene transcription has provided one of the most thoroughly studied examples of enhancer-mediated spatial/temporal control of transcription. The expression of sequential embryonic, fetal, and adult β-globin genes was found to be under the control of the long-range interaction between enhancers and promoters [192, 193]. The β-globin locus control region (LCR) consists of cis-acting regulatory elements that control high level and tissue-specific expression that is

crucial for a normal development process [192, 194, 195]. The early enhancer of Hoxc8 is another excellent example of long-range regulation of expression [196]. The 200 bp highly conserved enhancer sequence located about 3 kb upstream of the Hoxc8 gene controls spatial patterning of Hoxc8 during embryogenesis [197]. The early Hoxc8 enhancer consists of 9 distinct motifs that affect Hoxc8 expression in the neural tube and the mesoderm. Combinatorial mutation/deletion studies of these elements have demonstrated that this enhancer controls Hoxc8 expression in a tissue- and temporal-specific manner [198, 199]. It has been proposed that, among other models, enhancers and promoters can interact with each other through protein-protein interaction to form chromatin loops during gene activation [200]. This model has gained supports from findings that various enhancers are in close juxtaposition to promoters, resulted from intrachromosome or even interchromosome interactions [201]. This kind of enhancer-promoter contact has been demonstrated for the control of $\beta$-globin, growth hormone and $T_H2$ cytokine locus [200, 202-204].

### 4.3.6 Evolutionarily Conserved Non-Coding Sequences Serve as Functional Enhancers

Unlike the promoter region, which can be predicted relatively easily based on the cDNA sequence of a gene, finding enhancers remain a major challenge to biologists. Despite extensive efforts in searching for the cis-regulatory elements in the vertebrate genome, only a small fraction of these elements has been identified and experimentally characterized *in vivo* [19, 205-208]. This paucity of regulatory element collections with defined activities has thus hindered our understanding of enhancers and their functions in regulating spatial/temporal-controlled transcription. For some genes with highly complex expression patterns, often those that function as key developmental control genes, the cis-regulatory elements can extend long distances over the transcription start site [37, 209-211]. Sequence comparison of various different species has revealed conservation of many non-coding regions [3, 19, 206, 212]. Functional studies have shown many of these CRs to be transcriptional regulatory elements [3, 5, 205]. Such sequence-conserved elements generally harbor sites for tissue-specific DNA-binding proteins (trans-acting factors) [213-216]. In

addition, these CRs are often identified as DNase I hypersensitive sites [191, 217], a known feature of enhancers.

### 4.3.7 Identification and Verification of Functional Enhancers: Computation and Wet Lab Approach

Previously, the discovery of functional cis-regulatory elements (e.g., enhancers) typically relied on extensive experimentation. Tissue-specific cis-regulatory elements were generally identified by promoter/enhancer deletion studies in transgenic mice [218] or by DNase I hypersensitivity mapping in expressing tissues [191, 217]. DNase I hypersensitivity mapping technique is based on the observation that local disruptions of the regular nucleosomal array create preferential targets for DNase I. Binding of transcription factors to the DNA at cis-regulatory elements is thought to cause the removal or dispersal of a nucleosome. Thus, DNase I hypersensitive sites are often found at active cis-regulatory elements. Genomic regions close to the promoter are sometimes further explored by footprinting and by electrophoretic mobility-shift assays (EMSA), which seek to identify regulatory protein-binding DNA regions [219]. Currently, the ability to evaluate the expression of thousands of genes across various experimental conditions has allowed bioinformatics approaches to these problems. Clusters of genes that show similar patterns of expression were searched within their upstream sequences for over-represented or conserved sequence motifs. This method has worked well in bacteria and yeast [220]; however, due to highly complex nature of the genome, finding cis-regulatory elements in vertebrates still remains a difficult problem [215]. However, the completion of the human genome sequencing along with other species has allowed comparative genomic approach to identify evolutionarily conserved functional enhancers [221]. We have taken this approach and identified several evolutionarily conserved non-coding DNA sequences around the Notch1 gene. The identified sequences were then tested for their ability to drive cell type-specific reporter gene expression in the developing mouse and chick retina.

In this study, we will confirm and characterize the function of computationally identified sequences N1CR1 and N1CR2 as true Notch1 enhancers. The role of N1CR3 and N1CR4 are currently under investigation. In addition, we will also examine the role of N1CR2 within the complex transcriptional network for Notch1 expression in progenitor/Müller glial cells. As Notch1 is known to maintain stem/progenitor cells (including Müller glia), finding the cis- and trans-element in regulating Notch1 expression will be invaluable in stem cell research and application in treating eye disease.

## 4.4    Materials and Methods

### 4.4.1    Computational Prediction of Notch1 Enhancers

In order to gain a better understanding of how the Notch1 gene is regulated, sequences surrounding the mouse Notch1 gene (highlighted in green, Fig. 17A) were searched for non-coding conserved regions (CR). Sequence retrieval and alignment were performed as describe in the Implementation section of Chapter 2 (2.3.8).

### 4.4.2    βGP-GFP

Negative controls (Fig. 18A-B), Enhancer test constructs (Fig. 18C), and positive controls (Fig. 18D) were generated by manipulation of the transfection control construct, CAG-GFP (Fig. 18E) (plamid 11150, Addgene, Cambridge, MA, USA) [100]. The CAG cassette was removed by restriction enzymes digestion using XbaI and SpeI (New England Biolabs, Ipswich, MA, USA). The linearlized DNA was then treated with Calf Intestinal Phosphatase (New England Biolabs, Ipswich, MA, USA) and purification by gel electrophoresis to give the GFP backbone. Next the β-globin promoter (βGP) was prepared. The human βGP sequence is: 5' GGGCTGGGCATAAAAGTCAGGGCAGAGCCATCTATTGCTTACATTTGCTTCTGACA 3'. The restriction enzyme recognition sequences for SbfI, FseI were added on to the 5' end the βGP sequence. These recognition sites could be used as insert sites to test for enhancer function of conserved sequences. Then over hang sequences for SpeI and XbaI were added to the 5' and 3' end

**Figure 17 – Highly conserved regions (CR) near the mouse Notch1 gene were isolated and tested for enhancer function**
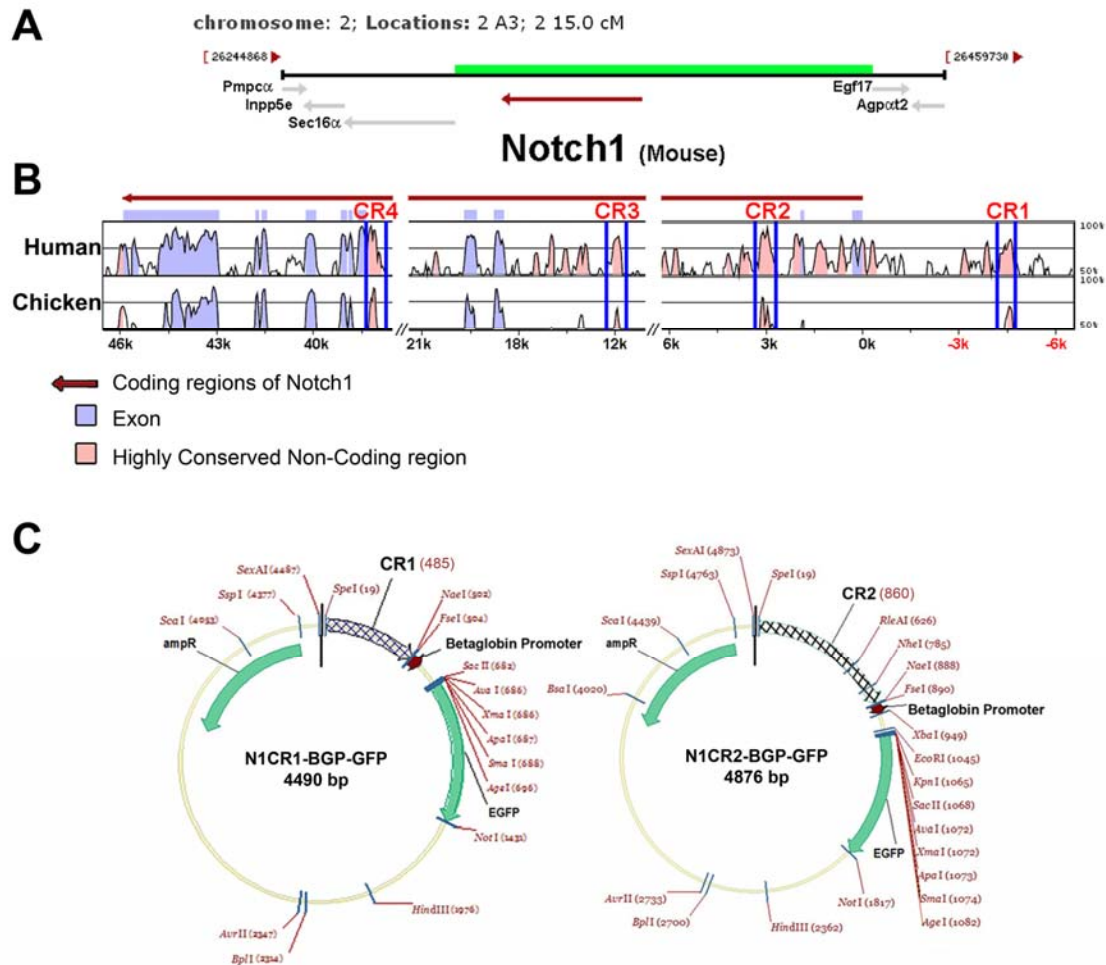
A mapping of a region of chromosome 2 from the mouse genome shows the relative location and size of Notch1 and its surrounding genes (A).  The non-coding sequence surrounding the mouse Notch1 gene (highlighted in green, A) was retrieved along with the homologous sequences for human and chicken.  Multiple sequence alignment revealed 4 highly conserved non-coding regions (B).  CR1 and CR2 were isolated from the genome and separately inserted into βGP-GFP to produce enhancer test constructs N1CR1-βGP-GFP and N1CR2-βGP-GFP (C).

respectively to allow for ligation with the GFP backbone.  The final forward sequence is 5'

ctagtcctgcaggggccggccGGGCTGGGCATAAAAGTCAGGGCAGAGCCATCTATTGCTTACATTTGCTTCTG

ACAt 3'.  Its complementary sequence is 5'

CTAGATGTCAGAAGCAAATGTAAGCAATAGATGGCTCTGCCCTGACTTTTATGCCCAGCCCGGCCGGCCC

CTGCAGGA 3'.   These sequences were synthesized by IDT (IDT technologies, Coralville, IA,

USA).  The single stranded DNA was annealed together to produce the double stranded βGP

insert.  The insert was prepared for ligation T4 Polynucleotide Kinase (New England Biolabs,

Ipswich, MA, USA).  The βGP insert was ligated with the GFP backbone using T4 DNA ligase (New

England Biolabs, Ipswich, MA, USA) to produce βGP-GFP.  The ligation product was transformed

into NEB 5-alpha Competent E. coli (New England Biolabs, Ipswich, MA, USA) and screened for

the presence of the βGP inserted by digestion with SbfI (New England Biolabs, Ipswich, MA,

USA). Once samples containing βGP were identified, sequencing was performed to verify that no

mutations have occurred during the insertion process.  Upon sequence verification, high

concentration βGP-GFP DNA was obtained using QIAGEN Plasmid Maxi Kit (QIAGEN, Valencia,

CA, USA).

| Table 6 – Modified PCR primer sequences for conserved sequences | | | |
|---|---|---|---|
| *Conserved Region* | *Primer* | *Sequence* | *Tm* |
| N1CR1 | Forward | cgatatatactagttttagagcttccgtcctctggctt | 57°C |
| N1CR1 | Reverse | cgatatatggccggcccgttcaccgtgagatgttccttgt | 57°C |
| N1CR2 | Forward | cgatatatactagtgcctttggcttgaaaggtgtccat | 57°C |
| N1CR2 | Reverse | cgatatatggccggcctctgctccatgttgggaactcctt | 57°C |
| NeuroD1CR2 | Forward | cgatatatactagtttctgggaagagcaagcacccta | 57°C |
| NeuroD1CR2 | Reverse | cgatatatggccggccttgttgccagttccctctgggata | 57°C |
| RhoCR3 (RER) | Forward | cgatatatactagtttctgtgaccttggtgacccactt | 57°C |
| RhoCR3 (RER) | Reverse | cgatatatggccggcctgcacccgggattcctagatgttt | 57°C |
| Sema3aCR20 | Forward | cgatatatactagtcgctgccatcctctcctatttcat | 57°C |
| Sema3aCR20 | Reverse | cgatatatggccggccggccaagagaacactgtagagtca | 57°C |

*4.4.3    Reporter Constructs for Enhancer Activity Assay*

PCR primers were designed to isolate CRs from the mouse genome.  A random extension

sequence (CGATATAT) and the SpeI recognition sequence (ACTAGT) was added to the 5' end of

the forward primer and the random extension sequence and FseI recognition sequence

(GGCCGGCC) to the 5' end of the reverse primer.  The random extension sequence ensured that

the added restriction enzyme recognition site would be functional.  These modifications produced

PCR products with ends that could be digested with their respective restriction enzymes to

produce sequence specific "sticky ends."  This allowed for sequence specific ligation in later steps

(The final sequences for the modified primers can be found in Table 6).  Mouse genomic DNA

was extracted from an adult mouse tail and used as the PCR template for all primers. PCR was performed using Taq PCR Kit (New England Biolabs, Ipswich, MA, USA) following the Routine Taq PCR Reaction protocol. PCR products were verified for correct size and concentration on an agrose gel prior to digestion with FseI and SpeI. The βGP-GFP construct also linearlized with FseI and SpeI and gel purified. After digestion the sticky end inserts were gel purified and ligated into the linearlized βGP-GFP backbone to produce enhancer test constructs (Fig 2C). Enhancer test constructs were isolated using QIAGEN Plasmid Maxi Kit (QIAGEN, Valencia, CA, USA) and diluted to a concentration between 3.0 – 6.0 μg/μl.

### 4.4.4   In Vivo Electroporation

*In vivo* electroporation was performed following the protocol detailed in Matsuda, T & Cepko C. L. [100] to target the retina (Fig.18J) of new born pups at postnatal day 0 (P0). To target the developing lens the protocol was slightly modified to inject the DNA into the vitreous (Fig. 18K) rather than the subretinal space and required 1.5 μl of DNA per eye. All of the animal experiments were approved by the Institutional Animal Care and Facilities Committee at Rutgers University.

### 4.4.5   In Ovo Electroporation

*In ovo* electroporation was performed on fertilized pathogen-free (SPF) white leghorn chicken (Gallus domesticus) eggs obtained from Sunrise Farms (Catskill, NY, USA). These eggs were incubated at 37.5°C and 60% humidity (GQF manufacturing, Savannah, GA, USA). Protocol found in Chen et. al. [130] was followed for injections targeting the lens of embryos at Hamburger and Hamilton stage 10 (HH10). Injection and electroporation was performed according to the. Injections targeting the retina were performed after incubating the eggs for approximately 90 hours (E4) when the embryos reach HH 21. Injection and electroporation was performed according to the protocols found in Doh et. al. [222].

**Figure 18 – In vivo electroporation of the β-globin promoter (βGP) Green Fluorescent Protein (GFP) construct system allows for direct visualization of an enhancer's tissue/cell type specificity**
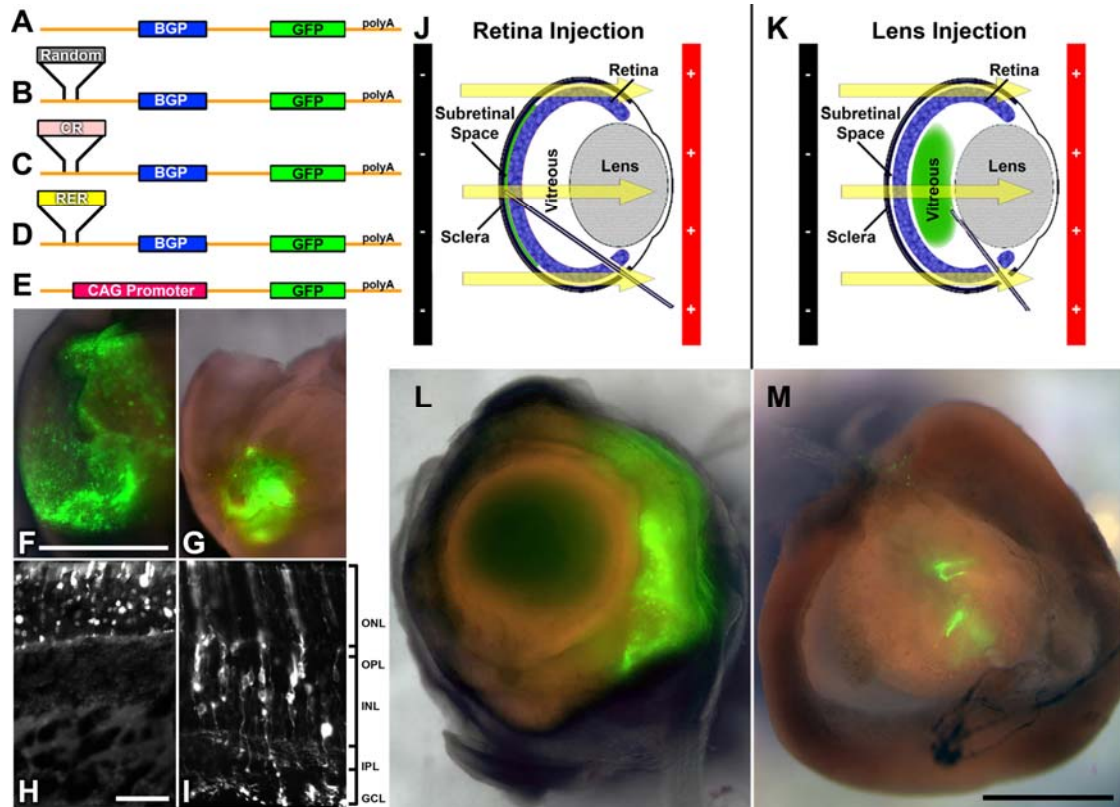
A schematic showing the key functional elements of the βGP-GFP plasmid and the different test conditions used to establish the system's ability to resolve the tissue/cell type specificity of an enhancer. Negative control constructs: βGP-GFP without an inserted sequence (A), βGP-GFP inserted with a random sequence (presumed to completely lack enhancer function) (B). Enhancer test construct: βGP-GFP inserted with a highly conserved non-coding regions (CR) (C). Positive control for tissue/cell type specificity: βGP-GFP inserted with RER, an enhancer for the Rhodopsin gene, which is known to possess photoreceptor specific function (D). Transfection control: CAG-GFP (E).

Mouse eyes were *in vivo* electroporated at postnatal day 0 (P0) with RER-βGP-GFP (F) and CAG-GFP (G) and harvested at P7 then cryosectioned. RER-βGP-GFP transfected retina (H) produced GFP only in the outer nuclear layer (ONL) where photoreceptors reside. GFP-positive cells were not observed in the inner nuclear layer (INL). CAG-GFP (I) was able to produce GFP expressing cells in the both the ONL and INL.

By injecting N1CR2-βGP-GFP into either the subretinal space (J) or into the vitreous (K), we were able to be targeted the retina (L) and lens (M), respectively, for *in vivo* electroporation.

(scale bar in F, M = 1mm, H = 50μm)

*4.4.6   Immunohistochemistry*

Tissues were harvested and fixed in 4% paraformaldahyde for 90 minutes and washed in PBS 3 times for 5 minutes.  Tissues were cryoprotected in 30% sucrose overnight at 4°C then embedded in OCT and stored at -80°C until ready to be sectioned.  Tissues were sectioned at 10-15 μm thickness using a cryostat (Thermo 0620E), mounted on Superfrost slides (Thermo Fisher Scientific, Waltham, MA, USA) and air-dried.  Two drops of PBS was added to each slide before covering with Shandon Coverplate (72110017; Thermo Fisher Scientific, Waltham, MA, USA) and mounted into a Shandon Slide Rack (73310017; Thermo Thermo Fisher Scientific, Waltham, MA, USA).  All volumes used with the Shandon Slide Rack/Coverplate system were 100 μl.  All washes used 100 μl and were for 5 min and repeated 2 times unless specified otherwise.  Sections were then prepared for staining by incubating in blocking solution (0.05% Triton X-100, 10% goat serum, 3% BSA in PBS) for 30 minutes at room temperature followed by a single PBS wash. Primary antibodies Anti-GFP (1:400 dilution; A-11122 Invitrogen c/o Molecular Probes, Carlsbad, CA, USA), Rho4D2 [75] (1:100 dilution; R.S. Molday, University of British Columbia, Canada), Lim1/2  [76-78] (1:10 dilution; 4F2 DSHB, Iowa City, IA, USA), Pax6 [80] (1:100 dilution; DSHB, Iowa City, IA, USA), PKCα [223] (1:400 dilution; sc-8393, Santa Cruz Biotechnology Inc, Santa Cruz, CA, USA), Brn3a [67] (1:100 dilution; MAB1585 Millipore, Billerica, MA, USA), CHX10 [99](1:200 dilution; sc-21692 Santa Cruz Biotechnology Inc, Santa Cruz, CA, USA), GFAP [224](1:100 dilution; G3893 Sigma-Aldrich, St. Louis, MO, USA), and Visinin (1:10 dilution; 7G4 DSHB, Iowa City, IA, USA), Vimentin (1:10 dilution; H5 DSHB, Iowa City, IA, USA), and Nestin [225] (1:10 dilution; rat-401 DSHB, Iowa City, IA, USA) were applied. Incubation was carried at 4°C overnight. As a negative control, serum and secondary antibodies were applied but no primary antibody was added to the staining solution. Slides were then washed with PBST (0.1% Tween-20 in 1x PBS) and DyLight 488 (for GFP) and DyLight 549 (for all other antibodies) from the appropriate host were applied as secondary antibodies (1:300 dilution; Jackson ImmunoResearch, West Grove, PA, USA). After 30 min incubation at room temperature, the

slides were washed with PBST then stained with DAPI (1:5 dilution; H-1200 Vector labs,

Burlingame, CA, USA) and cover slipped.

### 4.4.7   Imaging

Microscopy and imaging analysis were performed using an upright fluorescence microscope Axio

Imager A1 (Zeiss, Thornwood, NY, USA) with a monochrome digital camera Axiocam MRM (Zeiss,

Thornwood, NY, USA) or a Confocal laser scanning microscope (Olympus Fluoview FV10i;

Olympus America Inc, Center Valley, PA, USA).  GFP expression was enhanced using rabbit anti-

GFP and the anti-rabbit Dylight 488 secondary antibody.   Molecular markers were visualized

using the Dylight 549-secondary antibody labeled cells.  Filters used to detect the Dylight

488/GFP, Dylight 549, and DAPI were FITC, DsRed, and DAPI filters, respectively. Using Adobe

Photoshop CS, images of FITC, DsRed, and DAPI channels were adjusted to optimize contrast

and brightness levels then merged to create pseudo-colored triple-labeled images.

### 4.4.8   Cell Counts

Cell counts were performed on RGB images first for GFP-positive cells using the green channel

and then for double labeled GFP cells by toggling on and off the red channel.  Staining results for

each antibody was obtained for at least 3 separate GFP-positive retinas for N1CR2-βGP-GFP and

CAG-GFP.  The average for each set was calculated along with the standard error of the mean.

For each developmental stage and antibody condition, N1CR2-βGP-GFP and CAG-GFP results

were compared using 1-tailed student T-test to test for statistically significant differences ($p < 0.05$ and $p < 0.01$) between the results.

### 4.4.9   EMSA

Double stranded DNA probes (Table 7) were designed to span the entire CR and DNase I

hypersensitive sites of the enhancer sequences.  Probes were synthesized by IDT (Coralville, IA,

USA) as single stranded oligonucleotides.  Single stranded oligonucleotides were biotinylated

**Table 7 – EMSA probes with sequence specific binding**

| Probe | bp | Forward Sequence | Nuclear Extract |
|---|---|---|---|
| N1CR1.1 | 32 | tttagagcttccgtcctctggcttacttcccc | Lens |
| N1CR1.4 | 21 | gcttgaacaatagcaggtaccgcacatctgtg | Lens |
| N1CR1.A | 25 | ccgagggttggcgtgggaatgttag | Lens |
| N1CR2 Emsa2 | 59 | tgtacattctgggaagccacgcataattaatcacacagcattaatcgcctcccaacaat | Retina |
| N1CR2 Emsa3 | 59 | aacaatagctgctgcccttctactgaatcccagctgtcggcctctgaatggaaggaaat | Retina |
| N1CR2 Emsa4 | 59 | ccagctgtcggcctctgaatggaaggaaataagatttagggcatcaagcgtccgtgagg | Retina |
| N1CR2 Emsa5 | 59 | aaagtagtgtgcattcattagtgtctgacagaggcacaatcggctttgtccaataaact | Retina |
| N1CR2 Emsa6 | 59 | acagggcgggccagccagggaggtggggctgcagcccacaggctgggtactggaggcag | Retina |
| N1CR2 Emsa7 | 59 | tggggctgcagcccacaggctgggtactggaggcagcagcacccgttgtcaaggggatg | Retina |
| N1CR2 EmsaC | 45 | gctttgtccaataaactgctcacagacctgcttaattggcttcagt | Retina |

using Biotin 3´ End DNA Labeling Kit (Thermo Scientific Pierce Protein Research, Rockford, IL, USA) and stored at -20°C until ready for use and annealed at room temperature an hour immediately prior to binding.  Unlabeled single stranded probes were annealed to be used as double stranded competition probes.  The ratio of 1000:1 was used for Competition probe to labeled probes.  Nuclear extracts were obtained for P7, P14, and P21 from dissected lens and retina tissue and concentrations were measured using a Nanodrop Spectrophotometer (NanoDrop Technologies Inc, Wilmington, DE, USA).  The EMSA binding reaction and competition reaction were performed according to the LightShift Chemiluminescent EMSA Kit (Thermo Scientific Pierce Protein Research, Rockford, IL, USA) protocol.  Mini (8 x 8 x 0.1 cm) gels with 10 % polyacrylamide were run at 100V for approximately 90 – 110 minutes depending on the size of the probe.

## 4.5    Results

### 4.5.1    Computational Prediction of Conserved Regions as Potential Enhancer of Notch1

To predict evolutionarily conserved non-coding sequence elements that may serve as enhancers for the expression of the Notch1 gene, we have performed comparative sequence analysis.  The intergenic sequences spanning the 5' and 3' regions as well as introns of Notch1 (region highlighted in green, Fig. 17A) from various species, including human, mouse and chicken were

retrieved using our recently developed non-coding sequence retrieval system (NCSRS) [226], and

aligned using LAGAN [18] to reveal highly conserved non-coding sequence regions (pink, Fig.

17B) as potential gene regulatory elements.  The resulting sequence alignments revealed four

highly conserved regions, and thus, predicted as Notch1 enhancer candidates (N1CR1-4, Fig.

17B).  One of the regions resides upstream of the Notch1 gene (N1CR1) while the other three

reside within the intronic regions of the gene.  The top two scoring regions (N1CR1 and N1CR2)

were amplified and isolated from the mouse genome using PCR.  These regions were then

inserted into the βGP-GFP construct upstream of βGP to make two separate constructs (Fig. 17C)

which were used for *in vivo* electroporation of P0 mouse pup eyes.

### 4.5.2   *Generation of Reporter Constructs for Enhancer Activity Assay*

In order to experimentally verify and characterize the function of a potential gene regulatory

element (GRE), a reporter assay system containing an enhancer element was designed.  This

system utilizes a minimal basal promoter, β-globin promoter (βGP) and the reporter gene, green

florescent protein (GFP).  To verify the enhancer activity of a gene regulatory element, i.e., the

expression of reporter GFP based on the spatial and temporal function of the enhancer, a number

of negative and positive control tests were performed.  For the negative control, the β-globin

minimal promoter will be fused to the reporter GFP without a DNA sequence-element (Fig. 18A)

or with a comparable sized random sequence, e.g., an internal coding sequence of the bacterial

LacZ gene (Fig. 18B). Neither constructs showed the ability to drive GFP expression *in vivo*. In

addition, several highly conserved non-coding sequences from Sema3a and NeuroD genes have

been tested for enhancer activity and failed to drive reporter GFP expression in the retina, which

indicates that not all conserved sequences are functional tissue-specific enhancers (Fig. 18C).

For the transfection control, a strong ubiquitous CAG promoter (chicken β-actin promoter with

CMV enhancer) is in place of the β-globin minimal promoter (Fig. 18E). As shown in the

preliminary studies, this transfection control construct CAG-GFP was able to drive reporter GFP

expression (Fig. 18G) in various retinal cell types in various retinal cell layers (Fig. 18I). For the

positive control, a known enhancer will be inserted into the reporter construct (Fig. 17D) to ensure that in the presence of a functional enhancer, the β-globin minimal promoter can drive tissue/cell-specific GFP expression. The RER enhancer for Rhodopsin gene [227] was able to direct photoreceptor-specific GFP expression (Fig. 18H) confirming the ability of the reporter construct generate GFP based on the spatial and temporal function of the enhancer.

*4.5.3   N1CR1 and N1CR2 Are Novel Enhancers with Function in the Lens of Postnatal Mouse*

To examine the possibility that these enhancer candidate sequences (N1CR1 and N1CR2), conserved among human, mouse and chick might represent enhancers, we explored their ability to direct tissue-specific gene expression with the use of a reporter assay system in both mouse and chick using *in vivo/ovo* electroporation methods. The corresponding mouse sequences of N1CR1 and  N1CR2 were individually cloned upstream of a human β-globin minimal promoter [228] coupled to a reporter gene, green fluorescent protein (GFP), and injected and electroporated into the developing mouse retina and lens at postnatal day 0 (P0) and into the chick lens or optic vesicle at Hamilton-Hamburger stage 10-12 (about embryonic day 2, E2), respectively, to transfect the developing lens (see Methods section for details). Transfected tissues were harvested at various developmental stages during development. *In ovo* electroporation of the embryonic chick lens with N1CR2-βGP-GFP resulted in GFP expression from E3 (Fig. 19A) to E6 (Fig. 19B).  N1CR1 was not observed to result GFP expression in the chick. *In vivo* electroporation of the mouse lens at P0 resulted in GFP expression in the developing lens between P7 and P21 with N1CR2-βGP-GFP (Fig. 19C), N1CR1-βGP-GFP (Fig. 19D-F).  Results were similar for both N1CR1-βGP-GFP (arrowhead Fig. 20A-D) and N1CR2-βGP-GFP in that GFP expression was observed in primary fiber cells at the center of the lens which generally were denucleated (lacked dapi staining).  These cells generally exhibited long slender cell morphologies and were oriented along the anterior-posterior axis of the lens. By comparing GFP expression resulting from transfection with CAG-GFP with that resulting from N1CR1 and N1CR2 the cell type specificity of the Notch1 enhancers was observed.  GFP expression with CAG-GFP

**Figure 19 – *In vivo/ovo* electroporation of Notch1 enhancer constructs were able to drive GFP expression in the embryonic chick and postnatal mouse**
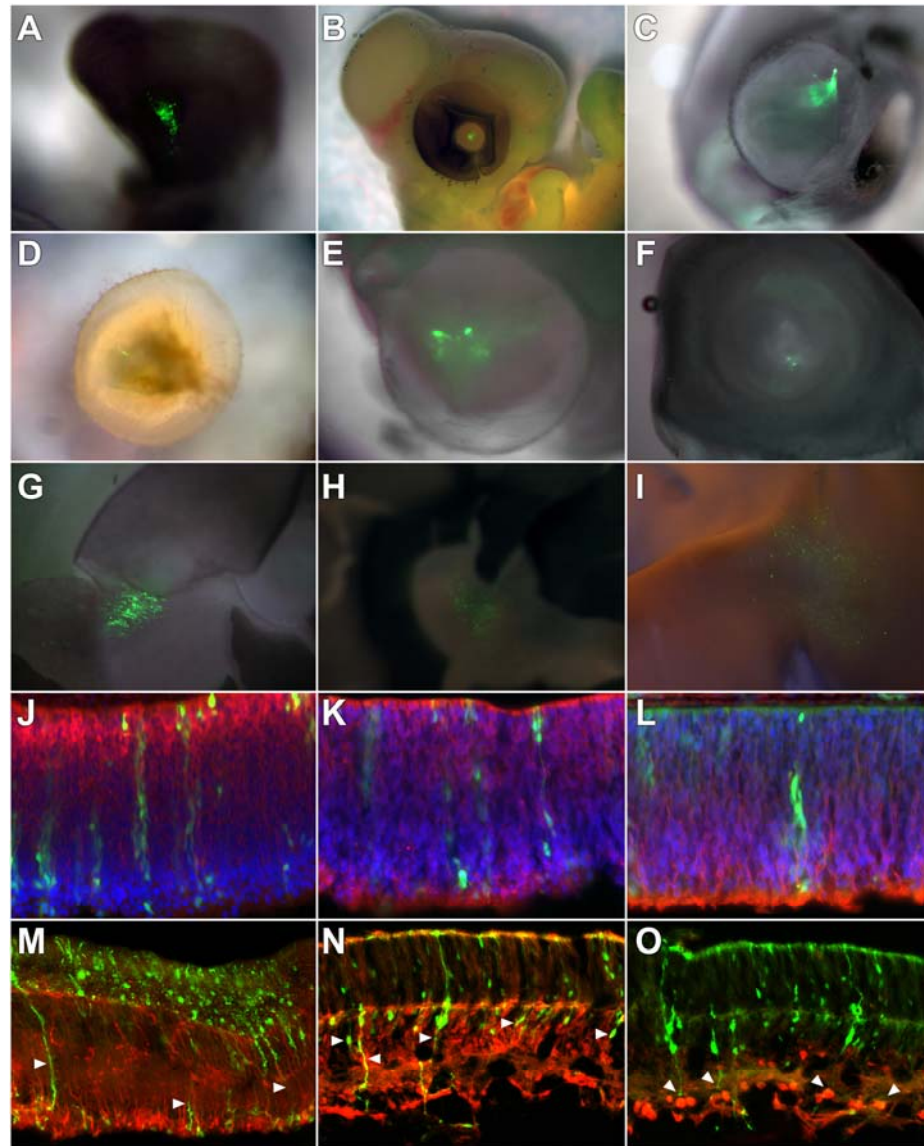
Whole mount images showing GFP expressing lens (A-F) and retinae (G-I) that were transfected using *in vivo/ovo* electroporation techniques. Chick embryos electroporated with N1CR2-βGP-GFP at embryonic day 2 (E2) showed GFP expression in the lens at E3 (A) and E6 (B). *In vivo* electroporation with N1CR2-βGP-GFP at P0 showed GFP expression in the lens at P7 (C). Similarly N1CR1-βGP-GFP transfected lens were shown to have GFP expression at P7 (D), P14 (E), and P21 (F). *In ovo* electroporation performed at E4 with N1CR2-βGP-GFP targeting the developing chick retina was able to generate GFP expressing retinal cells at E6 (G), E7 (H), and E10 (I). Sections of E7 chick retina transfected with N1CR2-βGP-GFP showing GFP expression (green) were labeled with Visinin (red, J), Nestin (red, K), Vimentin (red, L), and Dapi (blue, J-L). Sections of P7 mouse retina transfected with N1CR2-βGP-GFP showing GFP expression (green) were labeled with Nestin (red, M), Notch1 (red, N) and Calretinin (red, O).

was observed in both the primary (arrowhead, Fig. 20E-F) and secondary fiber cells (arrow, Fig.

20F) of the lens and in both denucleated and nucleated cells (Fig. 20F).  This result shows that

N1CR1 and N1CR2 were restricted to primary fiber cells of the lens by the cell type specific

enhancer function and not because of the electroporation technique.  These results show that

N1CR1 has enhancer function in primary fiber cells of the postnatal mouse lens and N1CR2 has

enhancer function in the lens that is conserved between the mouse and chick.

**Figure 20 – *In vivo* electroporation targeting the developing lens with N1CR1-βGP-GFP and CAG-GFP showed different patterns of expression.**
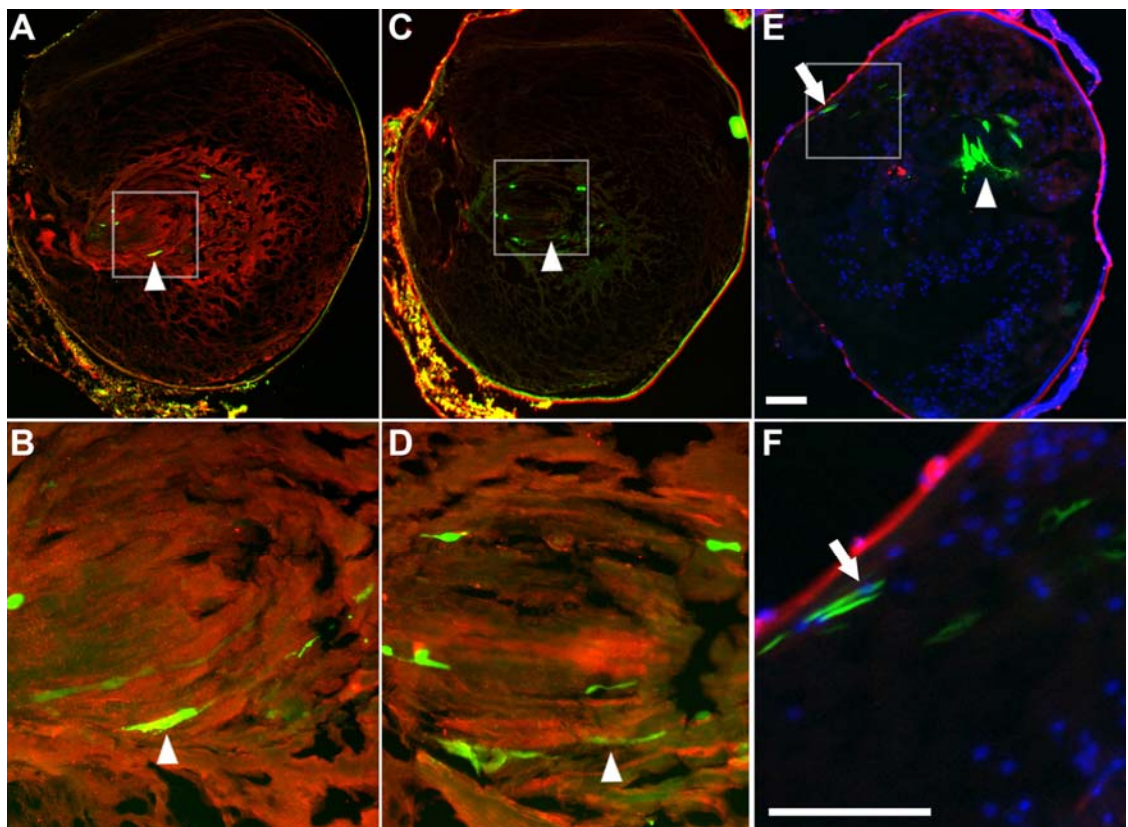


Cryosections of mouse lens *in vivo* electroporated at P0 with N1CR1-βGP-GFP (A-D) or CAG-GFP (E-F) and harvested at P14.  Sections were stained with GS (red, A-B), Notch1 (red, C-D), or DAPI (blue, E-F).  Higher magnification views show primary lens fiber cells (arrowhead, A-E) and secondary fiber cells (arrow, E-F) expressing GFP. (scale bar = 100µm)

*4.5.4    N1CR2 Has Enhancer Function in the Embryonic Chick and Postnatal Mouse Retina*

Similarly in the retina, *in vivo/ovo* electroporation, using N1CR1-βGP-GFP or N1CR2-βGP-GFP was

performed targeting the subretinal space of the retina in new born (P0) mouse pups or chick

embryos at HH21 (E4). N1CR1 failed to produce GFP in the retina of both mouse and chick at all

stages observed. N1CR2 was shown to reproducibly drive GFP expression specifically in the

developing retina of both the mouse at P7-P21 (Fig. 18L) and chick at E6-E10 (Fig. 19G-I). GFP

expression in E7 chick retina transfected with N1CR2-βGP-GFP was labeled with Visinin (Fig. 19J),

Nestin (Fig. 19K), and Vimentin (Fig. 19L). GFP expressing cells were clustered together into

columns spanning across all the layers of the retina. In the mouse retina, a significant portion of

GFP-expressing cells resulting from the N1CR2 construct transfection were shown to be Müller

glial cells that span all the retinal layers, possess radially polarized processes, and have

arborizations called "end-feet" toward the GCL (Fig. 19M-O) [97]. It is known that Müller glial

cells can function as retinal/neural stem cells [160, 165, 229-231]. To further determine the

identity of transfected cells (GFP-expressing cells), transfected tissues resulting from N1CR2

construct transfection were sectioned and immunostained with antibodies against Nestin (Fig.

19M) and Notch1 (Fig. 19N) to label neural progenitor cells. GFP-expressing cells in the mouse

retina were shown to express both Nestin and Notch1 (arrowheads, Fig. 19M-N). The end feet

processes of GFP expressing Müller glial cells seem to synapse with ganglion cells labeled with

Calretinin (arrowheads, Fig. 19O).

### 4.5.5 *N1CR2 is Preferentially More Active in Postnatal Progenitors and Nestin Positive Müller Glial Cells*

To characterize the enhancer function N1CR2 in the postnatal mouse retina, GFP expression

patterns of N1CR2-βGP-GFP were compared to those of a transfection control CAG-GFP at P7 and

P21. In both cases, GFP expression in the GCL failed to colocalize with DAPI staining (Fig. 21-22,

blue). Brn3a [91], a ganglion cell marker, colocalized well with the DAPI staining observed in the

GCL but failed to colocalize with GFP. Therefore the GFP expression observed in the GCL were

not ganglion cells but were processes of cells residing in other layers, such as end feet of Müller

glial cells. Immunolabeling with Lim1/2, a horizontal cell marker, also failed to colocalize with

GFP. The lack of GFP-positive horizontal and ganglion cells suggests that these cell types cannot

be transfected using *in vivo* electroporation at P0. Previous reports had similar findings showing only late born cells (rod photoreceptor, bipolar, amacrine, and Müller glial cells) were able to express GFP following *in vivo* electroporation of CAG-GFP at P0 [100, 232, 233]. To identity the cell types for GFP-positive cells (Fig. 21-22, green) at P7 (Fig. 21-22, A-I) and P21 (Fig. 21-22, J-R), cell-type specific markers (Fig. 21-22, red), e.g, GFAP for Müller glia [224](Fig. 21, A-B, J-K), Rho4D2 for rods [75](Fig. 21, D-E, M-N), and and PKCα for bipolar cells [223](Fig. 21, G-H, P-Q) were used to co-stain GFP-positive cells. Nestin (Fig. 22, A-B, J-K), CHX10 (Fig. 22, D-E, M-N), and Pax6 (Fig. 22, G-H, P-Q) were used to identify GFP-positive progenitor cells [98, 99, 234]. The GFP-positive cells labeled with various markers were counted and the percentages each individual cell types that also GFP-positive were calculated for both N1CR2-βGP-GFP and CAG-GFP (Fig. 21-22). The distribution of GFP-positive cells for N1CR2-βGP-GFP was compared to the transfection control CAG-GFP to determine whether there was a difference in enhancer activity in the various cell types. The results at P7 showed that, compared to control, there was a significant increase in the percentage of cells identified as Müller glia by GFAP staining (Fig. 21C) and progenitor cells by Nestin (Fig. 22C), CHX10 (Fig. 22F), and Pax6  (Fig. 22I) staining. A small increase was also observed in the number of GFP expressing cells identified as rods for N1CR2 at P7 but may be due to the labeling of rod progenitors. By P21, only Nestin labeling showed a significant difference compared to control (Fig. 22L). Comparisons of the percentage of GFP-positive cells labeled with PKCα did not show a statistically significant difference ($p < 0.05$) between N1CR2 and CAG-GFP at both P7 and P21. This suggests that while the N1CR2 enhancer was active in a wide array of differentiated cells types including rods, bipolar, and Müller glia, it was preferentially more active in progenitor cells at P7 and Nestin positive Müller glial cells at P21.

### 4.5.6   *Regions of N1CR1 and N1CR2 Showed Sequence Specific Binding*

Electrophoretic mobility shift assay (EMSA) was used to test for binding of proteins of characterized or uncharacterized protein factors; it provides a simple, rapid, and sensitive method

**Figure 21 – *In vivo* electroporation targeting the developing retina with N1CR2-βGP-GFP and CAG-GFP labeled with cell type specific markers**
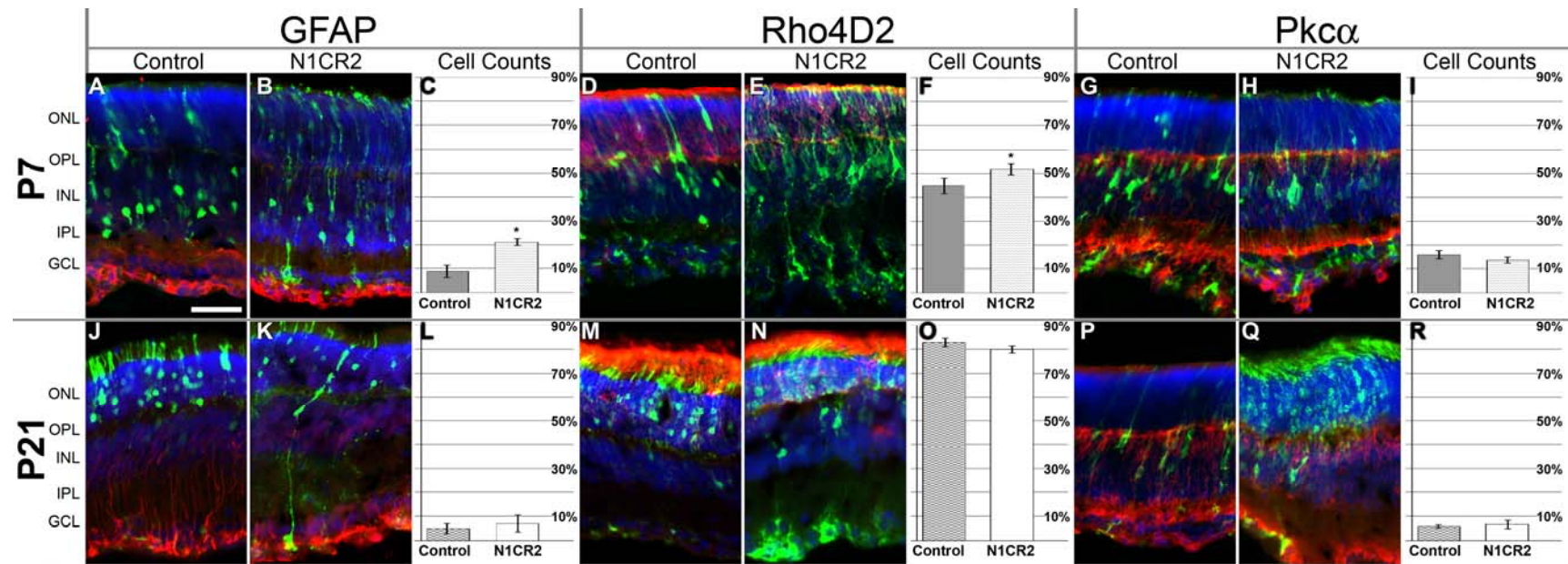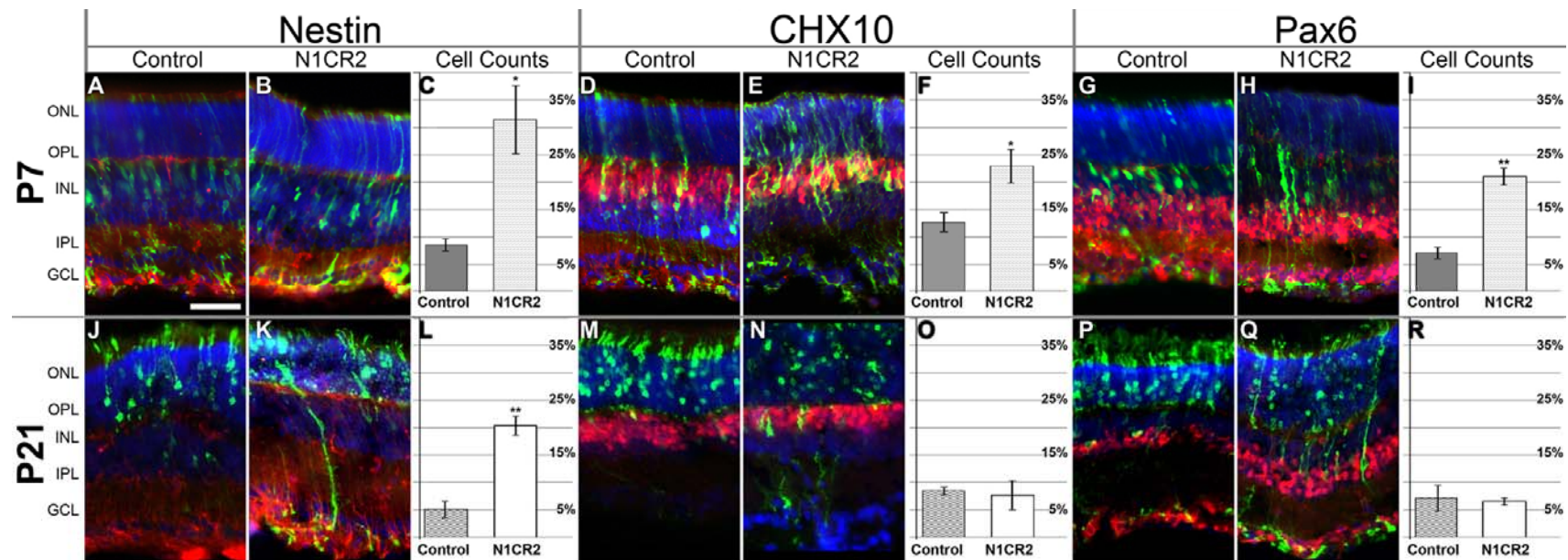
Cryosections of mouse retinae *in vivo* electroporated at P0 with N1CR2-βGP-GFP (N1CR2) or CAG-GFP (control) were harvested at P7 and P21. Sections were stained for Müller Glia cells with GFAP (A-B, J-K), photoreceptors with Rho4D2 (D-E, M-N), and bipolar cells with PKCα (G-H, P-Q). Cell counts were performed for each condition (C, F, I, L, O, R) with average values shown and standard error of the mean shown as error bars. One-tailed student t-test was used to calculate p-values and determine statistical differences between N1CR2 and control. (GFP – shown in green, cell type specific marker – shown in red, DAPI staining – shown in blue, n=3 for all conditions, * indicates p-values < 0.05, scale bar = 50μm)

for detecting sequence-specific DNA-binding proteins. Protein factors that bind specifically to an end-labeled DNA probe retard the mobility of the DNA during polyacrylamide gel electrophoresis, resulting in discrete bands corresponding to protein-DNA complexes of a particular molecular weight. To identify the specific regions with enhancer activity within N1CR1 and N1CR2, short double stranded DNA probes (< 60 bp) were designed for use in EMSA.  These short probes span the sequences of N1CR1 and N1CR2.  Nuclear extracts were prepared from lens and retina tissues from mice at various ages between P0 and Adults.  Multiple probes spanning N1CR1 were screened.  Probe 1, Probe 4 and Probe A (EMSA Probes, Fig. 23A) showed sequence specific binding with lens nuclear extracts prepared from mouse lens tissue (Fig. 23B).  Probes 1 and 4 reside within the predicted regulatory feature ENSMUSR00000011990[42] which was shown to be a DNase1 Hypersensitivity site (Fig.23A).  Similarly for N1CR2, seven probes (EMSA Probes, Fig. 23C) showed consistent, strong, sequence specific binding with nuclear extracts prepared from mouse retinal tissue of various developmental stages (Fig. 23D).

*4.5.7    Identifying Minimal Functional Sequence Elements of N1CR1 and N1CR2*

EMSA binding shows the potential for DNA:protein interactions in vitro, these may not be indicative of the *in vivo* mechanisms regulating the function enhancer activity.  Therefore, subsequent subregions were tested (subregion constructs, Fig. 23A, C) for their enhancer functions, based on the probes of N1CR1 and N1CR2 that were capable of sequence specific binding as shown through EMSA.  These subregions were synthesized and individually inserted into βGP-GFP plasmid then tested using the same methods previously used for the larger sequence fragment.  For N1CR1, GFP expression in the lens from transfection N1CR1-βGP-GFP (Fig. 23E) was similar with that of N1CR1.4-βGP-GFP (Fig. 23F) at P7. However, the subregion 1.4 generated GFP expression in the lens at a lower frequency of animals injected (N1CR1 ~ 50%, N1CR1.4 ~ 25%) than the full length N1CR1. The subregion constructs 1.1 and 1.A failed to produce detectable GFP expression in the lens between P7 and P21.

For N1CR2 a slightly different strategy was taken because of the greater number of probes that

**Figure 23 – Isolation of minimal functional enhancers by *in vivo* electroporation of constructs designed using EMSA binding results**
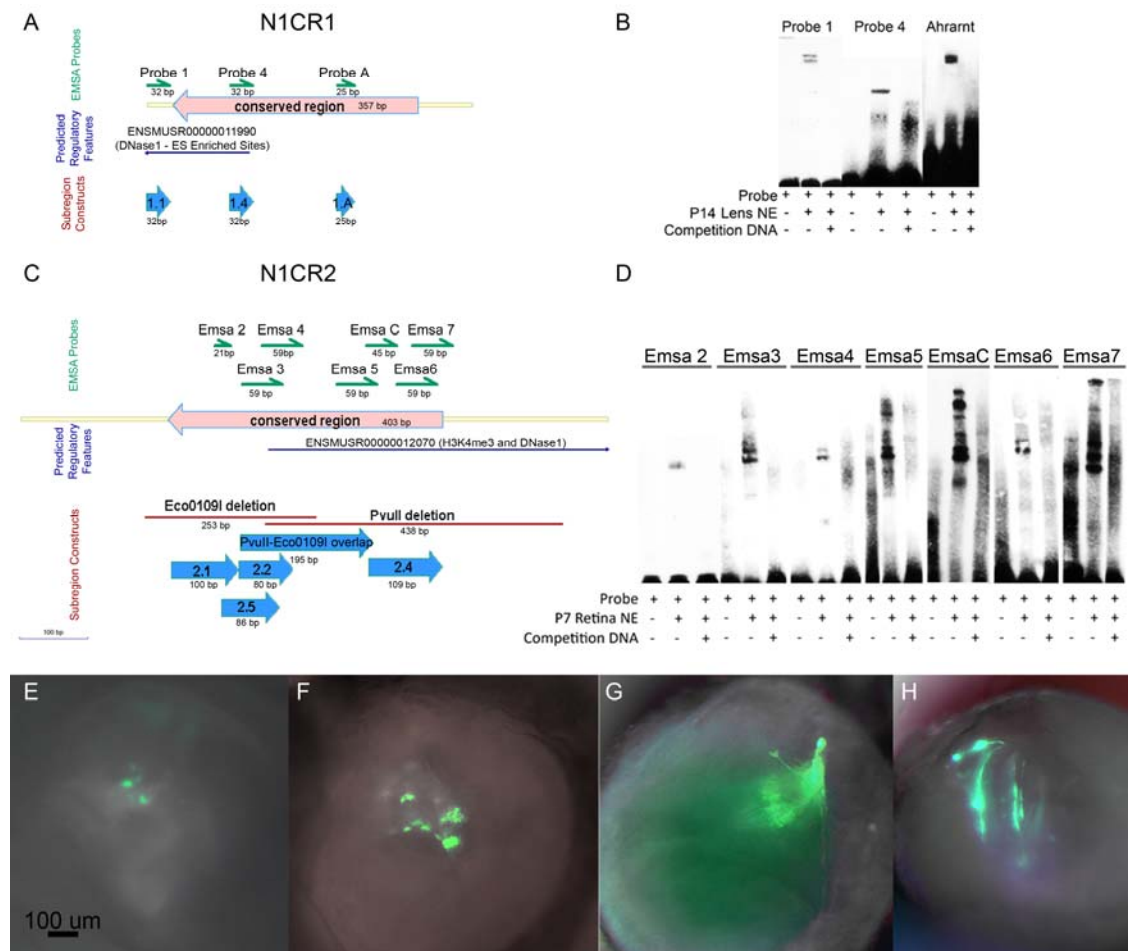
EMSA probes were designed to span the conserved regions of N1CR1 (A) and N1CR2 (C). EMSA results showing sequence specific binding using Probe 1, Probe 4, and Probe A with nuclear extracts isolated from P14 mouse lens tissue (B). Probes for N1CR2 showed sequence specific binding with nuclear extracts isolated from P7 mouse retina tissue (D). Sequences of N1CR1 and N1CR2 that correspond to EMSA probes with binding that were inserted into βGP-GFP to generate subregions constructs (Subregion Constructs, A and C). Using a process of elimination method, N1CR2 sequences were deleted by restriction enzyme digestion and relegation to test the remaining sequences for enhancer function (deletion regions represented by red bars in C). Whole mount images of P7 lens *in vivo* electroporation at P0 with N1CR1-βGP-GFP (E), N1CR1.4-βGP-GFP (F), N1CR2-βGP-GFP (G), and N1CR2.5-βGP-GFP (H).

*4.6.1    Reporter Construct Enhancer Activity Assay is a Fast and Flexible Method for Identifying Novel Enhancers*

In this study, we have developed a rapid enhancer verification method based on reporter assay with *in vivo/ovo* electroporation techniques. We demonstrated that the enhancer reporter assay

system was able to produce GFP based upon the spatio-temporal regulatory function an

enhancer using a number of negative control conditions (βGP-GFP alone, random-βGP-GFP), and

a positive control condition (RER-βGP-GFP). This system allowed for the direct visualization of

the spatio-temporal regulatory function of an enhancer. An advantage of this method is its

flexibility. It can be applied to wild type animals without altering normal development or

transgenic animals those missexpress genes without affecting the missexpression. This allows

for the potential study of enhancers function in the context of a particular disease state or

regulatory pathway. However because of the limitations of *in vivo* electroporation technique in

the mouse the time frame and tissues that can be tested are limited in the mouse to those that

could be easily accessed such as the retina [232], lens, and brain [235]. This system can be

used with *in utero* methods to study embryonic development but the tissues that can be targeted

are limited to the eye [236], brain[237], and spinal cord [238]. An earlier developmental time

frame and greater variety of tissue types can be targeted in the chick using *in ovo* techniques but

the potential for greater differences in regulatory mechanisms between chicks and humans may

make it more difficult to translate results into therapeutic applications. The constructs generated

in this system can be also applied to generate transgenic animals. Therefore the reporter assay

system in combination with *in vivo/utero/ovo* electroporation techniques may prove valuable as a

screening method from which CRs of interest can be identified based on preliminary results

before undertaking the costly and labor intensive work of generating transgenic animals. Using

this system, we identified 2 novel enhancers of the Notch1 gene, N1CR1 and N1CR2, and

established their tissue/cell type specificity. Our results indicate that Notch1 expression during

development may be regulated by the enhancers N1CR1 and N1CR2. For the lens, both N1CR1

and N1CR2 were found to have enhancer activity in primary fiber cells of the mouse lens

between P7 and P21. While these enhancers both showed similar cell type specificity in the

postnatal lens they may possess distinct regulatory functions at earlier stages as suggested by

the results in the chick lens where only N1CR2 had enhancer function. Further characterization

will be needed to better determine these differences. In the early postnatal retina (P0-P7) the

enhancer N1CR2 has increased activity in progenitor cells.  Notch1 is known to play a key role in maintaining the progenitor cell state [177, 181] and is also expressed in differentiated cells [239].  The ability of N1CR2 to drive expression of GFP in progenitors, rods, bipolar cells, and Müller glia between P0-P7 suggests that N1CR2 plays a role in maintaining Notch1 expression in a broad range of cell types.  These results further supports that Notch1 is involved in the regulation of differentiation in general rather than the development of any specific cell type.

*4.6.2   N1CR2 has Increased Enhancer Activity in Retinal Progenitor Cells and Nestin Positive Müller Glia*

Retinas transfected with either the N1CR2 construct of CAG-GFP were labeled with various cell type specific markers and colocalization of GFP and marker were calculated at P7 and P21 (stage/construct/marker, i.e. P7/Control/Pax6, would indicate colocalization results obtained for P7 retina transfected with CAG-GFP and labeled with Pax6).  Compared to the P7/Control, P7/N1CR2 showed a significantly higher percentage of GFP-expressing cells that colocalized with retinal progenitor cell markers CHX10 (Fig. 22F) [99, 240] and Pax6 (Fig. 22I) [98, 99]as well as the neural stem cell marker Nestin (Fig. 22C) [240-242].  While CHX10 and Pax6 label retinal progenitor cells and suggest that the enhancer function of N1CR2 is related to retinal progenitor cells, they also label mature retinal cell types after differentiation, e.g, CHX10 labels bipolar cells [243] and Pax6 labels amacrine and ganglion cells [98].   In order to eliminate the possibility that N1CR2 is preferentially more active in bipolar cells, colocalization with PKCα [102], another bipolar cell marker, was observed for both the N1CR2 enhancer and CAG-GFP.  A significant difference was not observed between N1CR2/PKCα and Control/PKCα at either P7 (Fig. 21I) or P21 (Fig. 21R).  This suggests that the enhancer is not preferentially active in bipolar cells and further supports that the difference observed between P7/N1CR2/CHX10 and P7/Control/CHX10 was due to the increased enhancer activity of N1CR2 in progenitors.

A significant difference was not observed between P21/N1CR2 and P21/Control for either Pax6 (Fig. 22R) or CHX10 (Fig. 22O).  The transient increase in colocalization with both

P7/N1CR2/CHX10 and P7/N1CR2/Pax6 suggests there may be a shared explanation for these results.  During histogenesis retinal progenitor cells are actively proliferating, replacing cells lost to differentiation, thereby maintaining a pool of progenitor cells [48, 244, 245].  While progenitor cells continue to differentiate, proliferation stops around P11 [49].  Without new progenitor cells being born to replace the ones lost to differentiation the number of progenitors decreases over time.  Given that both markers are able to label retinal progenitor cells.  The decrease in colocalization between P7/N1CR2 and P21/N1CR2 with Pax6 (Fig. 22I vs. Fig. 22R) and CHX10 (Fig. 22F vs. Fig. 22O) observed can be explained either by the loss of Pax6 and CHX10 expression or a decrease in enhancer activity as differentiation occurs. Colocalization remained consistent between P7/Control/Pax6 and P21/Control/Pax6 and only a slight decrease was observed between P7/Control/CHX10 and P21/Control/CHX10.  This suggests that the level of Pax6 and CHX10 expression does not drastically decrease between P7 and P21.  Therefore N1CR2 has increased activity in progenitor cells compared to differentiated cells.

### 4.6.3   *N1CR2 Plays a Role in Maintaining Progenitor Cell Properties in Nestin Positive Müller Glia and May Allow for the Manipulation of Stem/Progenitor Cell Properties*

Previous studies have linked Notch1 function to radial glial development and maintenance in the brain [150, 151, 246].  Other findings have suggested Notch1 has a related role for the radial glia analogue in the retina, Müller glia [118].  The Nestin antibody is a marker for progenitor cells including Müller glia precursors in the retina [234, 240, 241].  The interfilament protein Nestin is involved in maintaining cell shape, controlling cell survival and motility [247].  The highly specialized cell morphology of Müller glial cells with radially elongated cell bodies and long thin processes may require the cell shape maintaining function of Nestin.  Both Nestin [248] and GFAP [132] are upregulated in Müller glial cells following injury, and may play a role in triggering gliosis.  A significant number of cells transfected with the N1CR2 construct possess cell morphologies resembling that of Müller glial cells with processes that are labeled by Nestin and GFAP.  The nearly four-fold increase in colocalization observed between P7/N1CR2/Nestin (Fig.

22C) and P7/Control/Nestin was maintained at P21 (Fig. 22L). One possible explaination is that

the relatively late onset of Müller glial differentiation causes a large pool of Müller glia fated

progenitors to be maintained later in development than other cell types. This could explain why

the levels of colocalization remained elevated for P21/N1CR2/Nestin. However colocalization was

higher for P7/N1CR2/GFAP than P7/Control/GFAP (Fig. 21C) but was not significantly different at

P21 (Fig. 21L). This pattern was similar to the progenitor specific antibodies (Pax6 and CHX10)

in that differences between observed at P7 were no longer present at P21. Another possible

explaination is that N1CR2 enhancer function is linked to the regulation of Nestin expression.

Given the ability of Notch1 overexpression to generate Müller glia and the direct interaction

between Notch1 and Nestin expression in gliomas [249], the N1CR2 enhancer may indirectly

upregulate Nestin expression by enhancing the expression of Notch1. This may explain how

Notch1 is able to regulate the progenitor cell properties of Müller glia. This would also explain

the increased presence of Nestin labeling which is maintained through P21 in N1CR2 transfected

GFP-positive cells. We propose the mechanism linking N1CR2 to Nestin expression in Müller glial

cells is similar to the one observed in gliomas. The N1CR2 enhancer increases Notch1

expression. Notch1 then becomes activated and interacts with the regulatory regions of Nestin,

resulting in the increase of Nestin expression. N1CR2 therefore may be an important target for

the manipulation of Notch1 and Nestin and allow for novel tissue engineering methods for

manipulating the stem/progenitor cell properties found in retinal progenitor cells and Müller glial

cells.

*4.6.4   N1CR2 Contains Multiple Regions of Enriched Transcription Factor Binding Sites*

While attempts to isolate a smaller subregion of the N1CR2 with the same enhancer activity in

the retina were not successful, the subregions tested indicate two major details of N1CR2. First

that there are multiple regions that possess functional elements that is collectively responsible for

the enhancer activity of N1CR2 in the retina. Second these regions are necessary, but not

sufficient to drive expression in the retina. However some are sufficient to produce expression in

the lens.  This suggests that the regulatory mechanisms involved in controlling Notch1 expression in the retina are more complex than in the lens.  This is not surprising given the greater diversity of cells and complexity in their organization present in the retina.  There were multiple sites observed to be capable of *in vitro* binding with retinal cell nuclear extracts by EMSA analysis, some of which have multiple binding elements.  This suggests a highly complex modular model for this enhancer.  Further supporting this theory, transcription factor binding site (TFBS) analysis found a high density of predicted binding sites within the core of N1CR2 (see the .xls file in Supplemental Data for Table 8).  This may indicate the high level of complexity involved in the regulation of Notch through this enhancer and how Notch1 expression can be precisely and specifically regulated and yet seem to be ubiquitously and continuously expressed.

## 4.7     Conclusion

Studies focusing on Notch1 expression during development and missexpression studies have shown Notch1 plays a significant role in development and regulating cell characteristics such as maintaining plasticity and the timing of differentiation [166, 178, 180, 183, 239, 250, 251]. Transient inactivation of Notch1 has been shown to regulate the timing of differentiation in neurons [244].  Further support comes from a separate study showing a transient down regulation of Notch1 expression at E12 and E16 [239] which are concurrent with the beginning of the first and second wave of differentiation in the retina [244].  The link between Notch1 and Nestin in regulating stem cell properties may prove to be a powerful tool to tissue engineering and biomedical research.  A fuller understanding of Notch1 enhancers may provide the ability to regulate proliferation, plasticity, and cell fate determination which is critical to the future of biomedical engineering and in particular to stem cell based therapies.   The manipulation or targeting of enhancer may someday allow for tightly controlled transient activation and inhibition of genes.  This will only be possible with a better understanding of the mechanisms behind spatio-temporal regulation involving enhancers.  Identification and characterization of enhancers

for key developmental genes such as Notch1 may provide powerful tools necessary for the

advancement of tissue engineering applications aimed at both regeneration and repair.

## CHAPTER 5    FUTURE DIRECTIONS AND SUMMARY

### 5.1    Summary

A better understanding of how genes are regulated and the identification of both cis and trans functional elements in this regulation is massively important to understanding the mechanisms behind development, disease, repair, and regeneration.  As is seen in the case of Notch1 and many other developmentally significant genes, expression during development must be carefully orchestrated to control the order and duration of events such as proliferation, differentiation, and apoptosis.  Reverse engineering the body's methods for development, repair, and regeneration may hold the key to developing therapies.  Enhancers play a central role in this orchestration and may hold the key to new drug targets sites, drug delivery modalities, and understanding the biochemical mechanisms behind diseases.  Enhancer based therapies may someday enable drug delivery methods that are capable of recognizing specific micro-environments such as a disease state or specific cell types to explicitly control the activation, dosage, or release of a drug. Enhancers also may give tissue engineers the tools necessary for making stem cell based therapies a reality by allowing them to control the expression of developmental genes.

We have demonstrated a two staged system.  First computational analysis was performed to predict gene regulatory elements and second the biological function of identified sequences was experimentally verified using *in ovo/vivo* electroporation methods.  In an effort to increase the speed and accuracy of the often an overlooked first step of all sequence analysis methods, sequence retrieval, the Non-Coding Sequence Retrieval System (NCSRS) was developed.  This system eliminates possible human errors introduced during manual retrieval and provides a single centralized source for sequence retrieval.  Multiple genome alignments were performed on non-coding sequences flanking 89 different developmental genes.  This resulted in the identification and analysis of 1053 conserved regions (CR) of which 502 were computationally predicted to

have a high likelihood of gene regulatory function. A web browser friendly database was built using the results from this analysis to allow for easy access and navigation.

In order to establish the chick retina as a useful animal model for studying retinal development a novel *in ovo* electroporation method was developed. This method improved upon conventional methods by changing the time of electroporation to embryonic day 4. This change allowed for the all the various cell types of the retina to be labeled. Combined with previously established immunohistochemical methods, the dynamic morphological and molecular changes of retinal development were examined.

In order to experimentally verify the enhancer function of these CR a reporter construct based enhancer activity assay was developed. This construct system allows for the direct visualization of the spatio-temporally regulation of gene expression by an enhancer through the detection of Green Fluorescent Protein (GFP). This system was then applied to the mouse and chick models using *in vivo/ovo* electroporation for fast and efficient analysis of enhancer function. Two highly conserved non-coding region located proximally to the Notch1 gene were verified for enhancer activity in this manner. The enhancer N1CR2 was of particular interest as it was found to have enhancer function in lens primary fibers, retinal progenitor cells, and Müller glial cells of the postnatal mouse as well as in the lens and retina of embryonic chicks.

## 5.2 Future Work

In order to further study this enhancer and characterize its ability to drive gene expression at earlier time points and in other tissues, transgenic animals that contain the N1CR2-βGP-GFP sequence are being generated. Previous work with chicken embryos suggests that this sequence has also enhancer activity in the developing brain and neural tube. These embryos should reveal confirm these results in the mouse. It will be interesting to see whether the enhancer activity of N1CR2 is inhibited or otherwise downregulated in the retina concurrently with the down regulation of Notch1 expression. This would provide a mechanism for the observed transient

downregulation of Notch1 expression at E12 and E16.  These animals will also provide tissue

samples that can be sorted using FAC for GFP expression indicating the cells in which the

enhancer is active.  These cells can then isolated and used in ChIP analysis to identify the

proteins that bind to the enhancer *in vivo* rather than *in vitro* as with the results obtained using

EMSA.  The identification of these proteins will help elucidate the regulatory network controlling

Notch1 expression.

# REFERENCES

1.      Frazer, K.A., et al., Cross-species sequence comparisons: a review of methods and available resources. Genome Res, 2003. 13(1): p. 1-12.
2.      Makalowski, W., The human genome structure and organization. Acta Biochim Pol, 2001. 48(3): p. 587-98.
3.      Woolfe, A., et al., Highly conserved non-coding sequences are associated with vertebrate development. PLoS Biol, 2005. 3(1): p. e7.
4.      Vavouri, T., et al., Parallel evolution of conserved noncoding elements that target a common set of developmental regulatory genes from worms to humans. Genome Biology, 2007. 8.
5.      Nobrega, M.A., et al., Scanning human gene deserts for long-range enhancers. Science, 2003. 302(5644): p. 413.
6.      Kellis, M., et al., Sequencing and comparison of yeast species to identify genes and regulatory elements. Nature, 2003. 423(6937): p. 241-54.
7.      Lander, E.S., et al., Initial sequencing and analysis of the human genome. Nature, 2001. 409(6822): p. 860-921.
8.      Brazma, A., et al., Predicting Gene Regulatory Elements in Silico on a Genomic Scale. Genome Research, 1998. 8: p. 1201-1215.
9.      Fujibuchi, W., J.S.J. Anderson, and D. Landsman, PROSPECT improves cis-acting regulatory element prediction by intergrating expression profile data with consensus pattern searches. Nucleic Acids Research, 2001. 29(19): p. 3988-3996.
10.     Roth, F.P., et al., Finding DNA regulatory motifs within unaligned noncoding sequences clustered by whole-genome mRNA quantitation. Nat Biotechnol, 1998. 16(10): p. 939-45.
11.     Bucher, P., Regulatory elements and expression profiles. Curr Opin Struct Biol, 1999. 9(3): p. 400-7.
12.     Stojanovic, N., et al., Comparison of five methods for finding conserved sequences in multiple alignments of gene regulatory regions. Nucleic Acids Res, 1999. 27(19): p. 3899-3910.
13.     Schwartz, S., et al., PipMaker--a web server for aligning two genomic DNA sequences. Genome Res, 2000. 10(4): p. 577-86.
14.     Schwartz, S., et al., Human-mouse alignments with BLASTZ. Genome Res, 2003. 13(1): p. 103-7.
15.     Schwartz, S., et al., MultiPipMaker and supporting tools: Alignments and analysis of multiple genomic DNA sequences. Nucleic Acids Res, 2003. 31(13): p. 3518-24.
16.     Mayor, C., et al., VISTA: visualizing global DNA sequence alignments of arbitrary length. Bioinformatics, 2000. 16(11): p. 1046-7.
17.     Frazer, K.A., et al., VISTA: computational tools for comparative genomics. Nucleic Acids Res, 2004. 32(Web Server issue): p. W273-9.
18.     Brudno, M., et al., LAGAN and Multi-LAGAN: efficient tools for large-scale multiple alignment of genomic DNA. Genome Res, 2003. 13(4): p. 721-31.
19.     Bejerano, G., et al., Ultraconserved elements in the human genome. Science, 2004. 304(5675): p. 1321-5.
20.     Xie, X., et al., Systematic discovery of regulatory motifs in human promoters and 3' UTRs by comparison of several mammals. Nature, 2005. 434(7031): p. 338-45.
21.     Levy, S., S. Hannenhalli, and C. Workman, Enrichment of regulatory signals in conserved non-coding genomic sequence. Bioinformatics, 2001. 17(10): p. 871-7.
22.     Thacker, C., et al., Functional genomics in Caenorhabditis elegans: An approach involving comparisons of sequences from related nematodes. Genome Res, 1999. 9(4): p. 348-59.
23.     Loots, G.G., et al., Identification of a coordinate regulator of interleukins 4, 13, and 5 by cross-species sequence comparisons. Science, 2000. 288(5463): p. 136-40.
24.     Kellis, M., B.W. Birren, and E.S. Lander, Proof and evolutionary analysis of ancient genome duplication in the yeast Saccharomyces cerevisiae. Nature, 2004. 428(6983): p. 617-24.

25.    Cliften, P.F., et al., Surveying Saccharomyces genomes to identify functional elements by comparative DNA sequence analysis. Genome Res, 2001. 11(7): p. 1175-86.

26.    Bergman, C.M. and M. Kreitman, Analysis of conserved noncoding DNA in Drosophila reveals similar constraints in intergenic and intronic sequences. Genome Res, 2001. 11(8): p. 1335-45.

27.    Dubchak, I., et al., Active conservation of noncoding sequences revealed by three-way species comparisons. Genome Res, 2000. 10(9): p. 1304-6.

28.    Boffelli, D., et al., Phylogenetic shadowing of primate sequences to find functional regions of the human genome. Science, 2003. 299(5611): p. 1391-4.

29.    Myers, C.L., et al., Discovery of biological networks from diverse functional genomic data. Genome Biol, 2005. 16(13): p. R114.

30.    Pastinen, T. and T.J. Hudson, Cis-Acting Regulatory Variation in the Human Genome. Science, 2004. 306: p. 647-650.

31.    Loots, G.G. and I. Ovcharenko, rVISTA 2.0: evolutionary analysis of transcription factor binding sites. Nucleic Acids Research, 2004. 32(Web Server): p. W217–W221.

32.    Lewandoski, M., Cre-ating Somatic Cell Genetic Mosaics in the Mouse. Nat Rev Genet, 2001. 2: p. 743-755.

33.    Matsuda, T. and C.L. Cepko, Electroporation and RNA interference in the rodent retina *in vivo* and in vitro. PNAS, 2004. 101(1): p. 16-22.

34.    Matsuda, T. and C.L. Cepko, Controlled expression of transgenes introduced by *in vivo* electroporation. PNAS, 2007. 3(3): p. 1027-1032.

35.    Timmer, J., J. Johnson, and L. Niswander, The Use of *In Ovo* Electroporation for the Rapid Analysis of Neural-Specific Murine Enhancers. genesis, 2001. 29: p. 123-132.

36.    Vavouri, T. and G. Elgar, Prediction of cis-regulatory elements using binding site matrices--the successes, the failures and the reasons for both. Curr Opin Genet Dev, 2005. 15(4): p. 395-402.

37.    Vavouri, T., et al., Defining a genomic radius for long-range enhancer action: duplicated conserved non-coding elements hold the key. Trends Genet, 2006. 22(1): p. 5-10.

38.    Mayor, C., et al., VISTA : visualizing global DNA sequence alignments of arbitrary length. Bioinformatics, 2000. 16(11): p. 1046-7.

39.    Stojanovic, N., et al., Comparison of five methods for finding conserved sequences in multiple alingments of gene regulatory regions. Nucleic Acids Res, 1999. 27(19): p. 3899-3910.

40.    Lazzarato, F., et al., RRE: a tool for the extraction of non-coding regions surrounding annotated genes from genomic datasets. Bioinformatics, 2004. 20(16): p. 2848–2850.

41.    Pruitt, K. and D. Maglott, RefSeq and LocusLink: NCBI gene-centered resources. Nucleic Acids Res, 2001. 29(1): p. 137-140.

42.    Curwen, V., et al., The Ensembl automatic gene annotation system. Genome Res, 2004. 14(5): p. 942-950.

43.    Kent, W.J., et al., The Human Genome Browser at UCSC. Genome Res, 2002. 12(6): p. 996-1006.

44.    Siddiqui, A., et al., cis-Regulatory Element Prediction in Mammalian Genomes, in IEEE Computational Systems Bioinformatics Worshop. 2005.

45.    Wasserman, W.W., et al., Human-mouse genome comparisons to locate regulatory sites. Nat Genet, 2000. 26(2): p. 225-8.

46.    Doh, S.T., et al., Non-coding sequence retrieval system for comparative genomic analysis of gene regulatory elements. BMC Bioinformatics, 2007. 8(94).

47.    Kaneko, A., Physiology of the retina. Annu Rev Neurosci, 1979. 2: p. 169-91.

48.    Young, R.W., Cell differentiation in the retina of the mouse. Anat Rec, 1985. 212(2): p. 199-205.

49.    Young, R.W., Cell proliferation during postnatal development of the retina in the mouse. Brain Res, 1985. 353(2): p. 229-39.

50.    Alexiades, M.R. and C. Cepko, Quantitative analysis of proliferation and cell cycle length during development of the rat retina. Dev Dyn, 1996. 205(3): p. 293-307.

51.    Gloor, B.P., L. Rokos, and S. Kaldarar-Pedotti, Cell cycle time and life-span of cells in the mouse eye. Measurements during the postfetal period using repeated 3H-thymidine injections. Dev Ophthalmol, 1985. 12: p. 70-129.

52.    Fujita, S., Kinetics of cellular proliferation. Exp Cell Res, 1962. 28: p. 52-60.

53.    Li, Z., et al., Modulation of cell proliferation in the embryonic retina of zebrafish (Danio rerio). Dev Dyn, 2000. 219(3): p. 391-401.

54.    Rapaport, D.H. and J. Stone, The topography of cytogenesis in the developing retina of the cat. J Neurosci, 1983. 3(9): p. 1824-34.

55.    Silva, A.O., C.E. Ercole, and S.C. McLoon, Plane of cell cleavage and numb distribution during cell division relative to cell differentiation in the developing retina. J Neurosci, 2002. 22(17): p. 7518-25.

56.    Das, T., et al., *In vivo* time-lapse imaging of cell divisions during neurogenesis in the developing zebrafish retina. Neuron, 2003. 37(4): p. 597-609.

57.    Cayouette, M. and M. Raff, The orientation of cell division influences cell-fate choice in the developing mammalian retina. Development, 2003. 130(11): p. 2329-39.

58.    Tibber, M.S., et al., The orientation and dynamics of cell division within the plane of the developing vertebrate retina. Eur J Neurosci, 2004. 19(3): p. 497-504.

59.    Tibber, M.S., A.V. Whitmore, and G. Jeffery, Cell division and cleavage orientation in the developing retina are regulated by L-DOPA. J Comp Neurol, 2006. 496(3): p. 369-81.

60.    Zigman, M., et al., Mammalian inscuteable regulates spindle orientation and cell fate in the developing retina. Neuron, 2005. 48(4): p. 539-45.

61.    Godinho, L., et al., Nonapical symmetric divisions underlie horizontal cell layer formation in the developing retina *in vivo*. Neuron, 2007. 56(4): p. 597-603.

62.    Zimmerman, R.P., E.H. Polley, and R.L. Fortney, Cell birthdays and rate of differentiation of ganglion and horizontal cells of the developing cat's retina. J Comp Neurol, 1988. 274(1): p. 77-90.

63.    Morrow, E.M., C.M. Chen, and C.L. Cepko, Temporal order of bipolar cell genesis in the neural retina. Neural Develop, 2008. 3: p. 2.

64.    Gamm, D.M., A.D. Nelson, and C.N. Svendsen, Human retinal progenitor cells grown as neurospheres demonstrate time-dependent changes in neuronal and glial cell fate potential. Ann N Y Acad Sci, 2005. 1049: p. 107-17.

65.    Blanks, J.C., et al., Lineage study of degenerating photoreceptor cells in the rd mouse retina. Curr Eye Res, 1997. 16(7): p. 733-7.

66.    Reese, B.E., W.F. Thompson, and J.D. Peduzzi, Birthdates of neurons in the retinal ganglion cell layer of the ferret. J Comp Neurol, 1994. 341(4): p. 464-75.

67.    Liu, W., et al., All Brn3 genes can promote retinal ganglion cell differentiation in the chick. Development, 2000. 127(15): p. 3237-47.

68.    Bruhn, S.L. and C.L. Cepko, Development of the pattern of photoreceptors in the chick retina. J Neurosci, 1996. 16(4): p. 1430-9.

69.    Morrow, E.M., T. Furukawa, and C.L. Cepko, Vertebrate photoreceptor cell development and disease. Trends Cell Biol, 1998. 8(9): p. 353-8.

70.    Furukawa, T., et al., Retinopathy and attenuated circadian entrainment in Crx-deficient mice. Nat Genet, 1999. 23(4): p. 466-70.

71.    Hamburger, V. and H.L. Hamilton, A series of normal stages in the development of the chick embryo. 1951.[see comment]. Developmental Dynamics, 1992. 195(4): p. 231-72.

72.    Nakamura, H. and J. Funahashi, Introduction of DNA into chick embryos by *in ovo* electroporation. Methods (Duluth), 2001. 24(1): p. 43-8.

73.    Harris, W.A. and S.L. Messersmith, Two cellular inductions involved in photoreceptor determination in the Xenopus retina. Neuron, 1992. 9(2): p. 357-72.

74.    Yamagata, K., et al., Visinin: a novel calcium binding protein expressed in retinal cone cells. Neuron, 1990. 4(3): p. 469-76.

75.     Hicks, D. and R.S. Molday, Differential immunogold-dextran labeling of bovine and frog rod and cone cells using monoclonal antibodies against bovine rhodopsin. Exp Eye Res, 1986. 42(1): p. 55-71.

76.     Cheng, L., et al., Lbx1 and Tlx3 are opposing switches in determining GABAergic versus glutamatergic transmitter phenotypes. Nat Neurosci, 2005. 8(11): p. 1510-5.

77.     Muroyama, Y., et al., Wnt signaling plays an essential role in neuronal specification of the dorsal spinal cord. Genes Dev, 2002. 16(5): p. 548-53.

78.     Tsuchida, T., et al., Topographic organization of embryonic motor neurons defined by expression of LIM homeobox genes. Cell, 1994. 79(6): p. 957-70.

79.     Herman, J.P., J.C. Victor, and J.R. Sanes, Developmentally regulated and spatially restricted antigens of radial glial cells. Dev Dyn, 1993. 197(4): p. 307-18.

80.     Ericson, J., et al., Pax6 controls progenitor cell identity and neuronal fate in response to graded Shh signaling. Cell, 1997. 90(1): p. 169-80.

81.     Wiechmann, A.F., Recoverin in cultured human retinoblastoma cells: enhanced expression during morphological differentiation. J Neurochem, 1996. 67(1): p. 105-10.

82.     Mullen, R.J., C.R. Buck, and A.M. Smith, NeuN, a neuronal specific nuclear protein in vertebrates. Development, 1992. 116(1): p. 201-11.

83.     Stern, C.D., The chick; a great model system becomes even greater. Dev Cell, 2005. 8(1): p. 9-17.

84.     Suga, A., M. Taira, and S. Nakagawa, LIM family transcription factors regulate the subtype-specific morphogenesis of retinal horizontal cells at post-migratory stages. Dev Biol, 2009. 330(2): p. 318-28.

85.     Margeta, M.A., Transcription factor Lim1 specifies horizontal cell laminar position in the retina. J Neurosci, 2008. 28(15): p. 3835-6.

86.     Poche, R.A., et al., Lim1 is essential for the correct laminar positioning of retinal horizontal cells. J Neurosci, 2007. 27(51): p. 14099-107.

87.     Boije, H., P.H. Edqvist, and F. Hallbook, Temporal and spatial expression of transcription factors FoxN4, Ptf1a, Prox1, Isl1 and Lim1 mRNA in the developing chick retina. Gene Expr Patterns, 2008. 8(2): p. 117-23.

88.     Edqvist, P.H., S.M. Myers, and F. Hallbook, Early identification of retinal subtypes in the developing, pre-laminated chick retina using the transcription factors Prox1, Lim1, Ap2alpha, Pax6, Isl1, Isl2, Lim3 and Chx10. Eur J Histochem, 2006. 50(2): p. 147-54.

89.     Huang, E.J., et al., Brn3a is a transcriptional regulator of soma size, target field innervation and axon pathfinding of inner ear sensory neurons. Development, 2001. 128(13): p. 2421-32.

90.     Nadal-Nicolas, F.M., et al., Brn3a as a marker of retinal ganglion cells: qualitative and quantitative time course studies in naive and optic nerve-injured retinas. Invest Ophthalmol Vis Sci, 2009. 50(8): p. 3860-8.

91.     Badea, T.C., et al., Distinct roles of transcription factors brn3a and brn3b in controlling the development, morphology, and function of retinal ganglion cells. Neuron, 2009. 61(6): p. 852-64.

92.     Wohabrebbi, A., et al., Downregulation of a unique photoreceptor protein correlates with improper outer segment assembly. J Neurosci Res, 2002. 67(3): p. 298-308.

93.     Wikler, K.C. and P. Rakic, An array of early differentiating cones precedes the emergence of the photoreceptor mosaic in the fetal monkey retina. Proc Natl Acad Sci U S A, 1994. 91(14): p. 6534-8.

94.     Rapaport, D.H., S.L. Patheal, and W.A. Harris, Cellular competence plays a role in photoreceptor differentiation in the developing Xenopus retina. J Neurobiol, 2001. 49(2): p. 129-41.

95.     Hatakenaka, S., et al., Immunohistochemical localization of chick retinal 24 kdalton protein (visinin) in various vertebrate retinae. Brain Res, 1985. 331(2): p. 209-15.

96.     Docherty, R.J., et al., Chick embryonic pigmented retina is one of the group of epithelioid tissues that lack cytokeratins and desmosomes and have intermediate filaments composed of vimentin. J Cell Sci, 1984. 71: p. 61-74.

97.     Moscona, A.A., et al., Antiserum to lens antigens immunostains Muller glia cells in the neural retina. Proc Natl Acad Sci U S A, 1985. 82(16): p. 5570-3.

98.     Marquardt, T., et al., Pax6 is required for the multipotent state of retinal progenitor cells. Cell, 2001. 105(1): p. 43-55.

99.     Belecky-Adams, T., et al., Pax-6, Prox 1, and Chx10 homeobox gene expression correlates with phenotypic fate of retinal precursor cells. Invest Ophthalmol Vis Sci, 1997. 38(7): p. 1293-303.

100.    Matsuda, T. and C.L. Cepko, Electroporation and RNA interference in the rodent retina *in vivo* and in vitro. Proceedings of the National Academy of Sciences of the United States of America, 2004. 101(1): p. 16-22.

101.    Xiang, M., H. Zhou, and J. Nathans, Molecular biology of retinal ganglion cells. Proc Natl Acad Sci U S A, 1996. 93(2): p. 596-601.

102.    Caminos, E., et al., A comparative study of protein kinase C-like immunoreactive cells in the retina. Brain Behav Evol, 2000. 56(6): p. 330-9.

103.    Haverkamp, S., F. Haeseleer, and A. Hendrickson, A comparison of immunocytochemical markers to identify bipolar cell types in human and monkey retina. Vis Neurosci, 2003. 20(6): p. 589-600.

104.    Shin, T., et al., An immunohistochemical study of protein kinase C in the bovine retina. J Vet Med Sci, 2006. 68(1): p. 71-4.

105.    Dowling, J.E., The retina. An approachable part of the brain. 1987, Cambridge, MA., USA: Belknap.

106.    Kahn, A.J., An autoradiographic analysis of the time of appearance of neurons in the developing chick neural retina. Dev Biol, 1974. 38(1): p. 30-40.

107.    Prada, C., et al., Spatial and Temporal Patterns of Neurogenesis in the Chick Retina. Eur J Neurosci, 1991. 3(11): p. 1187.

108.    Wai, M.S., et al., Morphogenesis of the different types of photoreceptors of the chicken (Gallus domesticus) retina and the effect of amblyopia in neonatal chicken. Microsc Res Tech, 2006. 69(2): p. 99-107.

109.    Morris, V.B., Symmetry in a receptor mosaic demonstrated in the chick from the frequencies, spacing and arrangement of the types of retinal receptor. J Comp Neurol, 1970. 140(3): p. 359-98.

110.    Sarnat, H.B., D. Nochlin, and D.E. Born, Neuronal nuclear antigen (NeuN): a marker of neuronal maturation in early human fetal nervous system. Brain Dev, 1998. 20(2): p. 88-94.

111.    Wolf, H.K., et al., NeuN: a useful neuronal marker for diagnostic histopathology. J Histochem Cytochem, 1996. 44(10): p. 1167-71.

112.    Fischer, A.J., et al., Heterogeneity of horizontal cells in the chicken retina. J Comp Neurol, 2007. 500(6): p. 1154-71.

113.    Edqvist, P.H. and F. Hallbook, Newborn horizontal cells migrate bi-directionally across the neuroepithelium during retinal development. Development, 2004. 131(6): p. 1343-51.

114.    Poche, R.A. and B.E. Reese, Retinal horizontal cells: challenging paradigms of neural development and cancer biology. Development, 2009. 136(13): p. 2141-51.

115.    Boije, H., P.H. Edqvist, and F. Hallbook, Horizontal cell progenitors arrest in G2-phase and undergo terminal mitosis on the vitreal side of the chick retina. Dev Biol, 2009. 330(1): p. 105-13.

116.    Cho SS, L.J., Hyndman AG., Transferrin binding protein is expressed by oligodendrocytes in the avian retina. Brain Res, 1999. 816(1): p. 229-233.

117.    Waid, D.K. and S.C. McLoon, Immediate differentiation of ganglion cells following mitosis in the developing retina. Neuron, 1995. 14(1): p. 117-24.

118.    Furukawa, T., et al., rax, Hes1, and notch1 promote the formation of Muller glia by postnatal retinal progenitor cells. Neuron, 2000. 26(2): p. 383-94.

119.    Meller, K. and W. Tetzlaff, Scanning electron microscopic studies on the development of the chick retina. Cell Tissue Res, 1976. 170(2): p. 145-59.

120.    Bhattacharjee, J. and S. Sanyal, Developmental origin and early differentiation of retinal Muller cells in mice. J Anat, 1975. 120(Pt 2): p. 367-72.

121.    Malatesta, P., E. Hartfuss, and M. Gotz, Isolation of radial glial cells by fluorescent-activated cell sorting reveals a neuronal lineage. Development, 2000. 127(24): p. 5253-63.

122.    Pinto, L. and M. Gotz, Radial glial cell heterogeneity--the source of diverse progeny in the CNS. Prog Neurobiol, 2007. 83(1): p. 2-23.

123.    Willbold, E., et al., Muller glia cells reorganize reaggregating chicken retinal cells into correctly laminated in vitro retinae. Glia, 2000. 29(1): p. 45-57.

124.    Willbold, E., et al., Muller glia stabilizes cell columns during retinal development: lateral cell migration but not neuropil growth is inhibited in mixed chick-quail retinospheroids. Eur J Neurosci, 1995. 7(11): p. 2277-84.

125.    Anezary, L., et al., Shape diversity among chick retina Muller cells and their postnatal differentiation. J Comp Neurol, 2001. 438(1): p. 32-49.

126.    Won, M.H., T.C. Kang, and S.S. Cho, Glial cells in the bird retina: immunochemical detection. Microsc Res Tech, 2000. 50(2): p. 151-60.

127.    Cuadros, M.A. and J. Navascues, The origin and differentiation of microglial cells during development. Prog Neurobiol, 1998. 56(2): p. 173-89.

128.    Santos, A.M., et al., Embryonic and postnatal development of microglial cells in the mouse retina. J Comp Neurol, 2008. 506(2): p. 224-39.

129.    Niwa, H., K. Yamamura, and J. Miyazaki, Efficient selection for high-expression transfectants with a novel eukaryotic vector. Gene, 1991. 108(2): p. 193-9.

130.    Chen, Y.X., C.E. Krull, and L.W. Reneker, Targeted gene expression in the chicken eye by in ovo electroporation. Mol Vis, 2004. 10: p. 874-83.

131.    Pizzarello, L., et al., VISION 2020: The Right to Sight: a global initiative to eliminate avoidable blindness. Arch Ophthalmol, 2004. 122(4): p. 615-20.

132.    Dyer, M.A. and C.L. Cepko, Control of Muller glial cell proliferation and activation following retinal injury. Nat Neurosci, 2000. 3(9): p. 873-80.

133.    Tackenberg, M.A., et al., Muller cell activation, proliferation and migration following laser injury. Mol Vis, 2009. 15: p. 1886-96.

134.    Perron, M. and W.A. Harris, Determination of vertebrate retinal progenitor cell fate by the Notch pathway and basic helix-loop-helix transcription factors. Cell Mol Life Sci, 2000. 57(2): p. 215-23.

135.    Rowan, S., et al., Notch signaling regulates growth and differentiation in the mammalian lens. Dev Biol, 2008. 321(1): p. 111-22.

136.    Nelson, B.R., et al., Notch activity is downregulated just prior to retinal ganglion cell differentiation. Dev Neurosci, 2006. 28(1-2): p. 128-41.

137.    Livesey, F.J. and C.L. Cepko, Vertebrate neural cell-fate determination: lessons from the retina. Nat Rev Neurosci, 2001. 2(2): p. 109-18.

138.    Masland, R.H., Neuronal diversity in the retina. Curr Opin Neurobiol, 2001. 11(4): p. 431-6.

139.    Masland, R.H. and E. Raviola, Confronting complexity: strategies for understanding the microcircuitry of the retina. Annu Rev Neurosci, 2000. 23: p. 249-84.

140.    Cook, J.E. and L.M. Chalupa, Retinal mosaics: new insights into an old concept. Trends Neurosci, 2000. 23(1): p. 26-34.

141.    Wassle, H. and H.J. Riemann, The mosaic of nerve cells in the mammalian retina. Proc R Soc Lond B Biol Sci, 1978. 200(1141): p. 441-61.

142.    Noctor, S.C., et al., Neurons derived from radial glial cells establish radial units in neocortex. Nature, 2001. 409(6821): p. 714-20.

143.    Campbell, K. and M. Gotz, Radial glia: multi-purpose cells for vertebrate brain development. Trends Neurosci, 2002. 25(5): p. 235-8.

144.	Merkle, F.T., et al., Radial glia give rise to adult neural stem cells in the subventricular zone. Proc Natl Acad Sci U S A, 2004. 101(50): p. 17528-32.

145.	Noctor, S.C., et al., Cortical neurons arise in symmetric and asymmetric division zones and migrate through specific phases. Nat Neurosci, 2004. 7(2): p. 136-44.

146.	Kriegstein, A., S. Noctor, and V. Martinez-Cerdeno, Patterns of neural stem and progenitor cell division may underlie evolutionary cortical expansion. Nat Rev Neurosci, 2006. 7(11): p. 883-90.

147.	Noctor, S.C., V. Martinez-Cerdeno, and A.R. Kriegstein, Distinct behaviors of neural stem and progenitor cells underlie cortical neurogenesis. J Comp Neurol, 2008. 508(1): p. 28-44.

148.	Bao, Z.Z. and C.L. Cepko, The expression and function of Notch pathway genes in the developing rat eye. J Neurosci, 1997. 17(4): p. 1425-34.

149.	Jadhav, A.P., K. Roesch, and C.L. Cepko, Development and neurogenic potential of Muller glial cells in the vertebrate retina. Prog Retin Eye Res, 2009. 28(4): p. 249-62.

150.	Anthony, T.E., et al., Brain lipid-binding protein is a direct target of Notch signaling in radial glial cells. Genes Dev, 2005. 19(9): p. 1028-33.

151.	Gaiano, N., J.S. Nye, and G. Fishell, Radial glial identity is promoted by Notch1 signaling in the murine forebrain. Neuron, 2000. 26(2): p. 395-404.

152.	Chambers, C.B., et al., Spatiotemporal selectivity of response to Notch1 signals in mammalian forebrain precursors. Development, 2001. 128(5): p. 689-702.

153.	Uga, S. and Smelser, Comparative study of the fine structure of retinal Muller cells in various vertebrates. Invest Ophthalmol, 1973. 12(6): p. 434-48.

154.	Reichenbach, A., et al., The structure of rabbit retinal Muller (glial) cells is adapted to the surrounding retinal layers. Anat Embryol (Berl), 1989. 180(1): p. 71-9.

155.	Lillien, L. and D. Wancio, Changes in Epidermal Growth Factor Receptor Expression and Competence to Generate Glia Regulate Timing and Choice of Differentiation in the Retina. Mol Cell Neurosci, 1998. 10(5/6): p. 296-308.

156.	Dyer, M.A. and C.L. Cepko, p57(Kip2) regulates progenitor cell proliferation and amacrine interneuron development in the mouse retina. Development, 2000. 127(16): p. 3593-605.

157.	Lillien, L., Changes in retinal cell fate induced by overexpression of EGF receptor. Nature, 1995. 377(6545): p. 158-62.

158.	Levine, E.M., et al., p27(Kip1) regulates cell cycle withdrawal of late multipotent progenitor cells in the mammalian retina. Dev Biol, 2000. 219(2): p. 299-314.

159.	Vetter, M.L. and K.B. Moore, Becoming glial in the neural retina. Dev Dyn, 2001. 221(2): p. 146-53.

160.	Roesch, K., et al., The transcriptome of retinal Muller glial cells. J Comp Neurol, 2008. 509(2): p. 225-38.

161.	Bernardos, R.L., et al., Late-stage neuronal progenitors in the retina are radial Muller glia that function as retinal stem cells. J Neurosci, 2007. 27(26): p. 7028-40.

162.	Turner, D.L. and C.L. Cepko, A common progenitor for neurons and glia persists in rat retina late in development. Nature, 1987. 328(6126): p. 131-6.

163.	Reh, T.A. and A.J. Fischer, Stem cells in the vertebrate retina. Brain Behav Evol, 2001. 58(5): p. 296-305.

164.	Reh, T.A. and E.M. Levine, Multipotential stem cells and progenitors in the vertebrate retina. J Neurobiol, 1998. 36(2): p. 206-20.

165.	Fischer, A.J. and T.A. Reh, Potential of Muller glia to become neurogenic retinal progenitor cells. Glia, 2003. 43(1): p. 70-6.

166.	Cagan, R.L. and D.F. Ready, Notch is required for successive cell decisions in the developing Drosophila retina. Genes Dev, 1989. 3(8): p. 1099-112.

167.	Wharton, K.A., et al., Nucleotide sequence from the neurogenic locus notch implies a gene product that shares homology with proteins containing EGF-like repeats. Cell, 1985. 43(3 Pt 2): p. 567-81.

168.	Wharton, K.A., et al., opa: a novel family of transcribed repeats shared by the Notch locus and other developmentally regulated loci in D. melanogaster. Cell, 1985. 40(1): p. 55-62.

169.	Kadesch, T., Notch signaling: a dance of proteins changing partners. Exp Cell Res, 2000. 260(1): p. 1-8.
170.	Louvi, A. and S. Artavanis-Tsakonas, Notch signalling in vertebrate neural development. Nat Rev Neurosci, 2006. 7(2): p. 93-102.
171.	Brown, M.S., et al., Regulated intramembrane proteolysis: a control mechanism conserved from bacteria to humans. Cell, 2000. 100(4): p. 391-8.
172.	Jarriault, S., et al., Signalling downstream of activated mammalian Notch. Nature, 1995. 377(6547): p. 355-8.
173.	Ohtsuka, T., et al., Hes1 and Hes5 as notch effectors in mammalian neuronal differentiation. Embo J, 1999. 18(8): p. 2196-207.
174.	Borggrefe, T. and F. Oswald, The Notch signaling pathway: transcriptional regulation at Notch target genes. Cell Mol Life Sci, 2009. 66(10): p. 1631-46.
175.	Yoon, K. and N. Gaiano, Notch signaling in the mammalian central nervous system: insights from mouse mutants. Nat Neurosci, 2005. 8(6): p. 709-15.
176.	Huppert, S.S., et al., Embryonic lethality in mice homozygous for a processing-deficient allele of Notch1. Nature, 2000. 405(6789): p. 966-70.
177.	Henrique, D., et al., Maintenance of neuroepithelial progenitor cells by Delta-Notch signalling in the embryonic chick retina. Curr Biol, 1997. 7(9): p. 661-70.
178.	Beatus, P. and U. Lendahl, Notch and neurogenesis. J Neurosci Res, 1998. 54(2): p. 125-36.
179.	Garg, V., et al., Mutations in NOTCH1 cause aortic valve disease. Nature, 2005. 437(7056): p. 270-4.
180.	Austin, C.P., et al., Vertebrate retinal ganglion cells are selected from competent progenitors by the action of Notch. Development, 1995. 121(11): p. 3637-50.
181.	Jadhav, A.P., S.H. Cho, and C.L. Cepko, Notch activity permits retinal cells to progress through multiple progenitor states and acquire a stem cell property. Proc Natl Acad Sci U S A, 2006. 103(50): p. 18998-9003.
182.	Jadhav, A.P., H.A. Mason, and C.L. Cepko, Notch 1 inhibits photoreceptor production in the developing mammalian retina. Development, 2006. 133(5): p. 913-23.
183.	Gaiano, N. and G. Fishell, The role of notch in promoting glial and neural stem cell fates. Annu Rev Neurosci, 2002. 25: p. 471-90.
184.	Yang, X., et al., Notch1 signaling influences v2 interneuron and motor neuron development in the spinal cord. Dev Neurosci, 2006. 28(1-2): p. 102-17.
185.	Yaron, O., et al., Notch1 functions to suppress cone-photoreceptor fate specification in the developing mouse retina. Development, 2006. 133(7): p. 1367-78.
186.	Cepko, C.L., The roles of intrinsic and extrinsic cues and bHLH genes in the determination of retinal cell fates. Curr Opin Neurobiol, 1999. 9(1): p. 37-46.
187.	Magdaleno, S., et al., BGEM: an in situ hybridization database of gene expression in the embryonic and adult mouse nervous system. PLoS Biol, 2006. 4(4): p. e86.
188.	Taatjes, D.J., M.T. Marr, and R. Tjian, Regulatory diversity among metazoan co-activator complexes. Nat Rev Mol Cell Biol, 2004. 5(5): p. 403-10.
189.	Levine, M. and R. Tjian, Transcription regulation and animal diversity. Nature, 2003. 424(6945): p. 147-51.
190.	Clarke, M.F., et al., Sequence-specific interaction of histones with the simian virus 40 enhancer region in vitro. J Biol Chem, 1985. 260(23): p. 12394-7.
191.	Elgin, S.C., The formation and function of DNase I hypersensitive sites in the process of gene activation. J Biol Chem, 1988. 263(36): p. 19259-62.
192.	Engel, J.D. and K. Tanimoto, Looping, linking, and chromatin activity: new insights into beta-globin locus regulation. Cell, 2000. 100(5): p. 499-502.
193.	Li, Q., S. Harju, and K.R. Peterson, Locus control regions: coming of age at a decade plus. Trends Genet, 1999. 15(10): p. 403-8.
194.	Magram, J., K. Chada, and F. Costantini, Developmental regulation of a cloned adult beta-globin gene in transgenic mice. Nature, 1985. 315(6017): p. 338-40.

195.     Kollias, G., et al., Regulated expression of human A gamma-, beta-, and hybrid gamma beta-globin genes in transgenic mice: manipulation of the developmental expression patterns. Cell, 1986. 46(1): p. 89-94.

196.     Wang, W.C., et al., Comparative cis-regulatory analyses identify new elements of the mouse Hoxc8 early enhancer. J Exp Zool B Mol Dev Evol, 2004. 302(5): p. 436-45.

197.     Lei, H., et al., The identification of Hoxc8 target genes. Proc Natl Acad Sci U S A, 2005. 102(7): p. 2420-4.

198.     Wang, W.C., et al., Comparative cis-regulatory analyses identify new elements of the mouse Hoxc8 early enhancer. J Exp Zoolog B Mol Dev Evol, 2004. 302(5): p. 436-45.

199.     Force, A., et al., Comparative genomics, cis-regulatory elements, and gene duplication. Methods Cell Biol, 2004. 77: p. 545-61.

200.     Tolhuis, B., et al., Looping and interaction between hypersensitive sites in the active beta-globin locus. Mol Cell, 2002. 10(6): p. 1453-65.

201.     Dean, A., On a chromosome far, far away: LCRs and gene expression. Trends Genet, 2006. 22(1): p. 38-45.

202.     Palstra, R.J., et al., The beta-globin nuclear compartment in development and erythroid differentiation. Nat Genet, 2003. 35(2): p. 190-4.

203.     Carter, D., et al., Long-range chromatin regulatory interactions *in vivo*. Nat Genet, 2002. 32(4): p. 623-6.

204.     Spilianakis, C.G., et al., Interchromosomal associations between alternatively expressed loci. Nature, 2005. 435(7042): p. 637-45.

205.     Pennacchio, L.A., et al., *In vivo* enhancer analysis of human conserved non-coding sequences. Nature, 2006. 444(7118): p. 499-502.

206.     Pennacchio, L.A., et al., Predicting tissue-specific enhancers in the human genome. Genome Res, 2007. 17(2): p. 201-11.

207.     Prabhakar, S., et al., Close sequence comparisons are sufficient to identify human cis-regulatory elements. Genome Res, 2006. 16(7): p. 855-63.

208.     Poulin, F., et al., *In vivo* characterization of a vertebrate ultraconserved enhancer. Genomics, 2005. 85(6): p. 774-81.

209.     Sabherwal, N., et al., Long-range conserved non-coding SHOX sequences regulate expression in developing chicken limb and are associated with short stature phenotypes in human patients. Hum Mol Genet, 2007. 16(2): p. 210-22.

210.     Kleinjan, D.A., et al., Long-range downstream enhancers are essential for Pax6 expression. Dev Biol, 2006. 299(2): p. 563-81.

211.     Sipos, L. and H. Gyurkovics, Long-distance interactions between enhancers and promoters. Febs J, 2005. 272(13): p. 3253-9.

212.     Hillier, L.W., et al., Sequence and comparative analysis of the chicken genome provide unique perspectives on vertebrate evolution. Nature, 2004. 432(7018): p. 695-716.

213.     Kurokawa, D., et al., Regulation of Otx2 expression and its functions in mouse forebrain and midbrain. Development, 2004. 131(14): p. 3319-31.

214.     Ma, G.C., et al., Retina-specific cis-elements and binding nuclear proteins of carp rhodopsin gene. FEBS Lett, 2001. 508(2): p. 265-71.

215.     Vavouri, T., et al., Parallel evolution of conserved non-coding elements that target a common set of developmental regulatory genes from worms to humans. Genome Biol, 2007. 8(2): p. R15.

216.     Young, J.E., et al., Conserved interactions of a compact highly active enhancer/promoter upstream of the rhodopsin kinase (GRK1) gene. Genomics, 2007.

217.     Kleinjan, D.A., et al., Aniridia-associated translocations, DNase hypersensitivity, sequence comparison and transgenic analysis redefine the functional domain of PAX6. Hum Mol Genet, 2001. 10(19): p. 2049-59.

218.     Pfeffer, P.L., et al., The activation and maintenance of Pax2 expression at the mid-hindbrain boundary is controlled by separate enhancers. Development, 2002. 129(2): p. 307-18.

219.    Knight, J.C., Functional implications of genetic variation in non-coding DNA for disease susceptibility and gene regulation. Clin Sci (Lond), 2003. 104(5): p. 493-501.

220.    Pilpel, Y., P. Sudarsanam, and G.M. Church, Identifying regulatory networks by combinatorial analysis of promoter elements. Nat Genet, 2001. 29(2): p. 153-9.

221.    Visel, A., et al., VISTA Enhancer Browser--a database of tissue-specific human enhancers. Nucleic Acids Res, 2007. 35(Database issue): p. D88-92.

222.    Doh, S.T., et al., Analysis of retinal cell development in chick embryo by immunohistochemistry and *in ovo* electroporation techniques. BMC Dev Biol, 2010. 10: p. 8.

223.    Greferath, U., U. Grunert, and H. Wassle, Rod bipolar cells in the mammalian retina show protein kinase C-like immunoreactivity. J Comp Neurol, 1990. 301(3): p. 433-42.

224.    Sassoe Pognetto, M., et al., Comparative study of glial fibrillary acidic protein (GFAP)-like immunoreactivity in the retina of some representative vertebrates. Eur J Histochem, 1992. 36(4): p. 467-77.

225.    Hockfield, S. and R.D. McKay, Identification of major cell classes in the developing mammalian nervous system. J Neurosci, 1985. 5(12): p. 3310-28.

226.    Doh, S.T., et al., Non-coding sequence retrieval system for comparative genomic analysis of gene regulatory elements. BMC Bioinformatics, 2007. 8: p. 94.

227.    Nie, Z., et al., RER, an evolutionarily conserved sequence upstream of the rhodopsin gene, has enhancer activity. J Biol Chem, 1996. 271(5): p. 2667-75.

228.    Yee, S.P. and P.W. Rigby, The regulation of myogenin gene expression during the embryonic development of the mouse. Genes Dev, 1993. 7(7A): p. 1277-89.

229.    Bringmann, A., et al., Muller cells in the healthy and diseased retina. Prog Retin Eye Res, 2006. 25(4): p. 397-424.

230.    Ohta, K., A. Ito, and H. Tanaka, Neuronal stem/progenitor cells in the vertebrate eye. Dev Growth Differ, 2008. 50(4): p. 253-9.

231.    Bhatia, B., et al., Distribution of Muller stem cells within the neural retina: Evidence for the existence of a ciliary margin-like zone in the adult human eye. Exp Eye Res, 2009.

232.    Matsuda, T. and C.L. Cepko, Controlled expression of transgenes introduced by *in vivo* electroporation. Proceedings of the National Academy of Sciences of the United States of America, 2007. 104(3): p. 1027-32.

233.    Matsuda, T. and C.L. Cepko, Analysis of gene function in the retina. Methods Mol Biol, 2008. 423: p. 259-78.

234.    Wiese, C., et al., Nestin expression--a property of multi-lineage progenitor cells? Cell Mol Life Sci, 2004. 61(19-20): p. 2510-22.

235.    Boutin, C., et al., Efficient *in vivo* electroporation of the postnatal rodent forebrain. PLoS ONE, 2008. 3(4): p. e1883.

236.    Garcia-Frigola, C., et al., Gene delivery into mouse retinal ganglion cells by *in utero* electroporation. BMC Dev Biol, 2007. 7: p. 103.

237.    Tabata, H. and K. Nakajima, Efficient *in utero* gene transfer system to the developing mouse brain using electroporation: visualization of neuronal migration in the developing cortex. Neuroscience, 2001. 103(4): p. 865-72.

238.    Saito, T., *In vivo* electroporation in the embryonic mouse central nervous system. Nat Protoc, 2006. 1(3): p. 1552-8.

239.    Ahmad, I., P. Zaqouras, and S. Artavanis-Tsakonas, Involvement of Notch-1 in mammalian retinal neurogenesis: association of Notch-1 activity with both immature and terminally differentiated cells. Mech Dev, 1995. 53(1): p. 73-85.

240.    Ahmad, I., L. Tang, and H. Pham, Identification of neural progenitors in the adult mammalian eye. Biochem Biophys Res Commun, 2000. 270(2): p. 517-21.

241.    Yang, J., et al., Nestin expression during mouse eye and lens development. Mech Dev, 2000. 94(1-2): p. 287-91.

242.    Chacko, D.M., et al., Survival and differentiation of cultured retinal progenitors transplanted in the subretinal space of the rat. Biochem Biophys Res Commun, 2000. 268(3): p. 842-6.

243.     Morrow, E.M., C.M. Chen, and C.L. Cepko, Temporal order of bipolar cell genesis in the neural retina. Neural Dev, 2008. 3: p. 2.

244.     Cepko, C.L., et al., Cell fate determination in the vertebrate retina. Proc Natl Acad Sci U S A, 1996. 93(2): p. 589-95.

245.     Dhomen, N.S., et al., Absence of chx10 causes neural progenitors to persist in the adult retina. Invest Ophthalmol Vis Sci, 2006. 47(1): p. 386-96.

246.     Yoon, K., et al., Fibroblast growth factor receptor signaling promotes radial glial identity and interacts with Notch1 signaling in telencephalic progenitors. J Neurosci, 2004. 24(43): p. 9497-506.

247.     Chen, H.L., C.H. Yuh, and K.K. Wu, Nestin is essential for zebrafish brain and eye development through control of progenitor cell apoptosis. PLoS ONE, 2010. 5(2): p. e9318.

248.     Xue, L.P., et al., Nestin expression in Muller glial cells in postnatal rat retina and its upregulation following optic nerve transection. Neuroscience, 2006. 143(1): p. 117-27.

249.     Shih, A.H. and E.C. Holland, Notch signaling enhances nestin expression in gliomas. Neoplasia, 2006. 8(12): p. 1072-82.

250.     de la Pompa, J.L., et al., Conservation of the Notch signalling pathway in mammalian neurogenesis. Development, 1997. 124(6): p. 1139-48.

251.     Kageyama, R. and T. Ohtsuka, The Notch-Hes pathway in mammalian neural development. Cell Res, 1999. 9(3): p. 179-88.

## ACKNOWLEDGEMENT OF PREVIOUS PUBLICATIONS

# CURRICULUM VITAE

**SUNG TAE DOH**

## EDUCATION

2003-2010   **Rutgers, The State University of New Jersey, New Brunswick, NJ**
Ph.D. in Biochemical Engineering

1998-2002   **Rutgers, The State University of New Jersey, New Brunswick, NJ**
Bachelor of Arts, Mathematics and Biology

## PUBLICATIONS

1. Doh ST., Zhang Y., Temple MH., Cai L. "Non-coding sequence retrieval system for comparative genomic analysis of gene regulatory elements," BMC Bioinformatics. 8:94, 2007 March.
2. Nair, S., Doh ST., Chan, JY., Kong AN., Cai, L. "Regulatory potential for concerted modulation of Nrf2- and Nfkb1-mediated gene expression in inflammation and carcinogenesis," British Journal of Cancer. 99(12):2070-82, 2008 Dec.
3. Doh ST., Hao H., Loh S., Patel T., Tawil H., Chen D., Pashkova A., Shen A., Wang H., Cai L. "Analysis of retinal cell development in chick embryo by immunohistochemistry and *in ovo* electroporation techniques," BMC Developmental Biology. 10:8, 2010 Jan.
4. Liu J., Sandoval J., López-Rodas G., Doh ST., Cai L., Casaccia P. "Epigenetic modifiers are necessary but not sufficient for reprogramming non-myelinating cells into myelin gene-expressing cells," PLoS ONE. Manuscript under review.
5. Doh ST., Cai L. "A novel Notch1 enhancer preferentially drives expression in mouse retinal progenitor and Nestin positive Muller glial cells," Manuscript in preparation.
6. Hao H, Doh ST, LaBouff E, Maffei J, Patel T, Tawil HY, Loh SC, Son AL, Zhou R, and Cai L. Ephrin-A5 regulates retinal neurite outgrowth and laminar formation during development. Manuscript in preparation.
7. Hao H, Doh ST, Tzatzalos E, Lin R, Lyu L, and Cai L. Role of Top2b in retinal development. Manuscript in preparation.